2016

Investigating the Role of the Nucleosome Remodeling Factor INO80 in Development and NURF in Anti-Tumor Immunity

zeinab abdallah elsayed Ms
Virginia Commonwealth University

Investigating the Role of the Nucleosome Remodeling Factor INO80 in Development and NURF in Anti-Tumor Immunity

A dissertation submitted in partial fulfillment of the requirements for the degree of Doctor of Philosophy at Virginia Commonwealth University.

By

ZEINAB ELSAYED
Bachelor of Science, Al-Azhar University, Egypt, 2001
Master of Cytogenetics, National Research Center, Egypt, 2011

Advisor: Joseph W. Landry, Ph.D.
Assistant Professor, Department of Human and Molecular Genetics
School of Medicine

Virginia Commonwealth University
Richmond, Virginia
December 2016

ACKNOWLEDGEMENT

First and foremost, thanks to God since his will and grace is the main reason for my success. God blessed me with the ability to meet extraordinary people who helped me reach this point in my life.

I would like to thank my advisor, Dr. Joseph W. Landry, for his patience during teaching me to finish my work, for giving me the opportunity to participate in such great projects and his support all of this time. I will be in his debt forever.

I would like to thank my committee members: Dr. Jolene Windle for giving me a tremendous amount of her time, listening to me and sincerely helping me find my way out; Dr. Swati Palit Deb for her continuous encouragement and help whenever I asked for it; and Drs. Lynne Elmore and Jim Lister for their continuous help and support since they joined my committee.

I would like to thank Dr. Gail Christie for accepting me into the MBG program and for her help in every step until now. In addition, I would like to thank Dr. Amal Mahmoud (head of the Cytogentics Department in Egypt), Dr. Nivin Helmy, and Dr. Hesham Fayek for their continuous support during my Ph.D. studies.

I cannot find appropriate words to thank my parents for their unconditional love and continuous support and prayers for me. I am lucky to have such parents and my brother in my life. I am blessed to have my husband beside me during these four years and I am speechless for his support and help. I would like to thank my kids for being responsible and making me smile.

Finally, I am very grateful and thankful for the Landry lab members for their contributions to the completion of this work.

Contributors

Dr. Joseph Landry: Establishment of mouse lines and mouse dissection.

Dr. Zhijun Qui: MEF and mESC isolation and characterization; ISH experiments, teratoma and embryoid body assays, mouse husbandry and genotyping.

Veronica Peterkin: Mouse genotyping and RT-PCR experiments.

Suehyb Alkhatib and Dorothy Bennett: NK cell depletion *in vivo*, Southern blot analysis and mouse genotyping.

Aiman Alhazmi: Microarray experiments and data analysis.

Kimberly Mayes: Data analysis, heparanse Western blot, RT-PCR and CHIP experiments, NK cell depletion *in vivo.*

Mark Roberts and Kristen Peterson: Establishment of rADV and *in vivo* tumor studies.

Nikhil Ailaney: Ncr1-Zeta chain reporter assay and qRT-PCR**.**

Table of Content

List of Figures

List of Tables

List of Abbreviations

ACF1	ATP-utilizing chromatin assembly and remodeling factor 1
ATP	Adenosine triphosphate
BAF	Brahma-associated factor
BAZ1	Bromodomain adjacent to zinc finger domain 1A
BMP	Bone morphogenetic protein
BMP4	Bone morphogenetic protein 4
Bp	Base pair
BPTF	Bromodomain PHD transcription factor
PBS	Phosphate-buffered saline-tween
PBS-T	Phosphate-buffered saline-tween
53BP1	p53-binding protein 1
BRG1	Brahma-related gene1
BRK	Brahma and Kismet domain
BRM	Brahma
BrdU	Bromodeoxyuridine
BSA	Bovine serum albumin
cm	Centimeter
CTL	Cytotoxic T-lymphocytes
C-terminal	Carboxy-terminal
CHD	Chromodomain, helicase and DNA binding
ChIP	Chromatin immunoprecipitation
CHRAC	Chromatin-accessibility complex
Co-IP	Co-immunoprecipitation

CTCF	CCCTC-binding factor
CTD	C-terminal domain
Cys	Cysteine
D	Aspartic acid
DCs	Dendritic cells
DBP	DNA binding protein
DIG	Digoxigenin
DNA	Deoxyribonucleic acid
DSBs	DNA double-strand breaks
DNMT	DNA-methyl transferase
DP	Double positive
DNMTi	DNA methyltransferase inhibitors
DVE	Distal visceral endoderm
ESC	Embryonic stem cell
FACT	Facilitates chromatin transcription
FAIRE	Formaldehyde assistance isolation of regulatory elements
FOG-1	Friend of GATA-1
ELISA	Enzyme-linked immunosorbent assay
E	Embryonic day
EPI	Epiblast
FACS	Fluorescence-activated cell sorting
FBS	Fetal bovine serum
H	Histone
H2AK119ub1	Monoubiquitination of H2AK119
H3K27ac	Acetylation of lysine 27 of histone 3
H3K36me3	Tri-methylation of lysine 36 of histone 3
H3K4ac	Acetylation of lysine 4 of histone 3

H3K4me1	Mono-methylation of lysine 4 of histone 3
H3K4me2	Di-methylation of lysine 4 of histone 3
H3K4me3	Tri-methylation of lysine 4 of histone 3
H3K9me3	Tri-methylation of lysine 9 of histone 3
H4K16ac	Acetylation of lysine 16 of histone 4
HAT	Histone acetyl transferase
HDAC	Histone deacetylase
His	Histidine
HP1	Heterochromatin protein 1
HBSS	Hank's balanced salt solution
HR	Homologous recombination
HS	Heparin sulfate
HSGAG	Heparin sulfate glycosaminoglycan
HSPGs	Heparin sulfate proteoglycans
IFNγ	Interferon gamma
Kb	Kilo base
KD	Knock-down
LB	Lysogeny broth
LDH	Lactate dehydrogenase
LE	Luminal epithelium
LIF	Leukemia inhibitory factor
Min	minutes
MDSC	Myeloid derived suppressor cell
MHC	Major histocompatibility complex
NCR	Natural cytotoxicity receptors
NHEJ	Non-homologous end joining

NK	Natural killer
NSG	NOD/SCID, IFNg2r$^{-/-}$ mouse strain
NURF	Nucleosome remodeling factor
PFU	Plaque forming unit, or one infectious viral particle
PrE	Primitive endoderm
PVDC	Polyvinyledine fluoride
rADV	Recombinant adenovirus
SDS	Sodium dodecyl sulfate
TIL	Tumor infiltrating lymphocyte
TME	microenvironment
TNF	Tumor necrosis factor
ZGA	Zygote genome activation

Abstract

Understanding how an epigenetic regulator such as ATP-dependent chromatin-remodeling complexes modulate processes such as development and/or immune response is essential for our comprehension of cell biology. Deletion of the ATP-dependent chromatin remodeling factor INO80 is known to be embryonically lethal, however, the mechanism is not known. To identify roles for INO80 in mouse early development we generated *Ino80* KO mice. *Ino80* KO ESCs (Embryonic stem cells) were viable when maintained at ground state pluripotency but fail to differentiate *in vitro* and *in vivo*. Gene expression analysis of *Ino80* KO early embryos by *in situ* hybridization showed elevated *Bmp4* expression and reduced expression of DVE (distal visceral endoderm) markers *Cer1*, *Hex,* and *Lefty1*. BMP4 is a known negative regulator of DVE differentiation in the early embryo. Molecular studies in *Ino80* KO ESCs demonstrated that INO80 is bound to the *Bmp4* promoter, and regulates its chromatin structure, to suppress the positive regulator SP1 from stimulating its transcription. These results, suggest that INO80 directly regulates the chromatin structure of the *Bmp4* promoter with consequences to mouse embryo development. These results are significant because they demonstrate a specific role of INO80 in establishing P-D embryonic axis.

NURF (Nucleosome remodeling factor) is another ATP-dependent chromatin remodeling complex that is overexpressed in many cancer types including breast cancer. To demonstrate the roles of NURF in breast cancer biology, we knocked-down the NURF essential subunit BPTF (bromodomain PHD finger transcription factor) in

mouse breast cancer cell lines. Transplantation of these cell lines into immune-competent mice revealed that BPTF KD enhances NK cell antitumor activity. BPTF KD enhanced NK-92 cytotoxic activity toward BPTF KD cells by NKp30 activation *in vitro*. NK-92 activity is reduced by the addition of heparin to the culture medium, further indicating the involvement of NKp30 (in human) and NCR1 (in mice) in killing of tumor cells. We found that BPTF controls the abundance of NKp30/NCR1 ligands (heparin sulfate proteoglycans (HSPGs) by regulation of heparanase expression (endoglycosidase that degrades HSPGs). In addition, BPTF depletion in established mouse breast tumors enhanced anti-tumor immunity, without affecting NK or T cell cytotoxic activity, providing a novel immunotherapy target.

PART I. Role of the Nucleosome Remodeling Factor INO80 in Development

Chapter 1. Background and Literature Review

1.1 DNA Packaging into Chromatin

The eukaryotic genetic information is stored in two meters of linear DNA. In order for this long DNA to fit into a 10 μm nucleus it has to be packaged into chromatin, which consists of DNA wrapped around histone proteins. Histone proteins are highly conserved proteins, and they are the main components of chromatin structure. The basic unit of chromatin structure is the nucleosome, which is composed of 145-147 bp DNA wrapped around an octamer of histones, which itself consists of two copies of the canonical histones H2A, H2B, H3, and H4. The nucleosome structure is stabilized by the interaction between negatively charged DNA and positively charged histones. It is also stabilized by the protein-protein interactions inside the histone octamer (Davey et al., 2002 and Rohs et al., 2009). Nearby nucleosomes are connected by linker DNA (10-90 bp) and linker histones (H1 and H5) to form a chromatin fiber. Interactions between these fibers through inter and intra-nucleosomal interactions give rise to the highly compacted chromatin that we see in the chromosomes (Tremethick et al., 2007).

Depending on the degree of chromatin condensation, chromatin can be divided into euchromatin and heterochromatin (Trojer and Reinberg, 2007). Euchromatin is less condensed chromatin and enriched with genes. Heterochromatin is highly condensed and can be further divided into constitutive and facultative heterochromatin

(Margueron et al. 2005). Constitutive heterochromatin is repetitive DNA sequences that are clustered at telomeres, centromeres and peri-centromeric regions of the chromosomes. Facultative heterochromatin is enriched with genes that are expressed at a specific developmental stage or in response to specific stimuli. Consequently, regions of facultative heterochromatin are different among different cell types. These different chromatin domains are separated from each other by insulator elements (Trojer and Reinberg, 2007). Chromatin in its high order structure is inaccessible to DBP (DNA binding proteins), which are involved in nuclear processes such as transcription, DNA replication, and DNA damage response. Therefore, cells have evolved mechanisms to modulate the chromatin from inaccessible to accessible conformation, which includes histone modifications, DNA methylation, incorporation of histone variants, ATP-dependent chromatin remodeling, and long non-coding RNA mediated modulation (C. David and Thomas, 2016).

1.2 Mechanisms of Chromatin Structure Modulation

1.2.1 Histone Modifications

Histones are chemically modified at the post-translation level mostly at their N-terminal and to a lesser extent at core residues or C-termini. The N-termini of histones is about 19-40 amino acids enriched in basic residues mainly lysine (K) and arginine (R) that are extended out from the nucleosome in the form of histone tails. The interaction between these tails in neighboring nucleosomes, or within the same nucleosome, help to modulate chromatin structure. Post-translation modification (PTM) of histones could

be in the form of methylation, acetylation, phosphorylation or ubiquitination. The presence of these modifications serve as a platform for the recruitment of chromatin modulators or transcription factors (Andrew and Tony, 2011).

Methylation occurs mostly on lysine and to a lesser extent on arginine. Methylation can be mono-, di-, or tri- and the methylated residue can be on K4 or K36, which are associated with active chromatin, or on K9/K27, which are associated with repressed chromatin. Genome-wide analysis showed that H3K4me3 is localized at active TSS (transcription start sites) considering them as mark of active promoters (Sims et al., 2005). H3K4me1 is co-localized at enhancers with p300 histone acetyl transferase. The presence of active methylation marks serves to recruit chromatin remodeling complexes, such as NURF or the CHD1 (chromo-domain helicase DNA binding1), to promoter regions to facilitate gene expression (Wysocka et al., 2006). The H3K36me3 mark is enriched at exons than introns, suggesting a possible role in alternative splicing or the transcript elongation (Barski et al., 2007, Spies et al., 2009 and Kolasinska et al., 2009).

Acetylation mainly occurs on lysine residues and many studies showed that H4 and H3 acetylation is a mark of open and accessible chromatin domains. Shogren-Knaak et al., showed that acetylation on H4K16 interferes with chromatin compaction (Shorgen-Knaak, et al., 2006). In addition, acetylation neutralizes the positively charged lysine residues on histone tails and weaken their interaction with negatively charged DNA, which facilitate chromatin accessibility (Luger et al., 1997). Cells with highly dynamic chromatin, like ESCs, have enrichment of H4K16ac at TSS of transcriptionally active genes (Taylor et al., 2013).

Phosphorylation of histones can occur on serine, threonine and tyrosine residues, and this modification plays a role in many processes such as chromatin compaction, DNA repair, and transcription. The most conserved form of histone phosphorylation in eukaryotes is H3 phosphorylation. Four residues are phosphorylated on the H3 N-termini, which are T3, S10, T11, and S28. However, the most documented mark is H3S10ph (histone 3 phosphorylation at serine 10). H3S10ph is associated with chromatin condensation during mitosis (Wei et al., 1999). In addition, the linker histone H1 is phosphorylated in a cell cycle-dependent manner especially during mitosis. H1 phosphorylation by the CDC2 kinase mediates its binding to HP1 to maintain more stabilize compacted chromatin structure while its phosphorylation by CDK2 disrupt this interaction and destabilize chromatin to promote cell progression (Hale et al., 2006). Moreover, the phosphorylation of H3S28 is involved in transcription regulation of EGF (epidermal growth factor)-responsive genes such as c-fos (Lau et al., 2011). In response to DNA damage, the histone variant H2AX is phosphorylated by the ATM kinase and it is commonly referred to as γH2AX. The phosphorylation of H2AX spreads around the DNA damage site to recruit repair proteins such as MDC1 (Stucki et al., 2005).

Ubiquitination occurs in the form of mono-ubiquitination on lysine residues. The most ubiquitinated histones in the nucleus are H2A and H2B. H2Aub is associated with repressed chromatin since H2Aub ligase is found in repression complexes such as PRC1 (polycomb repressive complex) (Ogawa et al., 2002). Another study showed that H2Aub prevents the recruitment of the histone chaperon FACT (facilitate chromatin

transcription) to RNAP II binding sites to facilitate transcription elongation (Zhou et al., 2008). In addition, the activity of H2A deubiquitinase (2A-DUB) in activating gene expression provides another supporting evidence for H2Aub associated repression (Zhu et al., 2007). However, H2Bub is mostly associated with gene activation. ChIP-chip experiments showed enrichment of H2Bub at actively transcribed genes (Minsky et al., 2008). ChIP-chip is chromatin immunoprecipitation (ChIP) followed by DNA microarray (chip) to identify the interactions between DNA and proteins in a genome wide scale (Aparicio et al., 2004). H2Bub is also involved in transcription elongation where they are required for maintaining the chromatin integrity during elongation by RNA Pol II (Xiao et al., 2005).

1.2.2 Incorporation of Histone Variants

Histone variants are different from canonical histones mainly at the C-termini by length or amino acid composition (Ausió et al., 2002). The replacement of canonical histones with histone variants alter the nucleosome structure and consequently its function. For example, the replacement of H2A with its variants which includes H2AZ, H2AX, H2ABBD (H2A-bar-body-deficient) and macro H2A alters cellular functions in diverse cellular pathways. H2AZ (Htz1 is the yeast homolog) is the most studied H2A variant, and it is encoded by an essential gene since its disruption in mice resulted in early embryonic lethality (Faast et al., 2001). H2AZ is required to maintain heterochromatin domains through preventing the spread of HP1 to active regions in the genome (Rangasamy et al., 2004). H2AZ incorporation modulates chromatin structure

to facilitate active transcription and as such, its incorporation prevents chromatin condensation (Park et al., 2004).

1.2.3 DNA Methylation

DNA modification by methylation is the major form of epigenetic regulation in which the cytosines is covalently linked to a methyl group at the primary sequence CpG dinucleotide. DNA methylation patterns are tissue- and cell type-specific through methylation of CpG at specific sites (Razin et al., 1980). DNA methylating enzymes Dnmt3a and Dnmt3b are involved in the *de novo* establishment of methylation during development while the Dnmt1 is required to maintain this pattern upon cell division. DNA methylation pattern affect the chromatin structure since hypomethylated DNA is associated with active chromatin while hypermethylated DNA is associated with repressed chromatin (Razin et al., 1977). DNA methylation silences gene expression by impeding the binding of positive transcription factors or the recruitment of MBPs (methylated DNA binding proteins), which in turn recruit a repressive complexes that silences gene expression. For example, the chromatin remodeling complex NURD (Nucleosome remodeling and histone deacetylase) contain MBD2 (Methyl binding domain 2) that binds methylated DNA, and this interaction stabilizes MBD2 binding and represses gene expression (Zhang et al., 1990). Chromatin modification drives specific DNA methylation, and there is a growing evidence for the interaction between histone-modifying enzymes, such as HDAC1 (Histone deacetylase 1) and HDAC2 (Histone deacetylase 2), and the DNA methylating enzymes Dnmt1, Dnmt3a (Fuks et al., 2000). For example, transcription factors induce specific genes acetylation by recruitment of

HATs (Histone acetyl transferases) and RNA Pol II, and this is followed by DNA demethylation (D'Alessio et al., 2007).

1.2.4 ATP-Dependent Chromatin Remodeling Complexes

The major regulators of chromatin structure are complexes that utilize ATP hydrolysis as an energy source to disrupt histone-DNA interaction, and they are known as ATP-dependent chromatin remodeling complexes. These complexes are involved in every aspect of genome metabolism such as transcription, DNA replication, gene expression, and DNA damage and repair responses. These complexes belong to the Snf2 (sucrose non-fermenting 2) family of ATP-dependent helicases, which is further divided into four subfamilies based on the sequence homology of the ATPase domain and additional domains within the ATPase subunit, which include SWI/SNF (Switching defective 2/sucrose non-fermenting 2) ISWI (Imitation switch); CHD (Chromodomain, helicase and DNA-binding) and INO80 (Inositol-requiring 80). All subfamilies share the highly conserved ATPase domain, including an ATP binding domain for enzymatic activity adjacent to a helicase domain, which is required for the remodeling function (Bartholomew et al., 2014). The remodeling activity could result in the sliding of a nucleosome, nucleosome eviction, nucleosome assembly, nucleosome spacing or exchanging histone variants as showed in Figure 1.1. Sliding can expose or mask transcription factor binding sites in DNA. Ejecting a nucleosome is required during nuclear processes such DNA replication, and the DNA damage response. Exchange of histone variants occurs when modulating the nucleosome structure, such as the deposition of γH2AX variant of H2A during a DNA damage response (Becker et al., 2013).

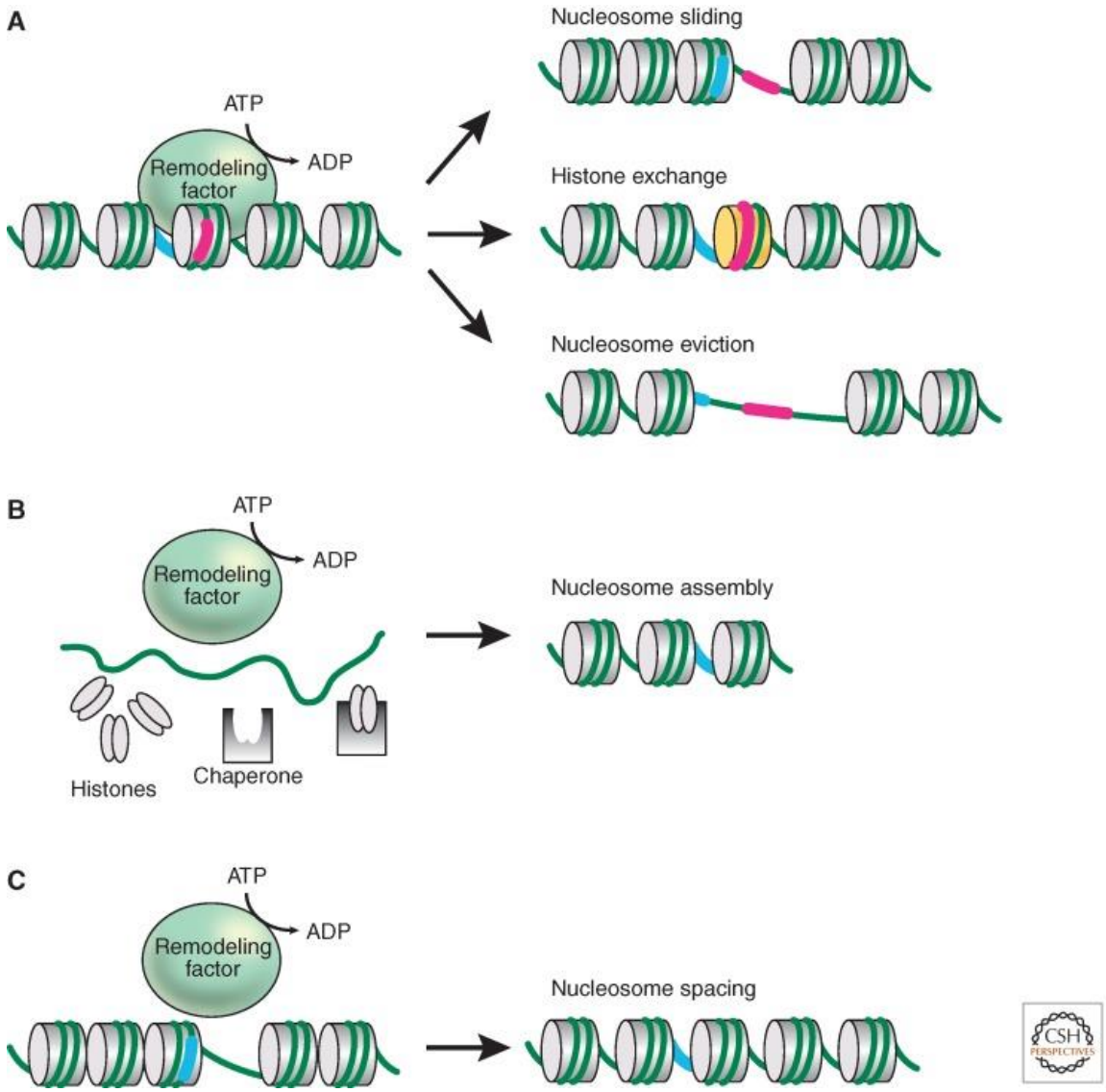

Figure 1.1: The Effect of ATP-Dependent Nucleosome Remodeling.
A) Remodeling can result in change of position or composition of nucleosomes.
B) ATP-dependent remodeler can cooperate with histone chaperones to assemble nucleosomes.
C) ATP-dependent remodeler can arrange the distances between nucleosomes during nucleosome spacing. (Becker et al., 2013).

1.3 Chromatin Remodeling and Development

ATP-dependent chromatin remodeling complexes are crucial for chromatin dynamic structure (assembly & disassembly) and regulation. Now, it is conceivable that these complexes have evolved as an adaptation to the major changes in chromatin regulation. During their evolution, they have expanded their gene families and utilized different combinatorial assemblies to form several hundred complexes with diverse biological functions beyond transcription in a different context (Wu et al., 2009).

1.3.1The SWI/SNF or BAF Complexes

BAF complexes change their subunit composition during ESCs differentiation from pluripotent to multipotent progenitor cell to a unipotent committed cell. The ATPase subunit of BAF complexes is encoded by two genes, *Brm* and *Brg1* (Brahma-related gene 1), and each complex contains only one of them. BAF complexes with different ATPase subunit exhibit diverse roles in different cell types (Lessard et al., 2007). In mammals, mRNA of oocytes is degraded after fertilization and zygote genes must be activated to initiate cell division. Brg1 is crucial for zygotic gene activation and, maternal KO of *Brg1* results in four-cell stage embryo that cannot undergo cleavage division (Scott et al., 2006). *Brg1* null embryos die before implantation stage where *Brg1* is required for ICM (inner cellular mass) and trophoblast cell survival through regulation of self-renewal and pluripotency genes (Scott et al., 2000). However, *Brm* null embryos develop normally with increased body weight that could be a result of high proliferation rates. *Brm* null MEFs fail to arrest the cell cycle in response to cell confluency or DNA

damage, suggesting that Brm is involved in the regulation of cell growth (Reyes et al., 1998).

1.3.2 ISWI Complexes

The core ATPase of ISWI complexes is SNF2H or SNF2L, which are found in different complexes with distinct functions. Both NURF and CERF (CECR2- Containing Remodeling Factor) complexes contain the SNF2L ATPase. Whereas the NoRC (Nucleolar Remodeling Complex) and the WICH (WSTF ISWI Chromatin Remodeling), ACF (ATP-Utilizing Chromatin Assembly and Remodeling Factor) and CHARC (Chromatin Remodeling by Chromatin Accessibility Complex) complexes contain the SNF2H ATPase. Embryos null for BPTF (Bromodomain PHD Finger Transcription Factor), the largest NURF complex subunit that is required for complex assembly, did not survive beyond the E8.5 days with the absence of DVE and AVE markers. Although BPTF null mESCs are viable, they fail to differentiate into endoderm or mesoderm (Landry et al., 2008). Knock-out of the remodeling subunit CECR2 in mice also resulted in neural tube defects in a strain-specific manner (Banting et al., 2005). Homozygous inactivation of the SNF2H resulted in embryo lethality after implantation since SNF2H is essential for the survival of ICM and trophoblast cells (Tomas et al., 2003).

1.3.3 CHD Complexes

The CHD complexes are classified into three subfamilies: subfamily I (CHD1 and CHD2), subfamily II (CHD3 and CHD4) and subfamily III (CHD5, CHD6, CHD7, CHD8 and CHD9). In mice, *Chd1* knock-out is lethal before implantation due to loss of

pluripotency. Depletion of CHD1 in bovine embryo reduced the number of blastocysts at early developing embryo, with no effect on the pluripotency marker *Nanog* or the trophectoderm marker *Cdx2*, however it reduced the deposition of the histone variant H3.3 (Zhang et al., 2016). The NURD complex consists of CHD3 or CHD4 which is the core ATPase subunit, MTA1, 2 or 3 (Metastasis Associated), MBD2 or 3 (Methyl-CpG Binding Domain), and RbBP4 or 7 (Retinoblastoma Associated Binding Protein). During the assembly of the NURD complex different combination of these mutually exclusive subunits are assembled in different cell types (Qin et al., 2001). MBD3, a NURD subunit that is required for complex assembly, knock-out resulted in post-implantation lethality due to a defective maturation of the ICM into epiblast, and dis-organization of the embryonic and extra-embryonic tissues (Kanji et al., 2007). CHD7 is the most studied member of this family since the human CHD7 mutations result in CHARGE syndrome, which is characterized by severe retardation in growth and development, heart defects, coloboma of the eye (abnormal structure of the eye) and ear abnormalities. Some of these features are recapitulated in mice with heterozygous loss of CHD7 (Hurd et al., 2007).

1.3.4 INO80 Family

The INO80 family include the INO80 and SWRI complexes that contain the INO80 ATPase subunit. The SWR1 and its homologue in mammals, Tip60/p400, is required to deposit the histone variant H2AZ *in vivo*. H2AZ incorporation is crucial for lineage commitment during mESCs differentiation (Creyghton et al., 2008). The INO80 complex is first identified in yeast where it regulates inositol responsive gene expression

(Ebbert et al., 1999). The INO80 subfamily complexes are known to directly regulate gene expression in yeast (Shen et al., 2000 and Korbor et al., 2004), mammals (Cai et al., 2007), flies (Klymenko et al., 2006) and plants (Deal et al., 2007 and Fritsch et al., 2004).

1.4 The INO80 Complex

The purified INO80 complex is approximately 1.2 MDa in mass and contains 15 subunits, which include the core catalytic ATPase INO80 subunit, RuvB-like (RuvBL1 or RuvBL2), actin (β-Actin) and actin-related proteins (ARP5, ARP8 and BAF53A) (Shen et al., 2000). The RvuBL1-2 subunits are homologous to the yeast Rvb1-2 subunits and functionally similar to the bacterial DNA helicase RuvB which is involved in DNA DSB (double-strand break) repair (Holliday et al., 1974). The actin and ARP (actin-related proteins) are required for the INO80 remodeling activity where they bind the HSA (helicase-SANT-associated domain) in the ATPase domain (Szerlong et al., 2008). Other subunits that are involved in the regulation of specific process, such as YY1 subunit, which recruits INO80 to target genes to activate their transcription (Cai et al., 2007). The INO80 complex is involved in many nuclear processes such as DNA replication, DNA repair, cell cycle checkpoint and DNA damage response. These diverse functions are due to the function of its distinct subunits. The ATPase subunit of INO80 is unique because of the presence of a spacer that splits the conserved ATPase domain and the deletion of this spacer prevents the assembly of the complex (Yunhe et al., 2007). The INO80 ATPase activity is stimulated *in vitro* in the presence of DNA or nucleosomes and this activity enhances nucleosomes sliding or eviction *in vivo* that

subsequently remodel chromatin structure to regulate access to DNA (Tsukuda et al., 2005). The remodeling activity of INO80 can be modulated by various mechanisms. One mechanism is the post-translation modification of the complex subunits. For example, upon DNA damage the Ies4p subunit of the yeast INO80 complex is phosphorylated by the kinases Tel1p and Mec1p (ATM and ATR in mammals), regulators of DNA damage response. However, this modification does not affect the complex localization to the DNA damage sites (Morrison et al., 2007). Small signaling molecules also modulate the activity of INO80. For instance, the inositol polyphosphate kinase Arg82p mediates the recruitment of INO80 to the promoters of phosphate responsive genes *Pho5* and *Pho84* in yeast (Shen et al., 2003).

1.4.1 INO80 in DNA Damage and Replication

To maintain genomic stability, cells have to efficiently repair DNA breaks. NHEJ (non-homologous end joining) and HR (homologous recombination) repair DNA DSBs (Hoeijmakers et al., 2001). In order for repair proteins to get access to their target DNA, chromatin around DNA breaks is remodeled. This remodeling could be accomplished by histone modifications, exchange of histone variants and/or ATP-dependent chromatin remodeling (Shen et al., 2003 and Loizou et al., 2006). Mouse INO80 is recruited to DSBs sites where it is involved in 5'-3' resection of DNA. It is also, required for the loading of the repair protein 53BP1 (p53-binding protein 1). 53BP1 is a DNA damage response factor that mediates the repair of DSBs (FitzGerald et al., 2009 and Gospodinov et al., 2011). In addition, mouse INO80 is required for the removal of H2AZ

from chromatin to facilitate HR of DSBs (Alatwi et al., 2015). The incorporation of H2AZ at DSBs restricts strand resection and its depletion reduces the recruitment of Ku70/Ku80 complexes to DSBs sites to promote DNA repair (Xu et al., 2012).

In mammals, DNA damage induces the phosphorylation of the C-terminal of H2AX by ATM into γH2AX, which is crucial component of the DNA damage response. Defects in H2AX phosphorylation alter the DNA damage checkpoint and drive genomic instability. γH2AX serves as docking sites for DNA repair proteins, such as INO80 (Nakamura et al., 2004). The mouse INO80 subunit BAF53A (Brg1-Associated Factor 53a) is associated with γH2AX and upon deletion; it reduces ARP recruitment of INO80 to DNA damage sites (Downs et al., 2004 and Morrison et al., 2004). In addition, the association of γH2AX and INO80 complex at DSB is required for nucleosome eviction around the DSB, which facilitates the binding and retention of repair proteins (Wu et al., 2007 and Morrison et al., 2007).

The yeast INO80 subunits Nh10p (non-histone protein 10), Arp4p (actin related protein) and Ise3p (Ino80 subunit) have unique roles in association with γH2AX to facilitate DNA repair. Mutations in the yeast Arp subunit of INO80 complex results in defective DSB repair through homologous recombination or non-homologous end joining pathways, which further support its importance in these pathways (Kawashima et al., 2007). In response to DNA damage, checkpoint pathways delay the cell cycle until DNA is repaired.

In yeast, Mec1p is a DNA damage checkpoint kinase that activates downstream

kinases to arrest the cell cycle, the INO80 subunit Ise4p is one of the Mec1p targets. Phosphorylation of Ise4p activates the S-phase checkpoint and delays replication origin firing until DNA repair is complete. Once complete then the S-phase checkpoint factor Tof1p promotes replication fork recovery to resume the cell cycle (Kattou et al., 2003 and Tourrie et al., 2005). Similarly, when the replication fork collapses due to DNA lesions or due to low levels of nucleotides, Ise4p subunit is phosphorylated to activate the S-phase checkpoint to delay the cell cycle progression. Recent studies in yeast showed that INO80 is enriched at replication origin, and higher levels of enrichment are found at stalled forks, suggesting its role in the recovery of stalled forks during DNA replication (Shimada et al., 2008, Papamichos-Chronakis et al., 2008 and Vincent et al., 2008).

1.4.2 INO80 and Telomeres, Centromeres and Chromosomes

Telomeres are repetitive DNA sequences at the end of the chromosomes, which decrease in length at each cycle of replication. Telomeres prevent the recognition of chromosome ends as a DSB by DNA repair machinery (d'Adda et al., 2004). The mouse INO80 is required for proper telomere replication where it prevents the formation of fragile telomeres. In addition, mouse INO80 prevents aberrant recombination between telomeres during their replication to prevent the activation of DNA damage response (Min et al., 2013).

INO80 is required to regulate telomere structure and function. It has been reported that deletion of Ies3p, Arp8p and Nhp10p subunits of yeast INO80 increased

telomere length indicating their roles in the regulation of telomere structure. In addition, the Ies3p subunit deletion induced telomere-telomere fusion events and reduced the cells' growth rate (Yu et al., 2007). During cell division, proper segregation of chromosomes is crucial to ensure faithful transmission of genetic material. INO80 has a role in chromosome segregation in yeast. The Arp4p and ATPase subunits of Ino80p bind directly to centromeres, and mutated Arp4p subunit results in defective kinetochore complex formation, and arrest of cell cycle. In addition, deletion of the Arp8 subunit increased the rate of sister chromatids separation (Ogiwara et al., 2007). Although the exact mechanism of INO80 in the regulation of chromosome segregation is unknown, it could be due to its ability to incorporate H2A histone variants into nucleosomes resulting in specialized structures with defined roles in centromeres, telomeres, and chromosomes.

1.5 Embryonic Stem Cells

Embryonic stem cells are pluripotent cells derived from the ICM before implantation, and after implantation they differentiate into the three germ layers of endoderm, mesoderm, and ectoderm. The expression of the core pluripotency genes, *Oct4* (encoded by *POU5F1*), *Sox2* (high mobility group- box transcription factor), *Nanog* (a homeobox transcription factor) and *Esrrb* are required for the maintenance of ESC pluripotency (Nichols et al., 1998, Avillion et al., 2003, Mitsui et al., 2003, Chambers et al., 2003 and Martello et al., 2012). The use of LIF (leukemia inhibitory factor) or BMP (bone morphogenetic protein) can keep ESCs in a naïve state (metastable state) where

they can self-renew. However, these growth conditions result in a heterogeneous population of cells with mosaic expression of pluripotency factors (Ying et al., 2003). Mechanistically, LIF binds the gp130 on the cell surface, activates STAT3 which then homodimerizes, and translocates to the nucleus to activate the transcription of core pluripotency genes (Graziano et al., 2013). BMP mediates its signaling through phosphorylation of SMAD1, 5, 8 which in turn activates the transcription of Id (inhibitors of differentiation) to block differentiation and keep cells pluripotent (Boyer et al., 2005). Differentiation mESC results in the secretion of FGF4, which binds the FGF receptor on ESC, acting as an autocrine, to activate the MAPK pathway driving differentiation (Kunth et al., 2007 and Stavridis et al., 2007). Consequently, the key to maintaining a homogenous population of pluripotent cells (the ground state) is to override the FGF4 differentiation signal and maintain the expression of core pluripotency genes at the same time, which is achieved by the use of 2i. 2i blocks the ERK (extracellular regulated kinase) to repress differentiation and Gsk3 (glycogen synthase kinase-3) pathways to activate pluripotency genes (Ying et al., 2008). The ground state pluripotency mimics the pluripotency state of ICM cells. Once LIF or 2i is removed from the media the ESCs is reprogrammed to a primed state where the cells are similar to the late epiblast after implantation (Nicholas and Smith, 2009).

The chromatin organization in mESC has a key role in the switch between pluripotency and differentiation states. Pluripotent ESCs have loosely associated chromatin architectural proteins such as linker histones and HP1 (heterochromatin

protein 1), which results in hyperdynamic chromatin. In addition, staining of the active histone marks H3K4me3/ H4K16ac and *in situ* hybridization of satellite DNA revealed less condensed constitutive heterochromatin in pluripotent ESCs (Park et al., 2004 and Meshorer et al., 2006). In addition, genome-wide mapping of epigenetic modifications of mouse ESCs indicated hypomethylated DNA in those cells (Meissner et al., 2008). Although maintaining pluripotency requires an open chromatin state to transcribe pluripotency genes, it also requires repression of differentiation genes to keep cells pluripotent. The key developmental genes in mESCs are mostly bivalent, which means that they have the active histone marker H3K4me3 and the repressive mark H3K27me3 at opposing H3 tails on the same nucleosome. The bivalency in these genes keeps them in a poised state. Once the cells differentiate into a specific cell lineage, bivalent genes become monovalent with either activating or repressive marks (Bernstein et al., 2006).

During differentiation, mESCs acquire more condensed, compact and less dynamic chromatin structure. Genome-wide analysis of the repressive histone modification H3K9me2 identified enrichment of these marks at the facultative heterochromatin (gene poor), which constitute 31% of genome in differentiated cells compared to 4% in pluripotent ESCs (Wen et al., 2009). In addition, the repressive histone mark, H3K27me3, expands into large domain during ESCs differentiation. Collectively, ESCs have to repress pluripotency and lineage inappropriate genes and activate lineage-specific genes with the help of chromatin modifiers to modulate the chromatin architecture according to their needs. Consistently, ESCs express high levels

of chromatin remodeling complexes such as BRG1, SNF2H, SSRP1 and SNF5, and their disruption resulted in early embryonic lethality suggesting their essential role in ESCs gene regulation (Bultman et al., 2000, Klochendler et al., 2000, Cao et al., 2003 and Stopka et al., 2003). INO80 is required for ESCs self-renewal (Chia et al., 2010; Hu et al., 2009), possibly due to its direct role in the regulation of the core pluripotency genes to maintain the ESC pluripotency state. In addition, INO80 occupies the promoters of pluripotency genes to maintain open chromatin structure and nucleosome depleted regions which facilitates the recruitment of RNA Pol II to initiate transcription (Li et al., 2014)

1.6 Mouse Early Development

Mammalian development is a very complex process, which starts with a single fertilized egg and gives rise to a whole embryo. Upon fertilization, the oocyte mRNA is degraded and transcription is initiated from the zygote genome, which is required for genetic reprogramming during development, a process known as ZGA (zygote genome activation) (Nothias et al., 1995). It has been shown that there is a transient phase of ZGA at 2-4 cell stage, which drives the transcription of reprograming genes and another phase of maternal genome activation at the 8 cell stage where a peak in transcription of adhesion molecules that is required for blastocyst polarity (Hamatani et al., 2004). After fertilization, the developmental stages of mouse embryo are determined by the embryo age. Embryos are staged by half-day intervals after the detection of a copulation plug, and is referred to as E (embryonic day) (Kojima et al., 2014). The fertilized egg undergoes three rounds of cell division to reach the eight-cell stage in which the embryo

is composed of four blastomeres. At the 8-cell stage, the nucleo-cytoplasmic ratio is increased, which induces these blastomeres to compact into a morula. During compaction, cells maximize their contact using tight junctions to form a compact ball of cells. Compacted cells form a gap junction to allow the passage of small molecules and ions for their nutrition (Fleming et al., 1992, Ducibella et al., 1975 and ziomek et al., 1980). Compaction establishes apical-basal polarity in the morula by asymmetrical loading the cellular polarity proteins such as PKC (protein kinase C), PAR3 and PAR6 (Pauken and Capco, 2000; Plusa et al., 2005) to the apical cells of the morula. However proteins such as Par1 (protease activator receptor 1) and E-cadherin (Hyafil et al., 1980; Shirayoshi et al., 2005) localize to the basolateral side of the morula by E2.5. Compacted morula undergoes two successive rounds of asymmetric cell division to form 16-32 blastocyst embryo.

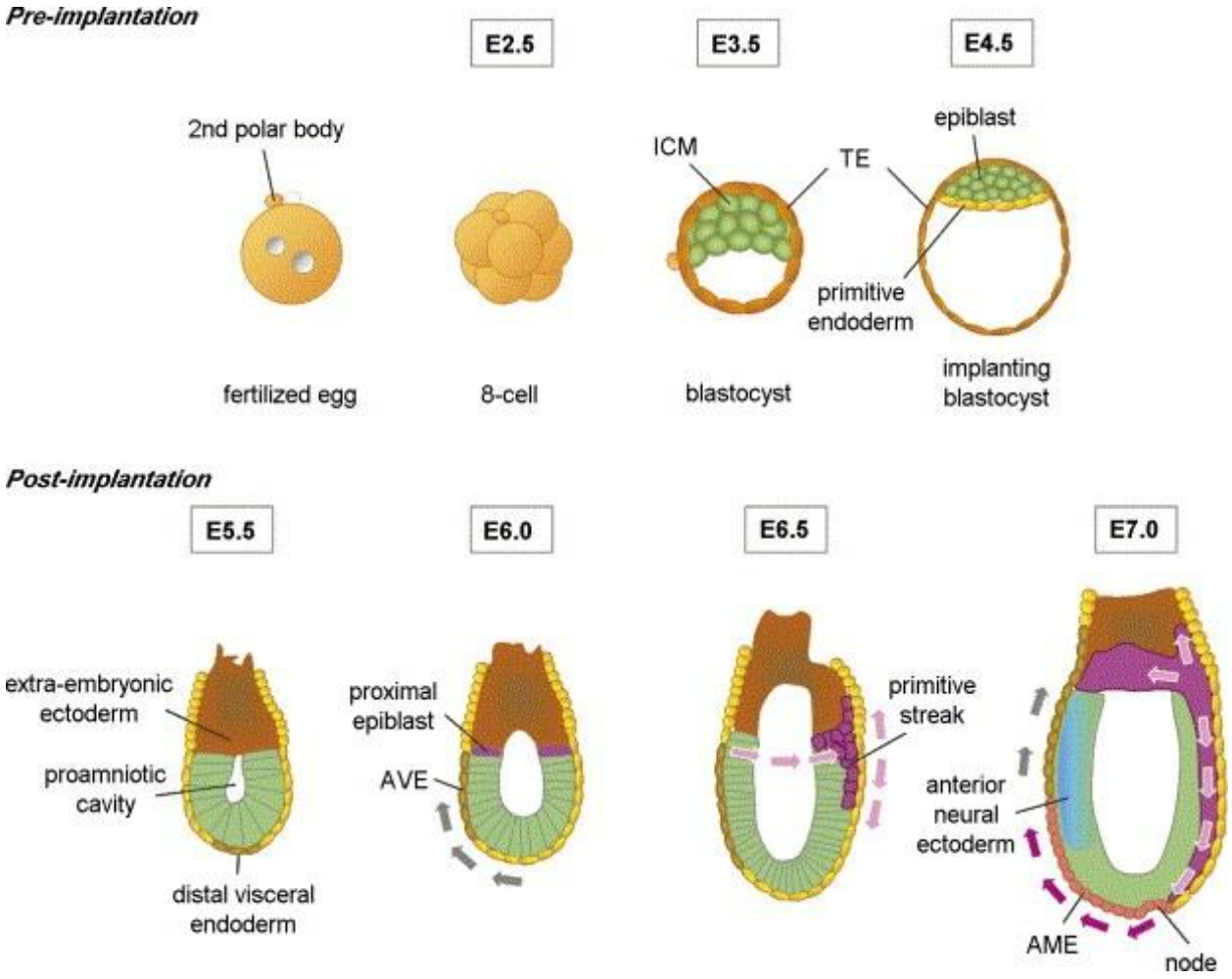

Figure 1.2: Cartoon to Illustrate Stages in the Early Mouse Development.
The morphological changes and the cell specification events that occur from fertilization to embryonic day E7.0. The morula stage at E2.5, the blastocyst stage at E3.5, and the gastrula stage at E6.5. The pre-gastrula stage starts at E5.5 where a subset of PrE cells differentiate at the distal part of the embryo to form DVE. From E5.5 to E6.5 these cells migrate to the anterior part of the embryo to form AVE. During this transition the AVE secretes inhibitors to the Wnt and TGF family of ligands, directing gastrulation at the posterior of the embryo. http://www.devbio.biology.gatech.edu/?page_id=8796.

A blastocyst is formed at E3.5 by cavitation; formation of a single cavity; and allocation of three cell lineages which include TrE (trophectoderm), PrE (primitive endoderm) and EPI (epiblast) as illustrated in Figure 1.2. TrE is the outer layer of cells that contact the LE (luminal epithelium) of the uterus to establish the site of implantation. TrE will form the chorion (abembryonic tissue), which is required for embryo nutrition and immunity at implantation site (Pedersen et al., 1987). The ICM is composed of pluripotent cells that will form the embryo proper (embryonic tissue). The segregation between these three different cell lineages (TrE, PrE and EPI) is defined by the expression of specific genes for each lineage. *Oct4*, *Sox2*, *Nanog* and *Nodal* genes are required for the formation and maintenance of the ICM, suppression of TrE formation and specification (Nichols et al., 1998, Avillion et al., 2003, Mitsui et al., 2003, Chambers et al., 2003 and Camus et al., 2006). TrE specification was thought to be due to the absence of *Oct4* expression, however Strumpf et al. showed that the *Cdx2* (a caudal type-homeodomain protein) is essential for TrE specification and its absence extends the expression domain of *Oct4* and *Nanog* into the outer layer (Strumpf et al., 2005). In addition, the T-box transcription factor, *Eomes*, is required for TrE cells proliferation (Russ et al., 2000). Similarly, PrE is specified by the expression of *Gata6*, which suppress the expression of *Nanog* (Mitsui et al., 2003 and Chambers et al., 2003).

In addition, epigenetic changes like histone modifications are key players in the molecular definition of these cell fates. For example, the levels of active histone markers, H4K8ac and H3K4me3, at the promoter region of *Oct3/4* are higher in the

ICM cells than in the TrE cells (VerMilyea et al., 2009). The behavior of these factors inside the cell also affect those cells fate. Monitoring the kinetics of *Oct3/4* nuclear export, import and retentions revealed that *Oct3/4* accessibility to its targets differ between four- and eight- cell stage (Plachta et al., 2011).

The embryonic-abembryonic axis specification is similar to the P-D (proximal-distal) axis of the embryo at the egg cylinder stage, which will determine the future dorsal-ventral polarity (Rossant and Tam, 2009). In addition, the inside-outside polarity of the blastocyst is also accompanied by differential asymmetric signaling of Hippo pathway in those parts of the blastocyst. Hippo signaling control cell contact-mediated inhibition of ICM proliferation. However, it is not active in the outer cell layer where the apical part of these cells is not in contact with other cells (Pan, 2007; Saucedo and Edgar, 2007). The peri-implantation blastocyst exhibits additional asymmetries, for example, the nuclear β-catenin is localized to a subset of blastomeres and *Nodal* is localized to another subset suggesting asymmetry at the level of canonical Wnt and Nodal signaling (Chazaud et al., 2006 and Granier et al., 2011).

In order for the blastocyst to implant, it has to be competent for implantation in the receptive uterus. Many factors affect blastocyst competency, for instance, cate-choloestrogens, endocannabinoid and anandamide are signaling molecules secreted in the uterus to activate the blastocyst (Paria et al., 1998 and Guo et al., 2005). The implantation process is divided into three stages; apposition, adhesion and penetration. Apposition, where TrE of the blastocyst closely oppose the LE of the uterus to prevent blastocyst dislodging (Daikoku et al., 2005). Once the blastocyst opposes the LE it

attaches by help of adhesion molecules such as integrin (Dey et al., 2004). After the blastocyst attaches, penetration occurs at the site of implantation to increase the vascular permeability by the action of prostaglandin (Lim et al., 1997). After implantation, the stromal cells of the uterus that envelop the blastocyst undergo decasualization to nourish the embryo and form the placenta, which is accompanied by increased angiogenesis (Matsumoto et al., 2002). Once the blastocyst is implanted, it develops into a cylindrical structure called the egg cylinder, which will undergo gastrulation (Patrick et al., 1997).

1.7 Gastrulation

Gastrulation is a blueprint for body plan determination and subsequent morphogenesis. Immediately after implantation (approximately at E5-6), the embryo mass is increased by about 40 fold mainly due to increased cell proliferation and reduced apoptosis rates. At this stage, an epithelization of ICM cells into a single cell layer surrounding the amniotic cavity forming a cup-shaped embryo (in the case of rodents), where the cup has two cell layers, the outer VE (visceral endoderm) and inner Epi (epiblast), forming an egg cylinder with two cell layers. The egg cylinder embryo has well defined extra-embryonic and embryonic regions that are polarized to P-D body axis. During gastrulation, a series of morphogenetic movements results in the formation of three germ layers: ectoderm, endoderm and mesoderm. The mouse gastrulation is accomplished by the differentiation, delamination, and migration of underlying embryonic ectoderm into the primitive streak to establish the A-P (anterior-posterior) axis of the embryo (Patrick et al., 1997).

As mentioned earlier PrE is the epithelial layer that surrounds the blastocoelic cavity. At E5.5, this layer forms the VE that surrounds the epiblast and parietal VE that surround the TrE. A subset of distal VE cells differentiates into DVE at E5.5 (Rossant and Tam, 2009; Takaoka and Hamada, 2012). DVE cells express both Nodal and Wnt antagonists, which are *Lefty1*, *Cer1* and *Dkk1* consequently (Yamamoto et al., 2004 and Kimura-modisha et al., 2005). Restriction of *Lefty1* expression to a subset of PrE cells could be regulated by three mechanisms: (1) *Lefty1* is regulated directly by Nodal through Nodal/FoxH1 responsive enhancer upstream of *Lefty1.* (2) Nuclear β-catenin is localized to Epi cells that face PrE suggesting that Wnt signaling activates *Nodal* which in turn regulate *Lefty1* expression (Chazaud and Rossant 2006). (3) Establishment of P-D axis is maintained by asymmetric expression of signaling molecules and asymmetric expression of *Nodal* restricts *Lefty1* expression to a subset of PrE cells (Granier et al., 2011).

From E4.5 to E5.5 the expression of *Lefty1* is auto-regulated by *Lefty1* itself (Christopher et al., 2001). At E5.5, DVE cells mature and express other DVE markers such as *Cer1* and *Hex1*. The restriction of DVE cells to the distal part of the embryo is maintained by inhibitory BMP signaling. *Bmp4* expression in the extraembryonic ectoderm generates a signaling gradient that allows DVE differentiation only at the distal part of the egg cylinder. This was further supported by the observation that ExE deletion resulted in DVE expansion (Roriguez et al., 2005 and Yamamoto et al., 2009). After the DVE matures, the VE cells get thicker and create a monolayer of tall-columnar cells (Takaoko et al., 2011), then DVE cells form a lamellopodia-filopodia like structure that

migrates to the anterior part of the embryo to establish the AVE and the A-P axis (Migeotte et al., 2010).

How the complicated process of animal embryonic development is regulated by epigenetics is just beginning to be unraveled. ATP-dependent chromatin remodeling complexes are essential for mammalian development where they regulate specific developmental pathways (Ho et al., 2010 and Chen et al., 2014). The chromatin remodeling complexes, NURD (Kaji et al., 2007), SWI/SNF (Bultman et al., 2000), and TIP60/p400 (Thomas et al., 2008) complexes are essential for pre-implantation development. While, other complexes including NURF (Landry et al., 2008) and CHD7 (Hurd et al., 2007) are involved in post-implantation development. Mammalian INO80 is also essential for development. Genome-wide siRNA screening show that *Ino80* is required for ESC self-renewal by promoting the expression of pluripotency genes such as *Oct4* and maintaining an open chromatin structure around pluripotency factors (Li et al., 2014). *In vivo*, *Ino80* KO mouse embryos implant but fail to develop to mid-gestation (Min et al., 2013), possibly due to abnormal gene expression because INO80 is well-known to regulate gene expression (Li et al., 2014). However, the exact mechanism by which INO80 regulates early mouse development is unknown. The purpose of this study is to characterize the role of the INO80 chromatin-remodeling factor in early mouse embryo, and identify the mechanisms by which it regulates development.

CHAPTER TWO

Methods

2.1 Generation of Conditional *Ino80* KO Mice.

This was done according to the standard protocol. The Animal Care and Use Committee of Virginia Commonwealth University approved all experiments and animal procedures under protocol AD10000372 and its modifications (Bouabe et al., 2013).

2.2 DNA Extraction & Genotyping

DNA was extracted from embryos for genotyping by digesting individual embryos overnight at 55˚C in 10 to 20 µl PBS **(**phosphate-buffered saline) (10 mM Na2HPO4, and 1.8 mM KH2PO4 [pH 7.4], 137 mM NaCl, 1.37 mM KCl), 0.1% tween 20 and 0.2 mg/ml PCR grade proteinase K (Roche). After digestion, proteinase K was heat inactivated at 100 ˚C for 15 min and 2 µl of digested embryo was used for PCR genotyping. Genomic DNA was extracted from tail biopsies or cells by overnight digestion in lysis buffer (50 mM Tris-Cl [pH 8.0], 100 mM EDTA, 100 mM NaCl and 1% SDS) containing proteinase K (0.5 mg/mL) at 53 °C. Following digestion, DNA was precipitated with isopropanol, washed with 70% ethanol and dissolved in water. The genotyping of *Ino80* was done using primers P1, P2, and P3 in a multiplex PCR reaction using recombinant Taq polymerase with Thermal Pol Buffer (NEB). PCR conditions were as follows: 94 °C for three minutes (min) for one cycle, 94 °C for 30 secs, 54 °C for 60 secs, 72 °C for 45 sec repeated for 40 cycles. Primer sequences are provided in Table 2.

Table 2.1: Primers Used for *Ino80* Genotyping

Ino80 Genotyping Primers	
P1	CTGGATGTGAAGGGAGAAGG
P2	CATCTCTCCAGCCAGCACACT
P3	TGCCACTCTACCTGCATCTG

2.3 Embryonic Cells Isolation and Maintenance

To generate *Ino80* KO ESCs, E2.5-day blastocysts were harvested in KSOM media until the blastocyst stage then induced to hatch in the presence of Tyrodes solution (Sigma T1788). Blastocysts were cultured on gelatinized plates for seven days in defined 2i + LIF media without serum (Millipore Cat# SF016-100). Individual outgrowths were removed by scratching from plate bottom with a fine glass pipette, dispersed into single cells with 0.25 % trypsin + EDTA, cultured in gelatinized 96 well plates in the presence of 15 % ESC grade FCS (Life Technologies) and 2i medium formulation (Life Technologies).

Primary MEFs were isolated from mouse pregnant females at E13-14. Mouse female was sacrificed by cervical dislocation and individual embryos were isolated from the uterine horns under aseptic conditions. Head and internal organs were removed and the embryo body was finely minced until it can be pipetted. Digested embryo was treated with 0.25% trypsin/EDTA in the presence of 100 K units of DNase I (USB) for 15 min at 37°C to obtain single cell suspension. Trypsin was inactivated by MEF culture medium (DMEM containing 10% FCS, 2 mM glutamine, 1 mM nonessential amino acids, penicillin, and streptomycin). Cells were then centrifuged, suspended in MEF

culture medium and plated on gelatinized plates. MEFs were treated with 10 ng/ml doxycycline in MEF culture

medium to knock-out *Ino80.* After two days of treatment, the medium was replaced with fresh medium and MEFs were cultured until subconfluency. *Ino80* deletion was verified by PCR.

2.4 Detection of MEFs Senescence by Lac-Z Staining

To measure β-galactosidase activity, MEFs were fixed in 4% buffered formaldehyde for five min, washed and stained with staining solution (35 mM potassium ferrocyanide, 35 mM potassium ferricyanide, 0.02% NP-40 and 2 mM MgCl2 [pH 6]) overnight with gentle rocking. Stained cells were washed and positively stained cells were counted using a microscope.

2.5 Alkaline Phosphatase Staining

AP activity was analyzed using the BM purple AP substrate (Roche Cat# 11442074001), according to the manufacturer's guidelines. Cell colonies were fixed in 0.2% glutaraldehyde, 0.02% NP-40, and 0.01% sodium DOC for five min followed by washing in 100 mM Tris-HCl [pH 9.5], 100 mM NaCl and 10 mM $MgCl_2$. Colonies were stained, washed, air dried and examined under light microscope.

2.6 Cell Doubling Time

To determine the doubling time, mESCs were plated in triplicates in 12 well plates. Cells were counted using a hemocytometer at time points 24, 48, 72, and 96 hours. I took the average cell count from each of the big four squares. and multiply by 10,000 then multiply by 2 to correct for trypan blue addition Population doubling times

were calculated using http://www.doubling-time.com.These measurements were repeated for three independent control and *Ino80* KO mESCs.

2.7 Teratoma and Embryoid Body Formation

Teratomas was generated by injection of 1×10^6 ESC into the flank of NOD/SCID mice (Jackson Labs Cat# 001303). Three weeks later teratomas were collected, embedded in OCT medium and frozen in liquid nitrogen. Teratomas were sectioned using a cryostat and sections were fixed in 10% neutral buffered formalin, stained with hematoxylin and eosin, and analyzed by light microscopy.

To create embryoid bodies 10×10^6 ESC were suspended in 13 × 100 mm polypropylene culture tubes. The cells were supplemented with 3 ml of complete ESC medium without addition of LIF or 2i to promote cells differentiation. Embryoid bodies were harvested at the indicated time points. For histological analysis, embryoid bodies were collected at day 9 and fixed in 10% neutral buffered formalin overnight, then embedded in OCT medium and frozen in liquid nitrogen. Sections were obtained by cryostat sectioning, stained with hematoxylin and eosin, and analyzed by light microscopy.

2.8 Whole Mount *in Situ* Hybridization

Embryos were collected at the indicated time points in PBS, fixed in 4% paraformaldehyde for 5 min. Fixed embryos were then dehydrated through a series of methanol (25%, 50%, 75%, and twice in 100%) and kept in 100% in methanol at −20°C until use. To prepare embryos for in situ hybridization they were rehydrated through 75%, 50%, and 25% methanol series then fixed again in 4% and 0.2%

glutaraldehyde in PBS-T (Phosphate-buffered saline 0.1% tween 20). To start hybridization, embryos were washed three times in PBS-T and mixed with pre-hybridization buffer (25ml formamide, 12.5 ml 20X SSC, 5ml 10% SDS and 7.3ml DEPC treated water) at 70°C for 1 hr. Hybridization buffer was then replaced with one ml of the same buffer mixed with ~ 1µg of DIG (Digoxigenin)-labeled probe and then incubated overnight at 70°C. Embryos were washed twice for 30 min using solution I (50% formamide, 4XSSC and 1% SDS) followed by 10 min wash in 1:1 solution I: solution II (500 mM NaCl, 10 mM Tris [pH 7.5] and 0.1% tween 20). Embryos were then washed three times 5 min each in solution ll at room temperature and incubated with solution II mixed with 100 µg/ml RNase at 37°C for 1 hr followed by one wash in solution ll and another wash in solution lll (50% formamide and 2XSSC). Embryos were then washed twice for 30 min each with solution lll at room temperature. Then washed three times for 5 min each with MABTL (100 mM maleic acid [pH 7.5], 150 mM NaCl, and 0.1 % tween 20 and 2 mM levamisole). To prevent non-specific staining embryos were incubated with 10% heat-inactivated sheep serum, 2% BMBR (Boehringer Mannheim Blocking Reagent) in MABT for 3 hrs. During the incubation period, anti-digoxygenin-AP (Roche) was mixed with 3 mg embryo powder, 2% BMBR and 10 µl of sheep serum in 1 ml of MABTL and rotated at 4°C for 3 hrs. Embryos were then incubated with the diluted antibody at 4°C overnight. Embryos were then washed for 5-8 times 1 hr each with MABTL and the color was developed with BM purple (Roche) after three washes with NTMTL buffer (100 mM Tris, [pH 9.5], 100 mM NaCl, 50 mM MgCl2, 0.1 %

tween 20 and 2 mM levamisole). For double ISH DIG-*Bmp4* and FITC-*Otx2,* labeled probes were detected by AP-conjugated anti-DIG Fab, which was detected by BM purple (Roche) and anti-FITC Fab fragment, which is detected by INT/BCIP (Roche), subsequently.

2.9 TUNEL Assay

Programmed cell death is characterized by DNA fragmentation, which can be quantified by the ability of the terminal deoxynucleotidyl transferase enzyme to incorporate labeled nucleotides to the 3' hydroxyl of fragmented DNA. To quantify apoptosis, we applied whole-mount tunnel staining procedure. Briefly, E6.5 embryos were fixed for 2 hrs at 4°C, washed with PBS-T and kept in 100% a methanol until use. Fixed embryos were then treated with 5:1 methanol: 30% hydrogen peroxide for three hours to reduce endogenous peroxidase activity. Then, they were washed in a methanol and treated with 20 µg/µl proteinase K for 3 min to digest proteins and facilitate the enzymatic addition of labeled nucleotides. After proteinase K treatment, embryos were fixed with 0.2% glutaraldehyde in 4% paraformaldehyde for 20 min at room temperature, washed three times with PBS-T and treated with sodium borohydride for 20 min to remove reactive aldehydes. Embryos were then washed with TdT buffer (30 mM Tris-HCl [pH 6.6], 200 mM potassium cacodylate, and 2.5 mM CoCl2). TdT buffer was replaced with labeling solution that contain 9:1: labeling solution (nucleotide mixture): enzyme (terminal deoxynucleotidyl transferase) and incubated at 37°C for 2 hrs. Then embryos were rinsed several times with PBST and incubated at 70°C with the labeling solution for another 20 min. To block non-specific binding, embryos were

treated with 10% heat- inactivated sheep serum at room temperature for 1 hr and then incubated with the converter-POD (anti-fluorescein antibody, Fab fragment from sheep, conjugated with horseradish peroxidase) at 37°C for 30 min followed by washing and color development using the DAB substrate. Samples were analyzed using fluorescent microscope and percent of apoptotic cells were normalized to the total number of DAPI positive nuclei in a 50-µm microscopic field.

2.10 Chromatin Immunoprecipitation (ChIP)

mESCs cells were induced to differentiate by culture in complete ESCs medium that lack both LIF and 2i. Cells were collected at the indicated time points and fixed in 1% PFA in PBS for 15 min. To remove the fixative, cells were washed three times in PBS and scrapped from the tissue culture dish by a cell scraper. Cells were suspended in lysis buffer and protease inhibitor and the chromatin was fragmented by sonication, using Bioruptor sonicator set at 15% amplitude for three sessions of 45 pulses (0.5 second on/0.5 second off), incubating the sample on ice for two min between sessions to fragment DNA to ~ 500bp fragments. After sonication, the cell suspension was centrifuged at 13,000 rpm for 10-20 min at 4°C. The supernatant was diluted at 5:1 by ChIP dilution buffer (16.7 mM Tris-HCl [pH 8.1], 167 mM NaCl, 1.1% triton X-100, 1.2 mM EDTA and 1 X protease inhibitor cocktail (Roche) then mixed overnight at 4°C with protein G Dynal beads (Life Technologies) pre-bound for 1 hr at 4°C with antibody (10 µl of beads with 5 µg antibody). For each pull-down, 20% input was saved for determination of pull-down efficiency using qPCR. The following antibodies were used for ChIP: Ino80 (VCU23, custom rabbit polyclonal), SP1 (Santa Cruz Biotech # sc-59),

pan-histone H3 (Abcam # ab1791), and H3K4me3 (Abcam # ab1012) and anti-BPTF (Millipore ABE1966). After overnight incubation, bound chromatin was subjected to a series of 5 washes (5 min each) on ice using the following buffers; low-salt buffer (20 mM Tris [pH 8.0], 150 mM NaCl, 1% triton X-100, and 2 mM EDTA), high-salt buffer (20 mM Tris [pH 8.0], 500 mM NaCl, 1% triton X-100, and 2 mM EDTA), LiCl buffer (10 mM Tris [pH 8.0], 0.25 M LiCl, 1% NP-40, 1% deoxycholic acid, and 1 mM EDTA) and two times with TE buffer (10 mM Tris [pH 8.0], 1 mM EDTA). The DNA was eluted from the beads by two washes with 250 µl elution buffer (0.1 M $NaHCO_3$, and 1% SDS) at room temperature. Both eluted DNA and the 20% input DNA were reverse cross-linked with 200 mM NaCl and incubated overnight at 65°C. Next, samples were treated with proteinase K for 4 hrs at 45°C. The DNA was extracted using phenol-chloroform extraction, precipitated with ethanol and dissolved in water treated with RNase A and then quantified by qRT-PCR. The sequence for primers used for ChIP-PCR are provided in Table 2.2

Table 2.2: Primers Used for *Bmp4* ChIP Analysis

Bmp4 ChIP Primers	
Amplicon1	For GTGCCCAAAGCATTTTGAAT
	Rev CACCCTACTTCCACCTCCAA
Amplicon2	For CCAGTGCTCTCTCACCTTCC
	Rev CAGGGGAGGTCACGAAGATA
Amplicon3	For TACAAACGAGGATGGGGAAG
	Rev CCAAGAACCGGAAATTGCTA
Amplicon4	For CCCAATGACCTCTCTTCCAA
	Rev TTGGCCTATTCCTCCTTCCT
Amplicon5	For ATGGCATGGTTGGTTGAGTT
	Rev ACGTAGTCCCAAGCATCACC
Amplicon6	For ATGACCGGGTTGAAAGATTG
	Rev GAAAGCCACACCTCCTTCTG

2.11 Formaldehyde-Assisted Isolation of Regulatory Elements (FAIRE)

Positive regulatory factors enhance nucleosomes eviction at their target DNA sequences. The idea of the FAIRE technique is to identify nucleosome-depleted DNA sequences (open chromatin). FAIRE is a simple technique to identify nucleosomes depleted DNA sequences and it is superior to DNase I hypersensitivity assay. The idea behind FAIRE technology is the crosslinking of proteins to DNA, fragmentation of the chromatin and enrichment of nucleosome depleted DNA sequences by phenol-chloroform extraction. To identify the chromatin status at *Bmp4* promoter in both WT and *Ino80* KO cells we applied the FAIRE technique. Briefly, cells were fixed in 1% paraformaldehyde and resuspended in FAIRE lysis buffer (50 mM Tris [pH 8.0], 1% SDS, 10 mM EDTA). Protein degradation was inhibited by addition of 1X protease inhibitor cocktail (Roche) to the lysis buffer. Samples were sonicated as indicated above and sonicated samples were centrifuged at 15,000 rpm at 4°C to remove cell debris. An equal volume of supernatant and phenol-chloroform were mixed, vortexed and centrifuged at 15,000 rpm to isolate FAIRE DNA in the aqueous phase. FAIRE DNA was ethanol precipitated in the presence of 0.3M sodium acetate and dissolved in TE buffer (10 mM Tris-HCl [pH 7.4], 0.5 mM EDTA). Dissolved DNA was treated with RNase at 100 µg/ml for 30 min at 37°C followed by proteinase K treatment at 55°C for 1 hr. After removal of residual RNA and proteins, FAIRE DNA was washed, mixed with DNA binding buffer at 2:1 ratio then purified using Zymo-I spin columns (Zymo research). The input DNA was prepared from the soluble chromatin after sonication where 50 µl of soluble chromatin was treated with RNase and proteinase K, as

described above, and cross-linked between DNA molecules was reversed by keeping samples at 65°C overnight. DNA was extracted by phenol-chloroform extraction followed by ethanol precipitation. Enrichment of individual loci was quantified by qRT-PCR. Primers were designed to amplify a control region that has similar enrichment in both WT and *Ino80* KO samples and a reference region that has different enrichment. Relative enrichment was quantified and calculated using the ΔΔCT method (Livak et al., 2001). Primer sequences are provided in Table 2.3.

Table 2.3: Primers Used for FAIRE Analysis

Bmp4 promoter FAIRE Primers	
Amplicon1	For CTTCCCTCCTCCCTTAATCG
	Rev1 GTGGCTGGATGGGAGGAT
Amplicon 2	For1 GTTGAAACAGGCTGTGAGCA
	Rev1 GGGGGAAAGTCACCTCCTAA
Amplicon 3	For1 AATTTCACACCCTGCCTCTG
	Rev1 TTCCCCATCCTCGTTTGTAA
Amplicon 4	For1 GATTGATTCCCTGCGTCACT
	Rev1 TCAGTCATTTTCGGTCTGG
Amplicon 5	For1 CAGGTAGAGTGGTGCATGCTT
	Rev1 GATCATCTGGCTGCCTCTGT
Control Primers	For1 ATACAACCAAACAGACACACAACC
	Rev2 CTACTGGCTGCCATGGCTTA

2.12 qRT- PCR

RNA was extracted from ESCs and embryoid bodies using Tri-Reagent (Sigma) according to manufacturer's instructions. 5 µg of isolated RNA was converted into cDNA using the reverse transcriptase Superscript II according to manufactures procedures (Life Technologies). cDNA was diluted and amplified using SsoAdvanced universal SYBR green supermix (Biorad) in 20 µl reaction that contains 300 nM of both forward

and reverse primers. Reactions were heated for 15 min at 95 °C, then cycled for 50 cycles at 95 °C, 30 secs, 60 °C 30 secs and 72°C 30 sec. Relative expression of target templates was normalized to GAPDH using the ΔΔCT method (Livak et al., 2001). Primers sequences are provided in Table 2.4.

Table 2.4: Primers Used for Quantification of Pluripotency and Differentiation Markers in mESCs

qRT-PCR Primers	
INO80	For CGAGGGAGCGAGCTAGGAG
	Rev TCAACTTGGCTTTAAGCTTCTTG
Nanog	For AGGGTCTGCTACTGAGATGCTCTG
	Rev CAACCACTGGTTTTTCTGCCACCG
Oct4	For TGAGGCTACAGGACACCTTTC
	Rev GTGCCAAAGTGGGGACCT
Klf4	For GCGAGTCTGACATGGCTGT
	Rev GAGTTCCTCACGCCAACG
Essrb	For CGATTCATGAAATGCCTCAA
	Rev CCTCCTCGAACTCGGTCA
Sox2	For TGCTGCCTCTTTAAGACTAGGG
	Rev TCGGGCTCCAAACTTCTCT
c-myc	For CACCAGCAGCGACTCTGAA
	Rev CCCGACTCCGACCTCTTG
n-myc	For AACACAGCGCTTGAGGATCA
	Rev GAGCGACTCAGATGATGAGGA
Cdx2	For GGAAGCCAAGTGAAAACCAG
	Rev CTTGGCTCTGCGGTTCTG
Bmp4	For CTGAGTATCTGGTCTCCGTCC
	Rev AAGGCTCAGAGAAGCTGCGGC
Fgf5	For CAGATCTACCCGGATGGCAAAG
	Rev GCGGACGCATAGGTATTATAGCTG
Nestin	For ACCTCAAGATGTCCCTTAGTCTGG
	Rev GGTGCTGGTCCTCTGGTATCC
Nodal	For GGGCCCACTCACCATTGACA
	Rev TCCTGAGGCCGGTTGGAGTA
T	For TGAGGAGATTACAGCCCTTAAA
	Rev GGTTCCTTAGAGCTGGGTAC
Wnt3	For GGGGCGTATTCAAGTAGCTG
	Rev GTAGGGACCTCCCATTGGAT
Gsc	For CGGTTCTGTACTGGTGTCTCCT

	Rev GAGCTGCTCATCGGTCAAGAT
Fgf8	For TCATTGTGGAGACCGATACTT
	Rev CAGCACGATCTCTGTGAATAC
Foxa2	For GCCAGCGAGTTAAAGTATGCG
	Rev TGTTGCTCACGGAAGAGTAG
Sox17	For CCATTTAGTGAAGAAACTGAAATATGGC
	Rev ATTCTCTTGATAGATACTTTGGGAGGAGT
Gata4	For AGGTAGTGTCCCGTCCCATCT
	Rev CCTGGAAGACACCCCAATCTC
Gata6	For AGTCAAAAGCTTGCTCCGGTA
	Rev ACCTATGTAGAGGCCGTCTTGA
Hex1	For GAGGTTCTCCAACGACCAGA
	Rev GTCCAACGCATCCTTTTTGT
Cer1	For CACGAAGTACACTGGGAGAC
	Rev GCCAAAGCAAAGGTTGTTCT
Hnf4a	For CTTCCTTCTTCATGCCAG
	Rev ACACGTCCCCATCTGAAG

2.13 Statistics

The standard deviation was used to calculate error bars throughout the study. *P* values were calculated using two tailed T-tests. The number of replicates are designated in the figure legends.

CHAPTER THREE

Results

3.1 Ino80 KO Embryos Fail to Develop After Implantation

Ino80 deletion is known to be embryonically lethal (Min et al., 2013 and Lee et al., 2014), however, its exact role in early mouse development is not identified. To investigate the role of *Ino80* in mouse early embryo, we used the Cre-loxP system in which the essential exons of *Ino80* were flanked by two loxP sites that were excised after crossing with mice that express Cre recombinase. Successful *Ino80* KO was verified in both *Ino80* KO MEFs using Western blot analysis (Figure 3.1 A). At the cellular level, *Ino80* KO in MEFs reduces cell proliferation and induces senescence (Min et al., 2014). To verify this observation using our model of *Ino80* KO in MEFs, we assessed the proliferation rate of *Ino80* floxed MEFs for about 12 days after their exposure to doxycycline in culture (Figure 3.1 B). As shown previously, *Ino80* KO MEFs ceased proliferation and started senescence as evidenced by their positive staining for β-Gal activity (Figure 3.1 C). These data suggested that our *Ino80* KO allele is a null allele.

To characterize the phenotypes of *Ino80* KO in mouse embryo we inter-crossed heterozygous mice to generate homozygous *Ino80* KO mice. However, we did not get

any homozygous KO mice, consistent with previous studies that showed that *Ino80* is essential for mouse embryo viability (Min et al., 2013 and Lee et al., 2014). To identify at which stage *Ino80* is essential for embryo viability, we collected mouse embryos at different stages of early development E5.5 (post-implantation), E6.5 (gastrulation) and E13.5 (mid-gestation). Genotyping of these litters revealed that *Ino80* KO embryos fail to survive after implantation. Phenotype analysis of E5.5, E6.5 and E7.5 embryos indicated that at E5.5 both WT and KO embryos had similar size and morphology, however, once they implanted *Ino80* KO embryos started to decrease in size and lose their structural integrity by E7.5 (Figure 3.1 D, and data not shown). These observations suggesting that *Ino80* KO embryos fail to develop after implantation.

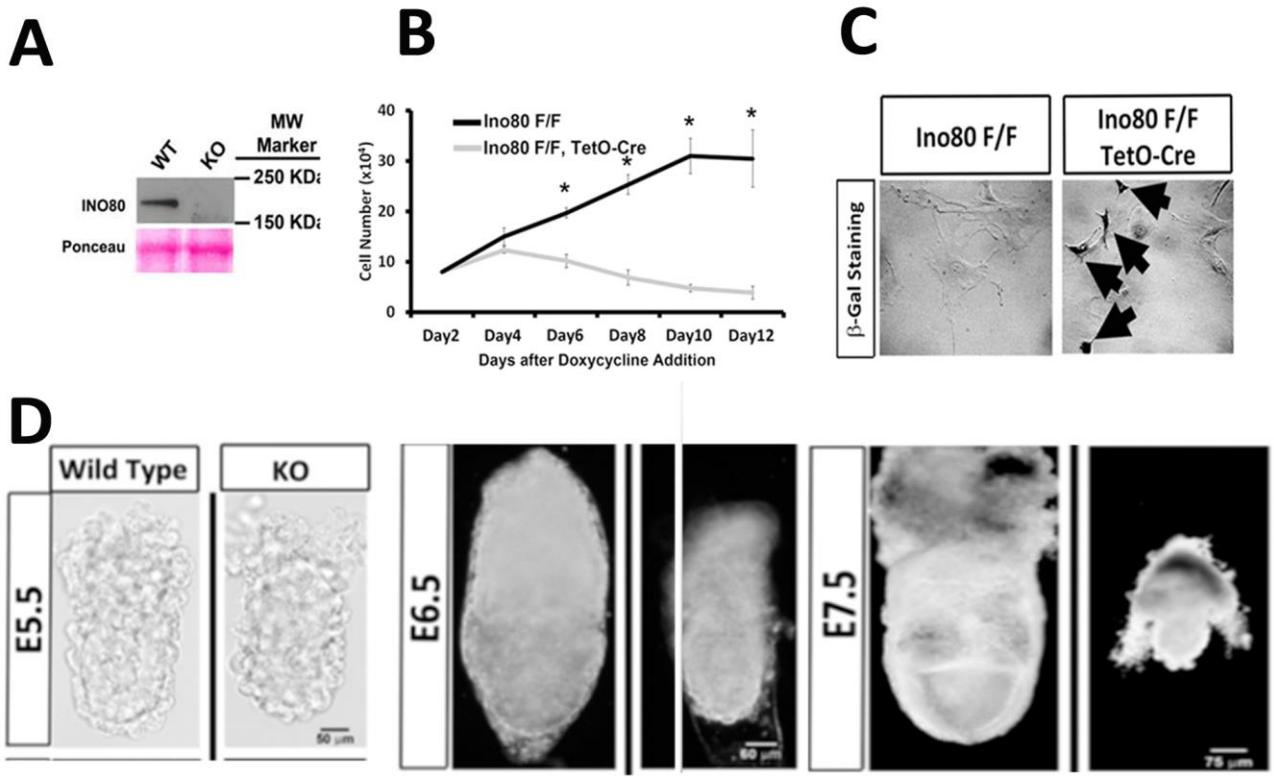

Figure 3.1: Ino80 is Crucial for Mouse Embryonic Fibroblast Survival and Early Embryonic Development.

A) Western blot analysis of Ino80 protein expression in wild type and *Ino80* KO ESCs.

B) Growth rate of conditional *Ino80* KO MEF induced by doxycycline treatment.

C) β-galactosidase activity of *Ino80* KO and WT MEFs at day 12 of culture,

Black arrows indicate β-galactosidase positive cells.

D) Microscopic Comparison of E5.5-, E6.5-, and E7.5-day wild-type and homozygous *Ino80* KO embryo. For all experiments, N ≥3. * = t-test p-value ≤0.05.

This figure is done by Dr. Zhijun Qui.

3.2 Ino80 KO Embryonic Stem Cells Are Viable and Pluripotent only in the Presence of 2i

To characterize the effect of *Ino80* KO on early embryo development further, we isolated mESCs from pre-implanted blastocysts at E3.5 after heterozygous inter-crossing. In order to maintain mESCs in culture, we have to use medium that maintains ESC self-renewal and pluripotency. We cultured both WT and KO blastocysts on gelatin-coated plates and culture media supplemented with LIF (Leukemia Inhibitory Factor) and 2i. Both WT and KO blastocysts outgrew and we successfully isolated mESCs from these outgrowths and maintained them at ground state pluripotency (homogenous population of pluripotent mESCs) by addition of 2i to the media in the presence of LIF (Figure 3.2 A). Under these conditions both WT and KO mESCs proliferate at similar rates and stained equally for alkaline phosphatase, a marker of pluripotency (Figure 3.2 B). However, upon 2i withdrawal from the media, *Ino80* KO mESCs started to scatter and differentiate suggesting that *Ino80* is required to maintain a metastable pluripotency state (Figure 3.2 C).

Moreover, the proliferation rate of *Ino80* KO mESCs was lower than that of WT cells even in the presence of 2i (Figure 3.2 D). Pluripotency and differentiation markers of WT and *Ino80* KO mESCs were quantified by qRT-PCR at different culture conditions (Figure 2 E&F). qRT-PCR data analysis revealed that at ground state pluripotency.

Ino80 KO ESCs express similar levels of pluripotency markers *Nanog, Oct4*, *Klf4*, *Sox2,* and *Essrb* compared to WT cell *Esrrb is a* down-stream target in the GSK3/Tcf3 pathway and it is critical for modulating ESCs self-renewal (Martello et al., 2012). Both *C-myc* and *N-myc* are required for pluripotency and self-renewal of ESCs(Varlakhanova et al., 2010). *Nanog, Oct4 and Sox2* are the core pluripotency markers, which are interconnected by autoregulation loop (Boyer et al., 2005). In addition, the levels of ectoderm, mesoderm, and endoderm markers were approximately equivalent in both WT and *Ino80* KO mESCs. In contrast, the levels of the respective pluripotency markers are reduced in *Ino80* KO mESCs under metastable pluripotency state (heterogeneous population of pluripotent mESCs) (Figure 3.2 E). Based on the above results, *Ino80* is required for metastable state but not ground state pluripotency of mESCs.

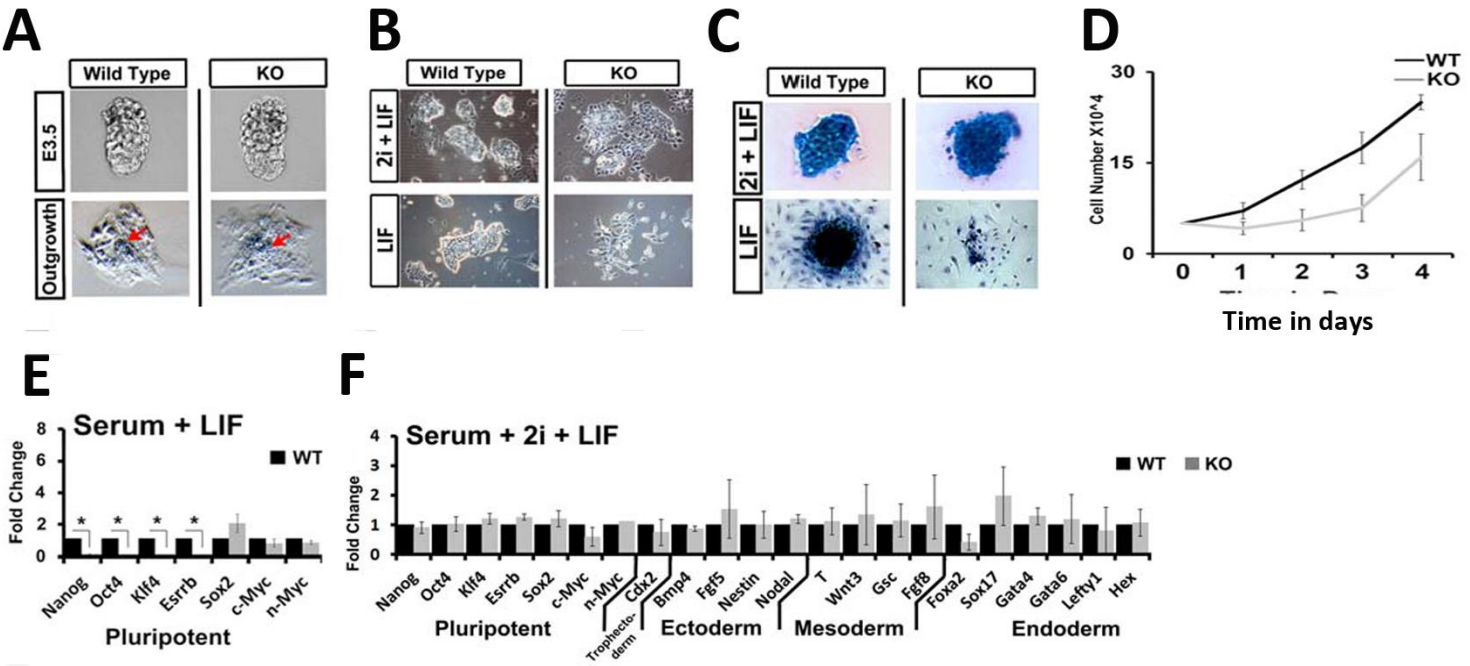

Figure 3.2: *Ino80* KO ESC Are Viable and Pluripotent only in the Presence of 2i in the Culture Medium.

A)Microscopic analysis of wild type and *Ino80* KO pre-implantation E3.5 blastocysts.

B) The morphology of wild type and *Ino80* KO ESCs grown in the presence of serum+2i+LIF or serum+LIF.

C) Comparison of Alkaline phosphatase activity in wild-type and *Ino80* KO ESCs after plating at in media containing serum+2i+LIF or serum+LIF.

D) The growth rate of both WT and *Ino80* KO cells.

E) Quantitative qRT-PCR analysis of gene expression in wild type and *Ino80* KO ESCs maintained in serum+2i+LIF.

F) q RT-PCR analysis of gene expression in wild type and *Ino80* KO ESCs maintained in serum+LIF. For all experiments N=3 biological replicates; * = t-test p-value ≤0.05).

A, B and C are done by Dr. Zhijun Qui. E and F are done by Veronica Peterkin.

3.3. *Ino80* KO ESCs Fail to Differentiate Using *In Vitro* Differentiation Models.

We utilized *in vitro* differentiation models to further characterize the role of Ino80 in mESCs differentiation. First, we created teratomas from both WT and KO mESCs maintained in ground state pluripotency medium by inoculating these cells into the opposing flanks of NOD/SCID mice. Once the control teratomas reached approximately 1cm in diameter we harvested tumors and conducted routine histological analysis on tumor tissues. WT tumors differentiated into tissues from the three germ layers, which include blood islands, keratin pearls, and neural rosettes from the ectoderm lineage, both striated and smooth muscle from mesoderm and ciliated endoderm from the endoderm lineage (Figure 3.3 A & B a',b',c',d',e' and f'). However, *Ino80* KO teratomas displayed undifferentiated mesenchyme surrounded by a single layer of epithelial cells (Figure 3.3 A & B g', h').

Secondly, we applied the embryoid bodies assay by suspension of WT and *Ino80* KO mESCs maintained in ground state pluripotency medium into medium deprived of 2i and LIF. We harvested mESCs aggregates at three-day interval over nine days and analyzed these tissues histologically. WT embryoid bodies formed an organized mesenchyme filled with small cavities and surrounded by a defined layer of endoderm, while KO embryoid bodies formed disorganized mesenchyme with discontinuous endoderm (Coucouvanis et al.,1999) (Figure 3.3 C). We then quantified the levels of pluripotency and differentiation markers in both WT and *Ino80* KO embryoid bodies. In contrast to pluripotency markers that exhibited approximately equal

levels in both WT and *Ino80* KO embryoid bodies, differentiation markers showed a significant difference between WT and *Ino80* KO embryoid bodies. The stem cell marker *Bmp4* was upregulated, and subsequently its downstream endoderm markers *Gata6* and *Gata4* (Cai et al., 2008 and Nemer et al., 2003). However, the levels of the ectoderm marker *Fgf5* (Herbet et al., 1990), the endoderm marker *Hnf4a* (Duncan et al., 1994) and mesoderm markers *Fgf8* (Crossley et al., 1995) and *T* (Wilkinson et al., 1990) (Figure 3.3 D) were reduced suggesting that pluripotency genes are *Ino80*-independent while differentiation markers are *Ino80*-dependent. To identify the expression domain of *Ino80,* we used RNA in situ hybridization to determine where and when *Ino80* is expressed starting with E5.5 embryo to the E7.5 embryo relying on sense and anti-sense probes. Results showed that *Ino80* was widely expressed in E5.5 and E6.5 embryos mostly in the EmE and ExE with less staining in the VE (Figure 3.4 A,B, C).

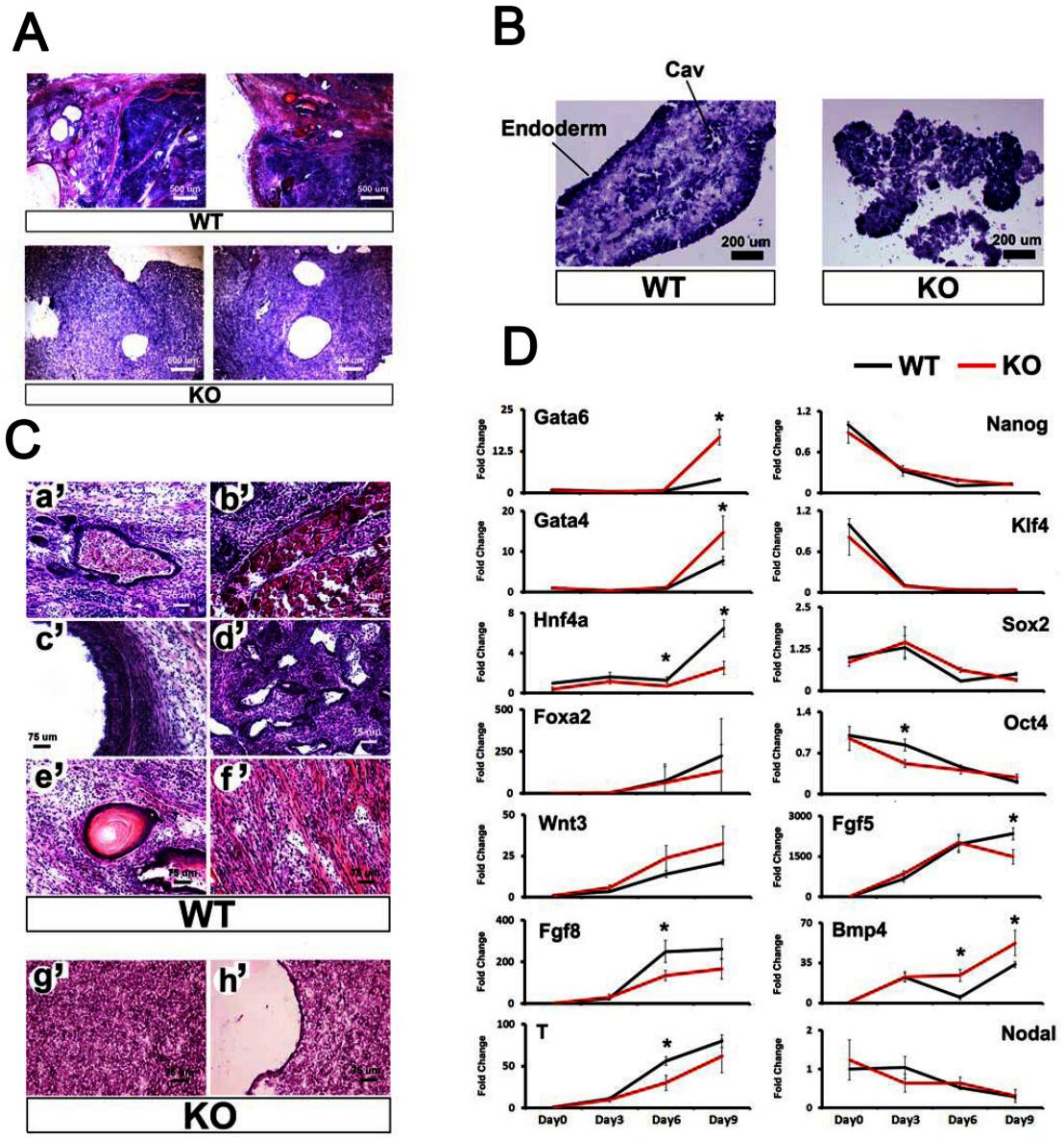

Figure 3.3: Ino80 is Essential for Embryonic Stem Cell Differentiation.
A) Low-magnification analysis of differentiation potential of teratoma derived from wild type and *Ino80* KO ESC (Scale bar = 500 µm).
B) High magnification analysis of teratomas derived from both wild type and *Ino80* KO ESCs (Scale bar = 75 µm).
C) H&E analysis of 9-day embryoid bodies derived from of wild type and *Ino80* KO 606 ESCs (Scale bar = 200 µm).
D) Gene expression analysis of differentiation markers in embryoid bodies derived from wild type or *Ino80* KO ESCs over 9 days. For all experiments, N=3 biological replicates; * = t-test p-value ≤0.05.
This figure is done by Dr. Zhijun Qui.

3.4 *Ino80* KO Embryos Fail to Gastrulate.

To further characterize *Ino80* KO embryos, we applied the whole amount ISH to determine the expression of known developmental markers at the pre-gastrulation and gastrulation stages. We started with E6.5 embryos, the latest stage that failed develop, yet retained structural integrity. E6.5 is the time of gastrulation where the formation of the three germ layers (ectoderm, mesoderm and endoderm) occurs. Therefore, we stained embryos with probes for the mesoderm marker Brachyury (*T*) that is first detected in the pre-mesoderm cells and plays a role in the formation and organization of mesoderm at the onset of gastrulation (Wilkinson et al., 1990). In contrast to WT embryos, *Ino80* KO embryos lack *T* expression, and presumably mesoderm differentiation is defective (Figure 3.4 D). Prior to gastrulation a subset of VE cells at the tip of the distal portion of the embryo migrate to the future anterior part to form the AVE that is identified by *Hex1, Lefty1 and Cer1* expression. Formation of the AVE is essential for gastrulation. An analysis of these markers demonstrated that *Ino80* KO embryos did not express the AVE markers *Cer1,* or *Hex1,* suggesting a failure to form the AVE. The ExE marker, *Bmp4* is a member of the TGFβ family members and it is known to inhibit the formation of AVE (Winnier et al., 1995). *Ino80* KO embryos exhibited very low expression of *Bmp4* in the ExE (Figure 3.4 D). Collectively, these

results support the hypothesis that *Ino80* KO embryos fail to gastrulate, do not specify the AVE and have abnormal *Bmp4* expression in the ExE.

Initiation of the P-D axis occurs at E5.5 when a subset of PrE cells differentiate at the distal part of the embryo to form the DVE. These cells are the precusors to the AVE. Because INO80 KO embryos lacked the AVE, we hypothesized that the DVE could be defective. Therefore, we measured the levels of *Cer1, Hex1* and *Bmp4* at E5.5 embryos using whole mount ISH. Results revealed that the DVE markers, *Cer1* and *Hex1,* were completely absent and the *Bmp4* expression domain is mislocalized to the EmE. To further verify the localization of *Bmp4* expression we performed a double staining of *Bmp4* and *Otx2*. *Otx2* is a known EmE marker at E5.5 embryos (Daisuke et al., 2004). As expected, we found an overlap between the two markers in the EmE (Figure 3.4 E) suggesting that *Bmp4* expression is lower in the EmE in *Ino80* KO embryos. Because, *Bmp4* is a known regulator of the DVE these results suggest that *In80* KO embryos fail to develop because of aberrant *Bmp4* expression, a known negative regulator of the DVE. However, the defects in DVE specification could also result due to a general defect in VE. To test this possibility, we measured the levels of *Hnf4a*. *Hnf4a* belongs to the steroid hormone receptor family and it is expressed in VE endoderm at E5.5 and in the proximal VE at E6.5-E7.5 (Duncan et al., 1994). We observed reduced levels of *Hnf4a* in *Ino80* KO embryos suggesting that *Ino80* KO

embryos fail to specify the DVE due to mis-regulation of the inhibitory molecule *Bmp4* and possibly a defective VE (Figure 3.4 D).

PrE is the origin of several extra-embryonic tissues including that VE, EmVE, ExE and DVE (Stephenson et al., 2012). At E4.5, a subset of PrE cells differentiates into DVE cells that are retained at the distal part of the embryo. Consequently, the defects in DVE formation could be due to defect in PrE differentiation. To test this hypothesis, we stained E4.5 embryos with DVE markers *Lefty1* and *Hex1* and observed similar levels of these markers in both WT and *Ino80* KO embryos suggesting normal differentiation of PrE cells. Also, the levels of the EPI specification marker *Nanog* in both WT and *Ino80* KO embryos was normal suggesting that its development in not INO80 dependent (Figure 3.4 D). The decreased embryo size at E6.5 is not likely due to cell death because TUNEL staining at this stage did not observe a significant difference between WT and *Ino80* KO embryos (Figure 4 F). Based on the above results, *Ino80* KO embryos fail to establish the P-D axis since they lack the ability to specify the DVE at E5.5. This could be due to abnormal expression of *Bmp4* in the EmE, a known negative regulator of DVE differentiation or defects in VE differentiation.

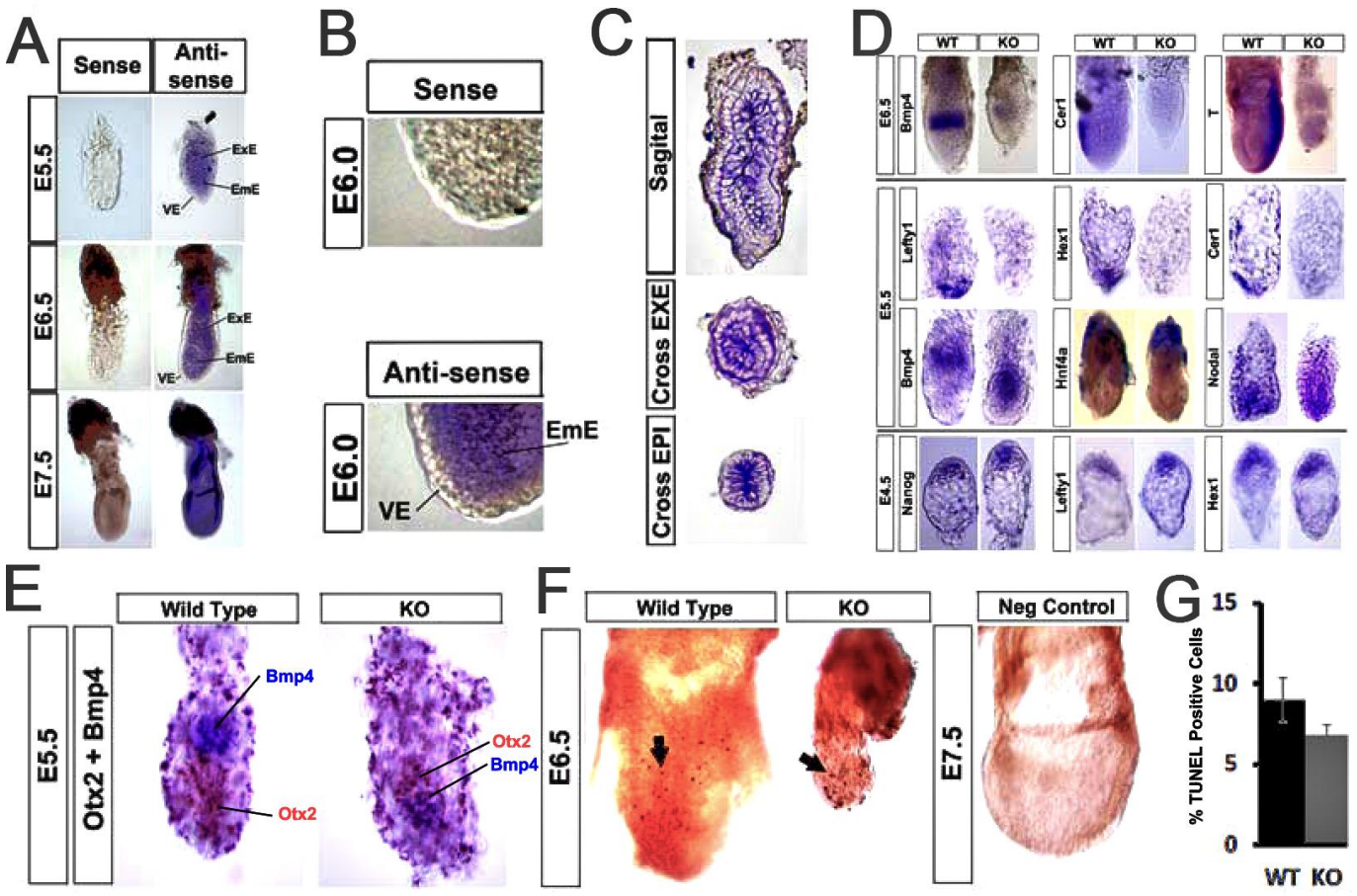

Figure 3.4: Ino80 is Widely Expressed in Embryonic Tissues and is Essential for Establishing the Proximal-Distal Axis of the Post-Implantation Embryo.
A) Whole mount RNA *in situ* hybridization using either sense or antisense *Ino80* riboprobes in embryos at E5.5, E6.5 and E7.5 embryos.
B) High magnification of *Ino80* ISH exhibits reduced antisense *Ino80* riboprobe staining in the visceral endoderm (VE) in E6.0-day embryos.
C)Frozen sections of sagittal and cross-sections through the ExE and EPI stained with antisense *Ino80* riboprobe.
D) Whole mount RNA in situ hybridization of E6.5, E5.5, and E4.5 embryos were performed with antisense riboprobes for markers of tissue differentiation. **All ISH are done by Dr. Zhijun Qui except *Hnf4a* ISH.**

E) Whole mount ISH of E5.5 embryos were performed with antisense probes to the ExE marker Bmp4 (purple color) and the EmE marker Otx2 (magenta color).

F&G) Whole mount analysis and quantification of TUNEL positive cells in wild type and *Ino80* KO E6.5 embryos. N=3 biological replicates.

3.5. *Ino80* Regulates *Bmp4* Expression During Embryonic Stem Cell Differentiation *In Vitro.*

Results from (Figure 3.3 D) showed upregulation of *Bmp4* in *Ino80* KO embryoid bodies. In addition, ISH experiments showed undetectable expression of *Bmp4* in the EXE, and its upregulation in the EmE, suggesting a possible direct role of *Ino80* in the regulation of *Bmp4* expression. To identify how INO80 regulates *Bmp4* expression, first we induced mESCs differentiation *in vitro* by LIF and 2i withdrawal from the media. LIF withdrawal from media is known to promote cell differentiation into mesoderm and endoderm lineages (Sharova et al., 2007 and Ying et al., 2003). We collected cells at three-day time interval over nine days. Then we quantified the RNA levels of *Bmp4* and other differentiation markers. Results from monolayer differentiated cells were consistent with embryoid bodies experiments where *Ino80* KO mESCs exhibited increased levels of *Bmp4* expression, reduced levels of DVE markers *Cer1*, *Hex1* and *Lefty1* and approximately equal levels of the endoderm markers *Gata4* and *Gata6* (Figure 3.5 A). In mESCs an upstream enhancer mediates transcription of *Bmp4* through interaction with Med23 and ETS1 (Wanqu et al., 2015).

We applied ChIP analysis using monolayer differentiated mESCs cells to identify which *Bmp4* regulatory element is occupied by INO80. As shown in Figure 3.5 B&C, Ino80 is preferentially localized to the promoter region of *Bmp4*. Next, we used FAIRE to detect the chromatin status at *Bmp4* promoter under the same condition. Results showed an open chromatin structure at ~ 1.5 Kb upstream of *Bmp4* promoter (Figure 3.6 A, B). SP1 is a transcription factor that is known to activate *Bmp4* expression (Ebara

et al., 1997), so we applied ChIP experiment to monitor its localization at the *Bmp4* promoter, and we observed that SP1 occupies the promoter region of *Bmp4* with enrichment of the active histone marker H3K4me3 (Figure 3.6 C, D). Based on the above data, we provide a model where the chromatin remodeling factor INO80 is required for DVE specification in pre-gastrula mouse embryo by negative regulation of *Bmp4* in the EmE and by positive regulation of *Bmp4* in the ExE (Figure 3.7) and also by its effect on VE differentiation through *Hnf4a* down-regulation.

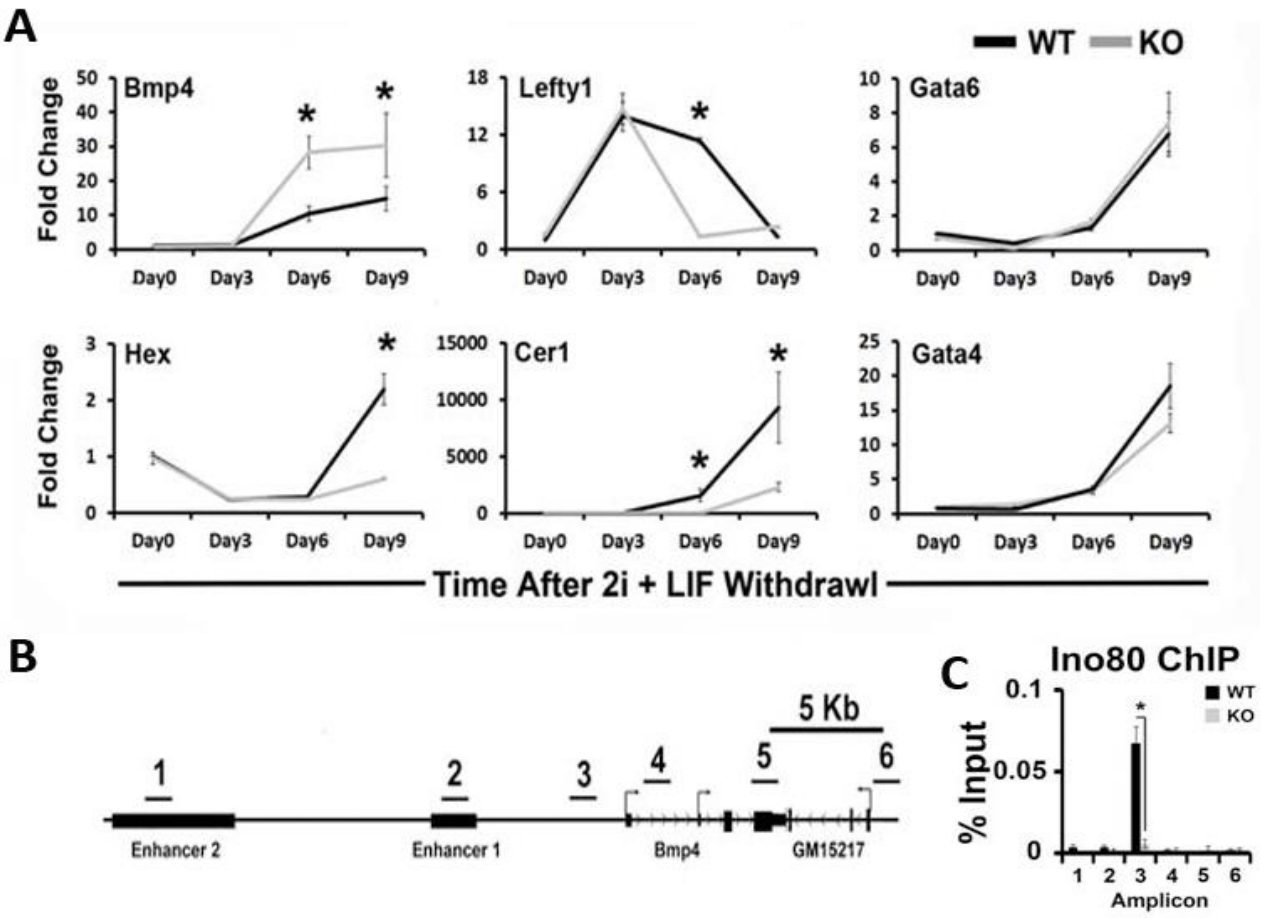

Figure 3.5: Ino80 Regulates *Bmp4* Expression by Occupying its Promoter.
A) qRT-PCR quantification of *Bmp4, Hex, Lefty1, Cer1, Gata6, and Gata4* during ESC differentiation in the absence of 2i+LIF in monolayer.
B) Cartoon showing the cis-regulatory elements of Bmp4 gene, location of upstream enhancers, and downstream gene Gm15217 to illustrate position of PCR amplicons used in ChIP experiments. Amplicons are shown as black bars labeled 1-6ChIP of both wild type and *Ino80* KO ESC after differentiation as a monolayer for 6 days in serum containing media in the absence of 2i+LIF.
For all of the above experiments N=3 biological replicates; * = t-test, p-value ≤0.05.

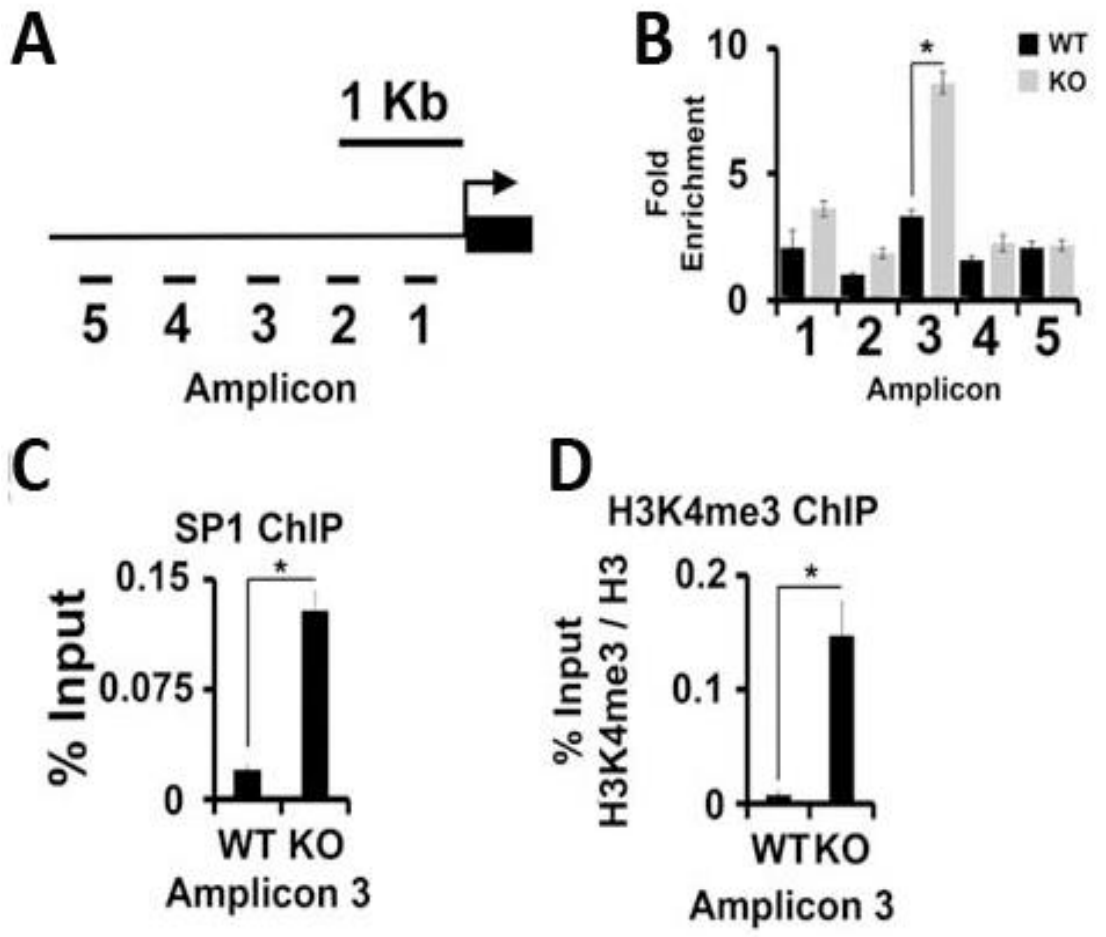

Figure 3.6: The *Bmp4* Promoter is More Accessible to Positive Regulatory Factors upon Ino80 Deletion.

A) Cartoon showing ~ 1.5Kb of the *Bmp4* promoter and the location of PCR amplicons used in FAIRE experiments.

B) FAIRE was performed with wild type and *Ino80* KO ESC after differentiations for 6 days in culture media containing serum and lack both 2i+LIF.

C) Increased occupancy of active chromatin mark H3K4me3 at *Bmp4* promoter in *Ino80* KO ESC as compared to WT. ChIP was performed using wild-type and *Ino80* KO ESC after differentiation as a monolayer for 6 days in serum containing media lacking 2i+LIF.

D) Increased occupancy of the positive transcription factor SP1 at *Bmp4* promoter in *Ino80* KO ESC as compared to WT ESCs. ChIP was performed with wild type and *Ino80* KO ESC after differentiation in serum containing media lacking 2i+LIF as a monolayer for 6 days.

For all of the above experiments N=3 biological replicates; * = t-test, p-value ≤0.05.

A Proposed Model INO80 Role in DVE Formation during Early Mouse Development.

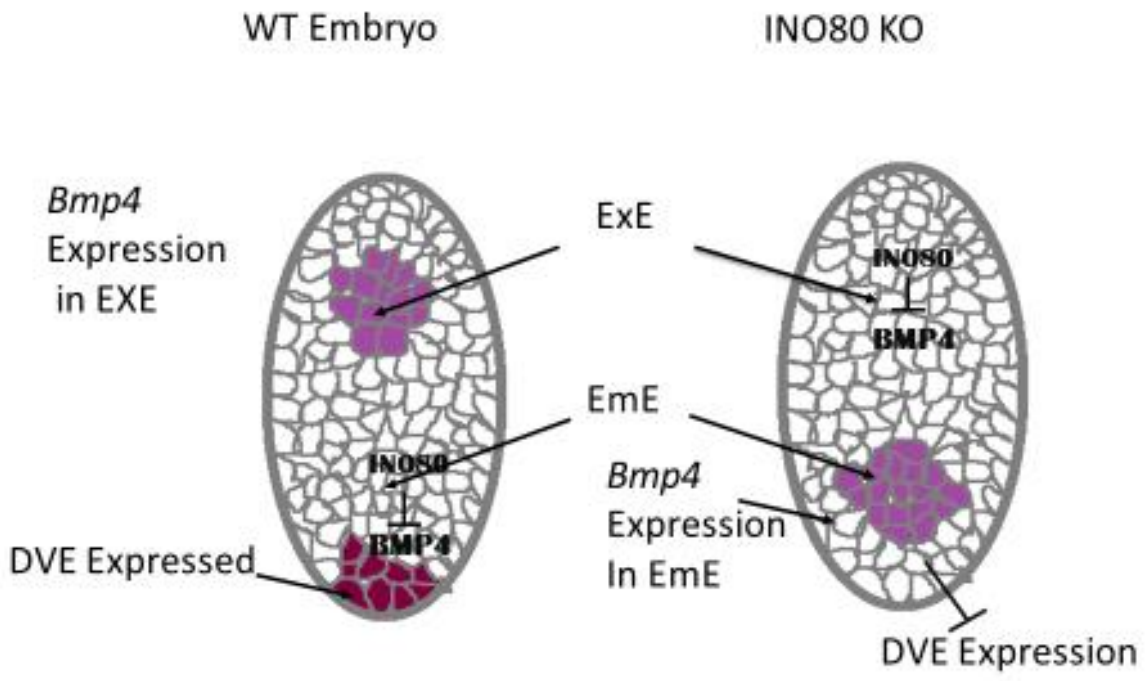

Figure 3.7: Model of Ino80 KO Effect on *Bmp4* Gene Expression and its Consequences on the Establishment of the Proximal-Distal Axis in Early Mouse Embryo.
We propose a model where *Ino80* KO embryos upregulate *Bmp4* expression in the EmE, which in turn repress the expression of the DVE markers *Cer1*, *Hex,* and *Lefty1*. Consequently, *Ino80* KO embryos lack the DVE in part due to mis-localized *Bmp4* expression and fail to gastrulate.

CHAPTER FOUR

Discussion and Future Directions

4.1 Discussion

4.1.1 Early Embryonic Lethality Due to Disruption of the ATP-Dependent Chromatin Remodeler INO80

Mammalian development is a complex process in which one cell zygote give rise to an organism. An organism is composed of multiple cell types that develop into specific tissues and organs. Although all these cells share the same genetic DNA sequence, the chromatin state (DNA packaging) is distinguished in each cell type to establish and maintain different cell identities. The chromatin state is modified by many mechanisms including histone post-translation modifications (for example, histone acetylation, and methylation), histone variants, and DNA modifications like cytosine methylation and/or ATP-dependent chromatin remodeling complexes (Ho et al., 2010 and Chen et al., 2014).

Genetic studies utilizing mouse models showed essential roles of chromatin remodelers in development. Chromatin remodelers are important for both pre- and post-implantation phenotypes suggesting that they regulate specific developmental pathways. NURD is required for maintaining the balance between self-renewal and differentiation. Pre-implantation lethality occurs upon deletion of the methyl CpG-binding domain protein 3 gene (MBD3) that encodes the core component of NURD (Kaji et al., 2007). MOF/TiP60 null embryos fail to implant and survived blastocysts are defective in

morphology and growth suggesting an essential role for the complex in cell survival, pluripotency and self-renewal (Thomas et al., 2008). Mouse embryos null for the SWI/SNF ATPase subunit Brg1 die before implantation suggesting a potential role of Brg1 in self-renewal and pluripotency in mESCs (Bultman et al., 2006). Other chromatin remodeling factors such as NURF and CHD7 exhibit post-implantation lethality upon deletion. NURF (BPTF) KO embryos are defective in gastrulation and differentiation of mesoderm and endoderm (Landry et al., 2008). CHD7 null embryos showed multiple defective tissues and perinatal lethality (Hurd et al., 2007). In the present study, we show that *Ino80* KO embryos fail to gastrulate and exhibit post-implantation lethality.

4.1.2 The Differential Effect of *Ino80* KO in MEFs and mESCs

DNA replication is an essential component of cell proliferation. Chromatin remodeling at replication origins is an essential step in DNA replication especially at stalled forks. *Ino80* is required for DNA replication where it disrupts nucleosomes in front of replication fork to facilitate polymerase movement and DNA unwinding at replication origin (Karina et al., 2012). It is also required to re-assemble disrupted nucleosomes behind the fork. Lee et al. showed that *Ino80* is stabilized by BAP1 through de-ubiquitination and BAP1 recruits *Ino80* to replication fork by its interaction with ubiquitinated H2A. These functions might explain in part the early embryonic lethality in *Ino80* KO mice, non-viable *Ino80* KO MEFs, and slow growth rate of *Ino80* KO ESCs (Min et al., 2013 and Lee et al., 2014).

Our results showed that *Ino80* KO MEFs have significantly higher beta-

galactosidase than WT MEFs. This is consistent with a recent study, which showed that *Ino80* is required for MEF proliferation, and its deletion delayed S-phase progression and decreased BrdU (bromodeoxyuridine) incorporation (Hur et al., 2010, Min et al., 2013 and Lee et al., 2014). Although the same study reported that *Ino80* KO ESCs were not viable. In our hands, *Ino80* KO ESCs were viable when cultured in medium supplied with 2i plus LIF to maintain ground state pluripotency. ESCs that grow in 2i medium exhibit global hypomethylation of DNA that is similar to hypomethylated ICM at E3.5 (Leitch et al., 2013). DNA hypomethylation alters chromatin structure to promote gene activation (Feinberg et al., 1983). INO80 is involved in regulation of gene expression (Ebbert et al., 1999), occupies the promoters of pluripotency genes in ESCs, and regulates their expression (Li et al., 2014). In addition, INO80 replaces the histone variant H2A.Z with H2A. H2A.Z occupies promoters of poorly transcribed genes (Zhang et al., 2005), possibly to facilitate their expression (Manolis et al., 2011). It is plausible, and I hypothesize that DNA hypomethylation of ESCs in ground state activates gene expression, compensating for INO80 functions in maintaining gene expression. These same compensatory effects would not be relevant in MEFs, which have hypermethylated promoters, and require INO80 to maintain gene expression.

In contrast to MEFs, mESCs exhibit unique characteristics to stay pluripotent. mESCs are characterized by the ability to self-renew *in vitro* while maintaining pluripotency, i. e. the capacity to differentiate into a broad number of cell types that originate from the three primary germ layers endoderm, mesoderm and ectoderm

(Evans and Kaufman, 1981; Martin, 1981). The potential to self-renew is marked by two main characteristics: highly rapid proliferation and high telomerase activity. The high proliferation rate of mESCs necessitate unique cell cycle, which have extremely short G1 phase that is devoid of regulation at the G1–S transition due to the absence of cyclin D and the presence of hyperphosphorylated retinoblastoma (RB1) protein (Savatier et al., 1996; Burdon et al., 2002). Both c-Myc and Klf4 are essential factors for mESCs pluripotency (Kazutoshi et al., 2006). Klf4, which is known to repress p53 directly (Rowland et al., 2005), while c-Myc, suppresses the expression of p21CIP1 (Seoane et al., 2002). Both p53 and p21CIP1 are involved in cell cycle regulation and their repression facilitate cell cycle progression in mESCs. mESCs express high levels of TERT and exhibit high telomerase activity. TERT is a ribonucleoprotein enzyme, which synthesis telomeres to maintain telomere homeostasis in mESCs and prevents telomeres fusion to keep cells genetically stable (Wong et al., 2010). This difference in cell cycle regulation and proliferation suggest that mESCs could compensate for *Ino80* KO while MEFs could not.

4.1.3 *Ino80* KO Effect on the Pluripotency of mESCs.

In our model, *Ino80* is required for metastable but not ground state pluripotency in *Ino80* KO mESCs as similarly observed for *Mbd3* KO mESCs (Kaji et al., 2007). *Ino80* KO mESCs exhibited WT pluripotent phenotype when those cells are maintained in medium that promote ground state pluripotency (2i+LIF). However, when those cells maintained in medium that induce metastable pluripotency (LIF only) they differentiate and lose their pluripotent phenotype. 2i can closely mimic the *in vivo* environment for

ICM pluripotency (Marks et al. 2012) and mask defective pluripotency due to *Ino80* KO. Our results contradict the finding that *Ino80* is required for mESCs pluripotency and pre-implantation (Wang et al., 2014). This could be due to difference in *Ino80* KO methods, since referenced study used siRNA to KD *Ino80*, which could affect both maternal and embryonic tissues (Li et al., 2014). In addition, the referenced study maintained the cells in culture medium that promotes metastable pluripotency, culture conditions that we have shown requires INO80. Another possibility, at the metastable pluripotency state, nucleosomes are highly modified by the activation marker H3K4me3 (Marks et al., 2012), which could recruit activating histone readers to promote gene expression and compensate for the loss of INO80. Under these conditions factors like *Sox2*, *Nanog*, *Oct4*, which require INO80 in the metastable state, would sufficiently transcribed maintaining pluripotency.

4.1.4 The Reduced Size of Epiblast in *Ino80* KO Embryos

The *Ino80* KO embryos have reduced size at E6.5, which could be due to reduced proliferation or increased apoptosis rates. *Ino80* KO did not affect the levels of apoptosis, as the rates of cell death were essentially similar in both WT and *Ino80* KO embryos. It has been shown that E5.5 embryo undergo dramatic increase in proliferation to attain a certain number of cells to start the gastrulation at E6.5 (Snow et al., 1977). Consequently, the reduced embryo size could be due to the reduced

proliferation rate of *Ino80* KO mESCs. This possibility could be further investigated by the determination of the epiblast proliferation rate at E6.5 through BrdU labeling of embryos and/or the measure of cell proliferation using immuno-histochemistry of phosphorylated histone H3 levels in the conceptus by at E6.5 and E7.5 (Landry et al., 2008).

4.1.5. *Ino80* KO Effect on the Proximal-Distal Axis Establishment

The A-P axis establishment is induced by AVE formation at the anterior part of pre-gastrula embryo, which in turn promotes gastrulation (Beddington and Robertson, 1999). Both TGF-β signaling molecules, Nodal and Bmps, are involved in the regulation of DVE formation at E5.5 (Brennan et al., 2001 and Soares et al., 2005). The antagonism between these two molecules at the distal part of the embryo is the molecular basis of DVE formation. Nodal -/- embryos fail to specify embryonic VE which is required to develop the DVE (Mesnard et al., 2006). Furthermore, inhibition of *Nodal* signaling abolished DVE formation, and promoted aberrant *Bmp4* expression at the DVE (Yamamoto et al., 2009). Although the levels of *Nodal* transcripts were similar in both WT and *Ino80* KO embryos, Nodal could be unprocessed, and therefore not functional in *Ino80* KO embryos, resulting in defective DVE formation for reasons discussed above (Mesnard et al., 2006).

In WT embryos, *Bmp4* is expressed in the EXE at the pre-gastrula and gastrula stages. Limited expression of *Bmp4* in the ExE is required for DVE establishment, because it is a negative regulator of the DVE (Rodriguez et al., 2005; Mesnard et al., 2006)(Yamammoto et al., 2009). In addition, *Bmp* signaling is required for VE

differentiation at E5.5, and it cooperates with *Nodal* signaling to promote epiblast proliferation. In our model, *Bmp4* expression is up regulated in the EmE thereby emitting an inhibitory signal for DVE formation. Defective DVE formation could be also result from impaired VE as suggested by the down-regulation *Hnf4a*, possibly also a result from aberrant *Bmp4* expression (Figure 4 D).

VE is the main expression domain of *Hnf4* during gastrulation and its disruption results in defective gastrulation (William et al., 1994). VE is an outer layer of epithelial cells around the embryo. The tight junctions between these epithelial cells are essential for nutrition and small molecule delivery to the embryo. It is also the main site for production of survival signals (Jollie et al., 1990). It would be interesting to examine the endocytic activity of VE in *Ino80* KO embryos, which could contribute to the lethality phenotype. Signals from ExE are required for VE patterning and DVE formation (Richardson et al., 2006). To determine if VE defects in *Ino80* KO embryos are the result of an overall defective ExE, we can monitor the expression pattern of additional ExE markers including, *Fgfr2*, *Plet1* and *Talia* using *in situ* hybridization (Stephen et al., 2007). FGF signaling is involved in the development of extraembryonic tissues and FGFR2 is required for ICM differentiation and specific functions of the trophectoderm (Arman et al., 1998). The initial establishment of the cardiovascular network occur during gastrulation at E6.5 (Nowotschin et al., 2010). This process is largely dependent on activation of the vascular endothelial growth factor (VEGF) signaling pathway. The vascular endothelial growth factor receptor 2 (VEGFR2/Flk1) is critical for the

development of the primitive capillary plexus during embryogenesis (Klagsbrun and Soker, 1993). *Flk1* is a receptor tyrosine kinase that is expressed in the extra-embryonic ectoderm. *Flk-1* KO embryos die at E8.5-E9.5 due to defect in the development of hematopoietic and endothelial cells (Shalaby et al., 1995). We can also quantify the expression of these angiogenic markers VEGFR2 and Flk1 at E6.5 to detect any defective angiogenesis phenotypes associated with *Ino80* KO. While defects in angiogenesis are unlikely to contribute the lethality of *Ino80* KO early embryos, it could reveal important functions for INO80 in these processes, which would have relevance to our understanding of INO80 in the adult.

4.1.6. INO80 Regulation of the *Bmp4* Promoter

The roles for INO80 as a chromatin-remodeling factor that regulates gene expression is well established. Towards this end, transcription factors can recruit INO80 to target genes where it can modulate chromatin and activate or repress expression. Our results demonstrated a differential regulation of *Bmp4* by INO80 at the transcriptional level in the ExE and EmE where *Bmp4* expression is inhibited in ExE and upregulated in EmE. More specifically in the EmE we predict that INO80 is modulating the chromatin structure at *Bmp4* to prevent access of regulatory factors such as SP1. How INO80 is recruited to the *Bmp4* promoter is unknown, but could be through interactions with unknown transcription factors. Also, enhanced H3K4me3 at the *Bmp4* promoter in *Ino80* KO ESCs could recruit other unknown regulatory factors that promote *Bmp4* expression beside SP1. For example, the mediator complex is a multi-protein

complex that mediates a connection between transcription factors and the mRNA polymerase II apparatus to regulate gene activity (Kagey et al., 2010). In ESCs, the mediator subunit *med23* recruit ETS1 (member of the ETS family transcription factors) to the *Bmp4* promoter and enhancer to facilitate their communication and enhance *Bmp4* expression (Wanqu et al., 2015). In addition, USF (upstream stimulatory factor) binds the *Bmp4* promoter and activate its expression (Ebara et al., 1997). The recruitment of either of these factors could be repressed by INO80 in the EmE. To test these hypotheses ChIP analysis of these factors at the *Bmp4* promoter in *Ino80 KO* ESC would be performed which could reveal additional regulatory factors of *Bmp4*.

4.2 Future Directions

The role of mouse INO80 in DNA repair, DNA replication, the cell cycle regulation and telomere replication demonstrates it's requirement for the maintenance of genomic stability (Wu et al., 2007 and Hur et al., 2010). Mouse *Ino80* deletion reduced the tumorigenic potential of oncogenic transformed cells by reduction in cell proliferation and impairment of their ability to form soft agar colonies (Min et al., 2013). In addition, mouse *Ino80* haploinsufficiency in a *p53* KO background induced a shifted in the tumor spectrum form lymphoma to sarcoma suggesting a role for *Ino80* in tumor suppression and determination of the cells fate that will initiate cancer (Min et al., 2013). A recent study showed that INO80 promotes cervical cancer proliferation through activation of *Nanog,* expression and its inhibition reduced cell proliferation *in vitro* and *in vivo* (Hu et al., 2016). The INO80 complex is an enzyme with multiple binding sites for its

substrates that could be targeted by small molecules to inhibit its activity. It has been shown that HSA/PTH and Snf2 ATPase domains of human Ino80 are essential for its remodeling activity (Lu et al., 2011). Targeting these subunits will inhibit the complex remodeling and enzynmatic acitivities. However, the consequences for INO80 depletion could be very detrimental to normal cells. The INO80 complex is crucial for essential cell processes such as DNA replication, cell cycle regulation, chromosomes segregation and telomere maintenance (Ashby et al., 2009).

Beyond cancer, the defective differentiation of *Ino80* KO ESCs suggests a possible role of *Ino80* in tissue regeneration. This could be tested by tissue specific KO of *Ino80* in the liver for example and chemical induction of liver injury followed by assessment of the recovery rate in both WT and KO mice (Dimitrios et al., 2013).

PART II. Role of the Nucleosome Remodeling Complex NURF in Anti-Tumor Immunity

Chapter 5. Background and Literature Review

5.1 The Immune System

The immune system is classically divided into innate and adaptive immune systems. The innate response is fast and it includes a broadly distributed variety of myeloid and lymphoid cells (e.g. monocytes, neutrophils, macrophages, dendritic cells and natural killer (NK) cells). However, the adaptive immune response is slow since it requires proliferation and differentiation of effector cells, which include T and B cells. T and B cells express an unlimited repertoire of antigen receptors that are produced by gene rearrangement (Vivier et al., 2011). NK cells are a type of lymphocytes that plays an important role in innate immune processes, including early defense against different pathogens and tumor transformation through a limited repertoire of germline-encoded receptors. They comprise up to 15% of peripheral blood lymphocytes and are found in peripheral tissues such as liver, spleen, peritoneal cavity and placenta (Trinchieri et al., 1989).

5.2 NK Cell Development

NK cells was first discovered by Rolf Kiessling, 40 years ago, when he characterized a subset of large granular lymphoid cells that directly lyse tumor cells *in vitro* without prior sensitization a phenomenon known as ‘natural cytotoxicity (Kiessling

et al., 1975). The evolutionary origin of NK cells is not completely understood. NK cells complete functional and phenotypic maturation in the bone marrow (BM) and their functional differentiation requires their direct interaction with BM stromal cells *in vitro* and *in vivo* (Caraux et al., 2006). The development of NK cells can be divided into several stages (Figure 5.1). The earliest stages involve the commitment of hematopoietic stem cell (HSC) in BM into a common lymphoid progenitor (CLP) that can give rise to NK, T and B cells. The CLP is characterized by expression of IL-7R (CD127), c-kit (CD117), Sca-1, and Flt-3 (CD135) (Kondo et al., 1997). The CLP differentiates into bi-potential T/NK progenitor cell reflecting the resemblance between NK and T cells (Rodewald et al., 1992 and Schmitt et al., 2006). In order for the T/NK cell progenitor to commit to NK progenitor, they acquire the IL-2/15Rα subunit (CD122). Accordingly, mice deficient in IL-15 receptor or its signaling components is defective in NK cell development (Suzuki et al., 1997, Ogasawara et al., 1998, and Kennedy et al., 2000). NK progenitors develop into immature NK (iNK) cells that lose IL-7R expression and acquire expression of NK1.1 (Rosmaraki et al., 2001). Immature NK cells develop into functionally mature NK cells by expression of CD11b, CD43, Ly49 receptors, and CD49b (DX5). Once mature these NK cells have the ability to lyse target cells and produce IFN-γ (Kim et al., 2002).

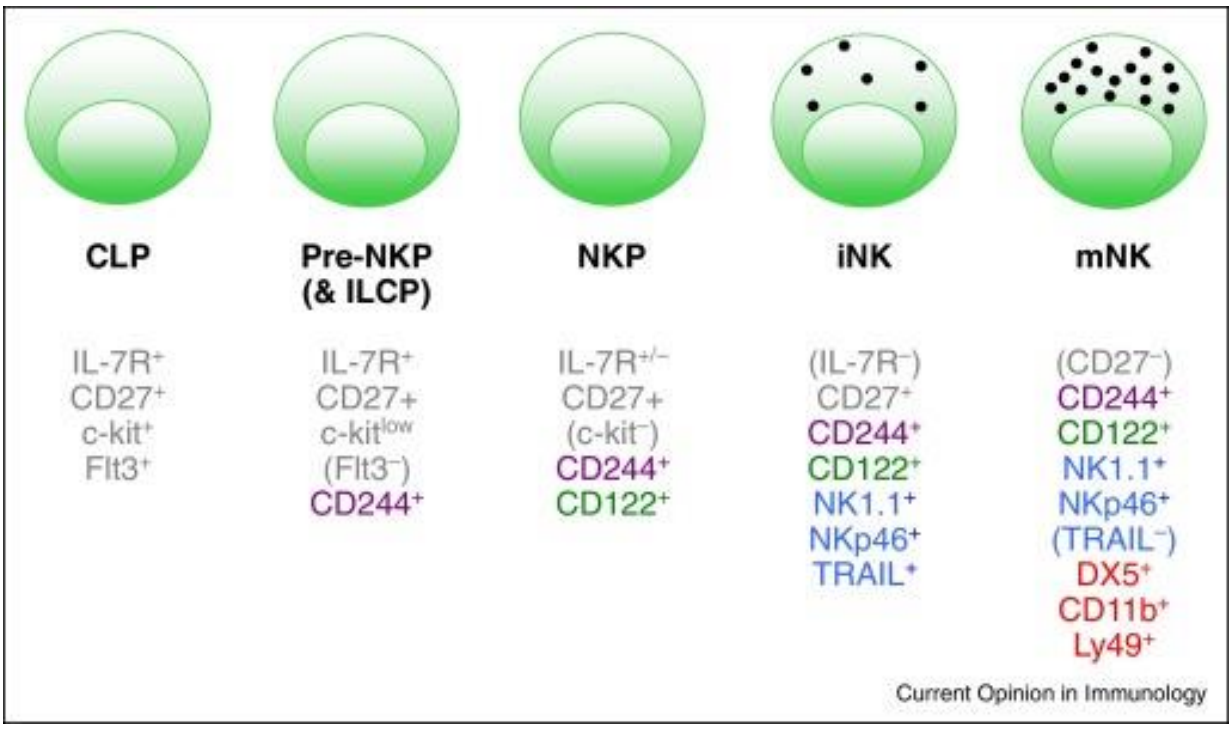

Figure 5.1: Cartoon Illustrating the Stages of NK Cell Development.
NK cells are derived from the CLP, which differentiates into NKP/ILCP population distinguished from the NKP by lack of CD122 expression. The NKP, begin to express NK cell markers NK1.1 and NKp46, and as they further mature they acquire expression of DX5 (CD49b) and CD11b while losing expression of CD27. As NK cells mature they also gain functional competence, expressing lytic molecules and cytokines such as IFNγ. Color-coded cell surface proteins indicate the stage where proteins are first expressed. Loss of a specific cell surface marker is indicated by parentheses (Geiger et al., 2016).

5.3 Regulation of NK Cytotoxicity

NK cell education/licensing is the process by which they become functionally competent (Fernandez et al., 2005). There are many models for NK cells' education: (1). The arming hypothesis proposes that the self-MHC class I specific receptors generate the signals necessary to confer the licensed phenotype, whereas signaling from inhibitory receptors mediates functional maturation in an active way. (2) The disarming hypothesis suggests the presence of a self-specific activation receptor. If unperturbed, the activation of this receptor results in chronic stimulation and an anergic-like, hypo-functional state. The self-MHC-I specific receptor then modulates the action of the activation receptor and leads to a licensed NK cell (Elliot et al., 2011). (3) The rheostat model suggests that NK cells' education depend on the strength of the inhibitory signal that is received which can be tuned up or down in a quantitative manner (Petter et al., 2010).

Once "educated", NK cells are able to kill pathogen infected or transformed cells without prior sensitization. NK killing occurs though a variety of mechanisms, including perforin/granzyme granule-mediated exocytosis, and/or signaling through the TNF death receptor family members (Smyth et al., 2005). The granule exocytosis pathway depends on NK cytotoxic and cytoplasmic granules, which resemble the secretory lysosomes. These granules contain the mediators of a diverse range of cell-death pathways that have evolved to rapidly kill target cells. The major components of these

granules are perforin, a membrane-disrupting protein, and granzymes. Both are related to a family of serine proteases with various substrate specificities. Perforin gene disruption in mice indicated that perforin is essential for NK cell cytotoxicity and it has an indispensable role in granzyme-mediated apoptosis (Kagi et al., 1994). Granzymes are highly redundant, there are eleven granzymes, ten of these (granzymes A–K, M and N) are expressed in mice, and five in humans (granzymes A, B, H, K and M) (Smyth and Trapani, 1995 and Trapani et al., 2000). Granzymes trigger cell apoptosis either directly or via activation of caspases (Heusel et al., 1994).

The death receptor pathways involve the interaction between a death receptor on target cells and their cognate ligands on NK cells, which results in caspase-dependent apoptosis. The death TNF (Tumor necrosis factor) ligands on NK cells includes TRAIL, FasL and other mediators. TRAIL (TNF-related apoptosis-inducing ligand), is a type II transmembrane protein that belong to the TNF superfamily. Both mouse and human NK cells express high levels of TRAIL in response to IL-2, IL-15 and IFN treatment indicating a broad role of TRAIL in innate immune response. The cytotoxic and anti-metastatic activity of NK cells toward TRAIL sensitive tumor cells is in part dependent on TRAIL (Takeda et al., 2001a) interaction with TRAIL-R1 (DR4) and TRAIL-R2 (DR5) resulting in an apoptotic signal (Degli-Esposti, 1999). In addition, FasL expression by NK cells suppress tumor growth *in vivo* (Bradley et al., 1998). In response to IFNγ secretion, NK cells directly induce Fas expression on tumor cells to kill them in a Fas-dependent manner (Screpanti et al., 2001). In addition, TNF deficient mice were

defective in rejection of NK sensitive tumor cells indicating that the death receptor pathway is an important mechanism for NK cells clearance of tumor (Smyth et al., 1998).

5.4 Regulation of NK Cells Activity

The regulation of NK cells is not dictated by one dominant receptor with high and specific affinity towards one particular antigen. Instead, each NK cell has broad specificity, which is mediated by the expression of multiple activating and inhibitory receptors. For many years, NK cells were considered as non-specific effectors until Klas-Karre first postulated his ‘missing self’ hypothesis in 1986 (Karre et al., 1986). According to this theory, NK cells can recognize and spare cells that express self-markers the MHC class I molecules. Based on this hypothesis, the activity of NK cells is based on their ability to sense what is missing on a target, but present in a healthy cell. The ‘missing self-hypothesis’ predicted that NK cells must express inhibitory receptors that interact with the self MHC class I molecules and deliver an inhibitory signal upon interaction. However, NK-mediated killing is regulated by other non-MHC ligands. Indeed, certain MHC class I negative molecules are resistant to NK killing and others with MHC class I molecules are NK susceptible targets. Thus, NK cell activity is not only dependent on the absence of the inhibitory signal but also require the engagement of their activating receptors (Moretta et al., 1995, Markel et al., 2002). The following sections will describe the central components that participate in the delivery of both inhibitory and activating signals and determine the overall regulation of NK activity, as known today.

5.4.1 Inhibitory Receptors

All of the well-defined NK inhibitory receptors contain one or more copies of the immune receptor tyrosine-based inhibitory motif (ITIM) in their cytoplasmic tail. Upon ligation of the receptor, the Tyr residues in the ITIM are phosphorylated (probably by Src family kinase) and recruit phosphatases via their SH2-domains. The recruitment of the phosphatases to a membrane proximal location dampen or prevents activating signals. Under normal circumstances, these inhibitory signals predominant those delivered by activating receptors (Lanier et al., 2005). However, experimental evidence shows that the degree of inhibition is proportional to the level of inhibitory ligands expressed on the target cells. In addition, when multiple costimulatory receptors are spontaneously engaged, or when a sufficient activating signal is delivered (by the ligation of a potent lysis receptor), NK cells are capable of overcoming the inhibition and destroy the target in spite of the existence of high levels of inhibitory ligands (Moretta et al., 2002).

NK inhibitory receptors can recognize ‘classical’ and ‘non-classical’ MHC class I ligands. The two major families of MHC-specific inhibitory receptors identified in humans include; The Ig superfamily, which includes the killer and leukocyte immunoglobulin-like receptors, designated as KIR and LIR, respectively and the C-type lectin receptor superfamily in both human and mice (Raulet et al., 2001). The KIR proteins belong to the Ig-superfamily of proteins have 2 or 3 immunoglobulin (Ig)-like domains and either a short or a long cytoplasmic tail. The KIR molecules with a long cytoplasmic tail signal via ITIMs to transduce a negative signal, whereas the KIRs with a short cytoplasmic tail

signal via ITAM mediated recruitment of DAP12 and thus inhibit the NK cell's activity (Raulet et al., 2001).

The KIR family in humans, the lectin-like Ly49 molecules in mice and CD94/NKG2A heterodimers in both species are the most relevant and best-studied inhibitory receptors. The KIR loci in human and the Ly49 loci in mice are highly polymorphic both in terms of gene numbers (14 genes and 2 pseudogenes) and alleles present. Other inhibitory molecules include KLRG1 (Killer Cell Lectin-Like Receptor Subfamily G member 1), TIGIT (T cell immunoreceptor with Ig and ITIM domains), NKR-P1A or LILRB2 (Leukocyte immunoglobulin-like receptor subfamily B member 2) (Aron et al., 2006). These molecules detect cadherin, CD155 and CD112 and/or a broad array of HLA-A, -B, -C and -G alleles and thus complement the capability to distinguish "self" from "altered self" or "missing self". All mentioned receptors signal via ITIMs that subsequently recruit and activate the phosphatases SHP1 and SHP2, thus decreasing the absolute signal strength.

Importantly, NK cells in one given individual can vary in terms of which KIR alleles are expressed and the level of expression creating different populations of KIR positive NK cells. The fact that KIR alleles are expressed in a largely random manner, unlinked from the host's HLA haplotypes, is troublesome as this potentially could cause NK cell mediated autoimmunity. Therefore, an education system exists in which developing NK cells acquire self-tolerance if they fail to bind to self-HLA. This state of hypo-responsiveness not only affects reactivity to self but also affects stimulation with MHC class I negative tumor cells, or plate-bound antibodies against various stimulatory

receptors. The same phenomena can be observed when mice or human individuals lack HLA class I molecules (Natalia et al., 2014).

5.4.2 Co-stimulatory NK receptors

Surprisingly, most the MHC class I-dependent inhibitory receptors have a stimulatory homolog counterpart. Under normal conditions, the affinity of stimulatory receptors to their MHC class I ligands is lower than their inhibitory counterparts are so, the inhibitory signal dominate the stimulating ones (Vales-Gomeset al., 1999). A possible explanation is that these receptors may be involved in a different context and recognize additional ligands. For example, both the CD94/NKG2C stimulatory and its inhibitory counterpart the CD94/NKG2A, recognizes HLA-E. However, NKG2C is activated by peptides derived from the heat shock protein Hsp60 bound to the HLA-E molecules under stress conditions (Michaelsson et al., 2002).

5.4.3 NK Activating Receptors

The difference between NK co-stimulatory and activating receptors is their ligand specificity. While the stimulatory receptors recognize MHC class I ligands, the triggering receptors recognize non-MHC ligands. Moreover, the activating receptors are able to mediate direct killing of targets and therefore considered as lysis receptors. In resting NK cells, the cytolysis activity requires synergistic stimulation of more than one receptor (Bryceson et al., 2005). Progress in the understanding of NK cell biology revealed that NK cell activation is not only dependent on the absence of the inhibitory signal; it also requires efficient activating signals. This theory is based on the discovery of a set of NK activating receptors that are able to directly induce cytotoxicity and cytokine production

upon engagement. The major NK activating receptors include the NKG2D, CD16 and the NCRs (natural cytotoxic receptors), which include NKp46, NKp44 and NKp30 (Moretta et al., 2002). In addition, some NK receptors are thought to serve as 'costimulatory' receptors that enhance signaling of active receptors but cannot mediate cytotoxicity on their own. The following sections will discuss the major NK triggering receptors and their ligands.

NKG2D is a type II transmembrane glycoprotein that is expressed on the surface of all human and mouse NK and a subset of T cells (Bauer et al., 1999 and Jamieson et al., 2002). The identified ligands for NKG2D include MICA, MICB and ULBP1-4 in human and H60, Rae1 in mice (Bauer et al., 1999, Castriconi et al., 2003 and Sutherland et al., 2002). These proteins are stress inducible cellular ligands that are structurally homologous to MHC class I proteins (Li et al., 2001). NKG2D is involved in anti-viral defense mechanisms. For example, CMV infection leads to upregulation of NKG2D ligands (Groch et al., 2001). In response to this challenge, CMV developed evasion mechanisms, which include the expression of UL16 protein (Cosman et al., 2001). UL16 binds NKG2D ligands and prevents their transport to the surface of infected cell to reduce NK cytolysis activity (Wu et al., 2003 and Dunn et al., 2003).

In tumors, NKG2D ligands are upregulated due to genotoxic stress and stalled DNA replication and *in vivo*, expression of NKG2D ligands induce NK-mediated elimination of NK-resistant tumor cell lines (Cerwenka et al., 2000 and Diefenbash et al., 2001). Tumor cells avoid NK-mediated killing via NKG2D receptor, by shedding of NKG2D ligand from their surface. Indeed, high levels of soluble MIC proteins were

detected in sera of cancer patients (Grosh et al., 2002). In addition, tumors upregulate TGF-β (a known immunosuppressive factor) that might induce downregulation of NKG2D receptor on lymphocytes (Castriconi et al., 2003).

The NCRs are highly conserved among species even at the level of their cellular ligands (Moretta et al., 2002). The only functional NCR homolog expressed in mice is the murine NKp46 (NCR1) (Biassoni et al., 1999). NCRs are preferentially expressed on NK cells and induce NK cytotoxicity upon cross-linking by specific monoclonal antibodies. A functional crosstalk between the three NCRs was suggested since upon ligation of a single NCR also induces signaling cascades of other NCRs (Augugliaro et al., 2003). Accumulating evidence suggested that NCRs have important roles in recognition and killing of tumor cells. NCRs blocking prohibited NK-mediated killing of many tumor cell lines and *in vivo*, downregulation of NCRs or their ligands in acute myeloid leukemia cells rendered them resistant to NK cytotoxicity (Biron et al., 2001 and Costello et al., 2002).

NKp46 is the first identified member of NCRs (Sivori et al., 1997). NKp46 is specifically expressed on NK cells, and a minor population of innate lymphoid cells (Gazit et al., 2004). NKp46 cross-linking induced calcium mobilization, cytotoxicity and cytokines release (Sivori et al., 1997). Upon engagement, NKp46 is associated with the adaptor molecules CD3ζ and FcyR, which have the activation ITAM motif (Pessino et al., 1998 and Falco et al., 1999). In humans, NKp46 is a 46KDa glycoprotein with two Ig-like extracellular domains and three potential glycosylation sites located at positions Thr125, Asp215 and Thr225 (Pessino et al., 1998). The membrane proximal domain of

NKp46 is sufficient for the binding of NKp46 to tumor cells. However, it has been suggested that the membrane-distal domain of the receptor is dispensable for its function (Arnon et al., 2004). Recently, it was reported NKp46 and NKp30 involve heparin sulfate in the recognition of tumor cells (Bloushtain et al., 2004). In addition, it has been shown that high cell surface heparanase (heparin sulfate degrading enzyme), or low heparin sulfate expression on tumor cells, rendered them less susceptible to NK-mediated killing. Similarly, the absence of heparin sulfate expression reduced NK mediated lysis (Bloushtain et al., 2004).

NKp44 encodes a 44 KDa surface glycoprotein. Antibody blocking of NKp44 partially inhibited cytotoxicity against NK susceptible targets (Vitale et al., 1998). However, simultaneous blocking of both NKp44 and NKp46 led to a significant inhibition of NK cells activity (Vitale et al., 1998), suggesting a functional cross talk among these receptors (Augugliaro et al., 2003). In contrast to other NCRs, NKp44 is not expressed on resting NK cells, but it is upregulated in response to IL-2 activation *in vitro* (Vitale et al., 1998). *In vitro* upregulation of NKp44 by IL-2 may explain the enhanced cytotoxicity of IL-2 activated NK cells towards non-MHC restricted targets. Very little information is known about the cellular ligands of NKp44. The only identified ligand for NKp44 so far is the hemagglutinin (Arnon et al., 2001).

NKp30 was shown to synergize with NKp46 and NKp44 to enhance cytotoxicity, however, it also induces killing of targets that are NKp46/44-independent (Pessino et al., 1998 and Moretta et al., 2000). NKp30 is expressed on resting as well as activated NK cells (Moretta et al., 2000). NK cells incubation with TGF-β1 reduces NKp30

cytolysis activity suggesting a possible mechanism by which tumor cells that produce TGF-β evade NK response (Castriconi et al., 2003). NKp30 was also suggested to interact with cell surface heparin sulfate as a co-receptor (Bloushtain et al., 2004). The identified ligand for NKp30 so far is the HCMV tegument protein, pp65 (Arnon et al., 2005).

5.5 NK Cells in Anti-Tumor Defense Mechanisms

The evidence for NK cells role in tumor clearance came from the "missing self" hypothesis when the MHC class I negative RMA-S cell line was rejected while the same parental (positive for MHC class I) was not (Karre et al., 1986). *In vivo* deficiency studies supported NK-dependent rejection of many tumor cell lines (Kim et al., 2000). NK rejection of tumors was shown to be dependent on perforin (Van den Broek et al., 1995 and Smyth et al., 1999), IFNγ (Straat et al., 2001) and TNF-α (Smyth et al., 1998). The molecular mechanisms by which NK cells execute their antitumor effect is not completely defined. Chronic DNA damage response in tumors results in upregulation of NKG2D ligands suggesting a central role for this receptor in tumor control (Gasser et al., 2005). NKG2D was also shown to play an essential role in tumor metastasis (Smyth et al., 2005). NCRs are also crucial for the killing of tumors by NK cells since NKp46 blocking *in vivo* inhibited the NK anti-tumor response toward some melanoma cell lines (Pessino et al., 1998). In addition, deletion of the mouse NCR gene in mice diminished the ability of NK cells to eliminate tumors (Gazit et al., 2004). Recently, NK cells were shown to modulate the innate and adaptive immune response. Active NK cells are known to secrete IFNγ, which modulates downstream immune responses (Biron et al.,

2001). When IFNγ released into tumor-drained lymph nodes by NK cells it primes a Th1 response. Naive T helper (Th) cells are activated by recognition of antigens presented on antigen-presenting cells (APCs) by the interaction with the T-cell receptor (TCR). Upon activation, these effector Th cells can be divided into three main types: Th type-1 (Th1); Th type-2 (Th2); Th type-17 (Th17) cells, with unique characteristics for each type. Th1 cells secrete interferon (IFN)-γ, and (TNF)-β, which is critical for development of cell-mediated immune response and consequently tumor cells elimination (Martin-Fontecha et al., 2004). It was shown that NK cells could behave like APCs through antigen uptake and presentation to CD8 T cells (Hanna et al., 2004). In 1999, a report showed an interaction between NK cells and DCs (dendritic cells) in anti-tumor response (Fernandez et al., 1999). NK cells can activate DCs in the presence of TNF-α (Piccioli et al., 2002). In addition, NK cells induce maturation of DCs *in vivo*, which activates CD8+ T cells generating an anti-tumor response (Mocikat et al., 2003). These observations suggest that NK cells mediate its anti-tumor role through two independent effector and helper pathways.

5.6 Cancer Immunoediting

Cancer is a multistep process that represent dysregulation of both oncogenes and tumor suppressor genes. Transformed cells acquire genetic and epigenetic changes that contribute to the tumor phenotype. In order for normal cells to become malignant they exhibit six alterations in their physiology which include; (1) self-sufficiency in growth signals, (2) insensitivity to antigrowth signals, (3) limitless replicative potential, (4) evasion of apoptosis, (5) sustained angiogenesis (6) tissue

invasion and metastasis, (7) reprogramming of cellular energy metabolism, (8) evasion of the immune system (Douglas et al., 2011). The ability of the immune system to detect and eliminate transformed cells is known as immunosurveillance. Ehrlich's first introduced the concept of immunosurveillance in 1909, when he demonstrated the ability of the immune system to identify and destroy tumor cells. Ehrlich's observation was supported 50 years later by Burnet and Thomas when they suggested that lymphocytes were responsible for the eradication of continuously arising tumor cells (Burnet et al., 1970). Since then a lot of research has been done using a variety of well-characterized gene-targeted mice, specific immune system activators, and blocking monoclonal antibodies highly specific for distinct immunologic components, to identify components of the immune system that indeed protect the murine host against tumors which include for example IFNγ and effector lymphocytes (T, NK and NKT cells). Although the evidence for immunosurveillance depends mainly on mouse models, there is evidence that humans also exhibit cancer immunosurveillance. For example, during transplantation the immune system of the patients must be suppressed, which results in more susceptibility to non-viral cancers. Birkeland et al. showed increased cancer incidence for colon, lung, bladder, kidney, ureter, and endocrine tumors in 5692 renal transplant patients (Birkeland et al., 1995). In addition, tumor-infiltrating lymphocytes (TILs) is a predictor of patient's five-year survival. Balch et al. analyzed Tumor-infiltrating lymphocytes from 120 different human cancers, including breast cancer, renal cell carcinoma, melanoma, sarcoma, and colon cancer (Balch et al., 1990).

Based on the above, immunosurveillance is a multifactorial process that requires the actions of different immune effectors and this diversity is dependent on the tumor's type, anatomic localization, tumor stage, tumor’s acquired genetic and epigenetic changes, and immunological recognition pattern. Therefore, the immune system could promote or eradicate tumors, which is described by a new term, immunoediting. Immunoediting could result in (i) Elimination - This phase represents the ability of the immune system to eradicate the developing tumor (Figure 5.2).

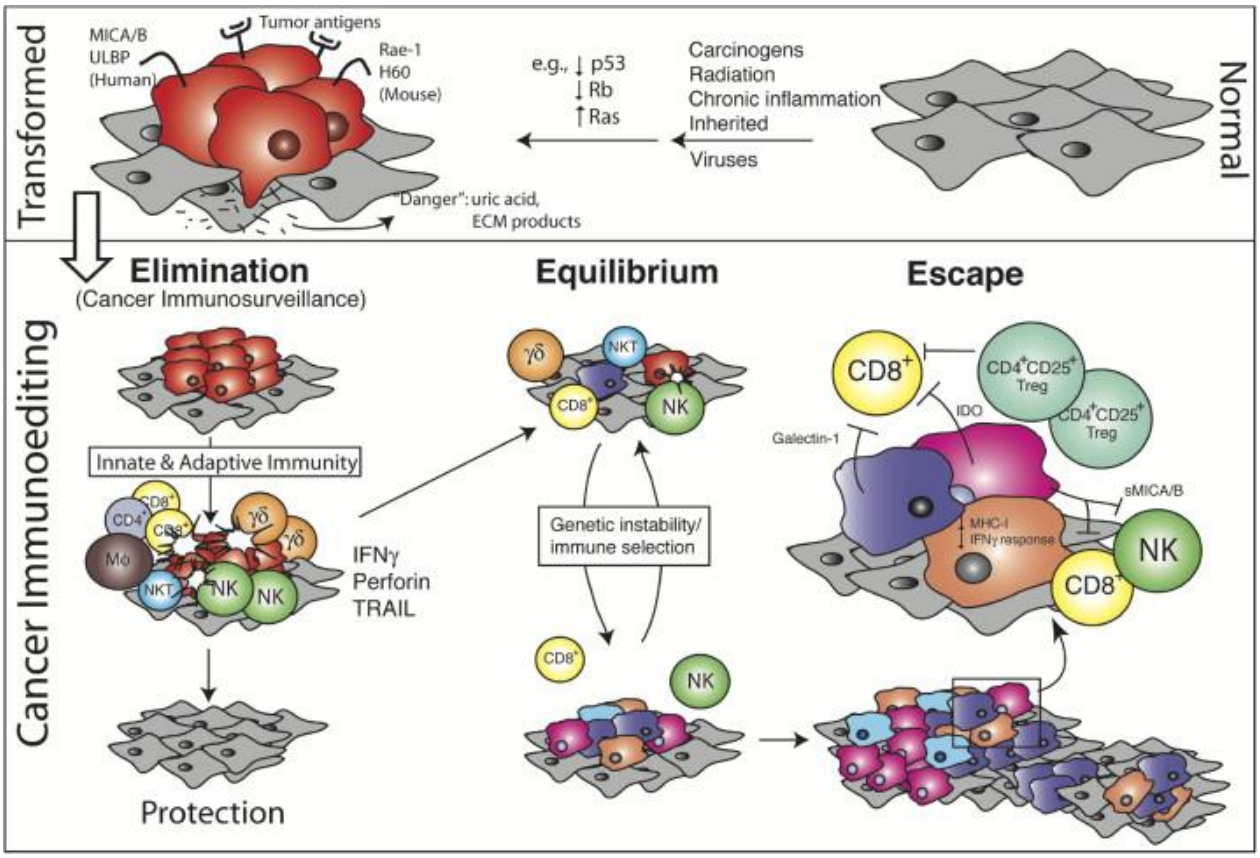

Figure 5.2: A Cartoon Illustrates the Three Phases of the Cancer Immunoediting Process. Normal cells (gray) are transformed to tumor cells (red) (top). In the elimination phase, cells and molecules of innate and adaptive immunity, may eradicate the developing tumor. However, if elimination fails, the tumor cells may enter the equilibrium phase where they may be either maintained chronically or edited by the immune system to produce tumor variants that may eventually evade the immune system by a variety of mechanisms and enter the escape phase (Dunn et al., 2004).

The elimination phase is initiated by disruption of tissue surrounding the tumor because of invasive growth and angiogenesis (Hanhan et al., 1996, Carmeliet et al., 2000 and Sternlicht et al., 2001). Stromal remodeling is accompanied by pro-inflammatory cytokines and chemokines production to recruit immune effector cells such as NK, T, NKT and /or macrophages to tumor site. The recruited immune cells are activated once they recognize their cognate ligands and secrete cytokines such as IFNγ, IL-2 and IL-12 that amplify the signal and recruit more CTL to tumor site (Hodge-Dufour et al., 1997). IFNγ can enhance the expression of tumoricidal products by macrophages, enhance NK cytotoxic function toward tumor cells and /or kill tumor cells by anti-proliferative, pro-apoptotic and angiostatic effects (Luster et al., 1993, Coughlin et al., 1998 and Qin et al., 2000). Dead tumor cells, in turn, become a source of antigens that could be directly cross-presented by DC to CD4 Th1 T cells to develop tumor specific CD8 T cells (Albert et al., 1998).

(ii) Equilibrium - In the equilibrium phase the tumor cells which survived the elimination phase enter a dynamic equilibrium with immune cells that exert selection pressure on these genetically unstable tumor clones. This phase is the longest of the three phases and it might take years for tumor cells in equilibrium to generate clones that are poorly recognized either by the immune system or that have acquired mechanisms to suppress immune effector functions (Loeb et al., 2005). (iii) Escape - In this phase, tumor cells at equilibrium acquire genetic and/or epigenetic modifications to avoid the immune system detection and elimination. Mechanisms of evasion include release of immunosuppressive factors such as TGF-β (Sakaguchi et al., 2001), induce

infiltration of regulatory T cells (Khong et al., 2002), antigenic drift, loss of MHC components (Marincola et al., 2000), shedding of ligands that induce cytotoxic activity of CTL (Groh et al.,2002) and /or development of IFNγ insensitivity (Kaplan et al., 1998). These mechanisms reflect how tumor cells can be edited by the immune system.

5.7 Breast Cancer & Immunoediting

Breast cancer is the most common cancer in women, approximately one in eight women developing breast cancer during their lifetime. Breast cancer is a heterogeneous disease with multiple subtypes and diverse histopathology that results in different clinical outcomes (Rosen et al., 2007). Tumor histological grade and tumor type are the most important tumor characteristics that can be estimated by histopathological analysis of breast cancer. There are many types of breast cancer which include adenocarcinomas, micro-papillary, metaplastic, medullary carcinomas and inflammatory. Tumor grade is an evaluation of the degree of differentiation, proliferative capacity that indicates the tumor's aggressiveness (Elston et al., 1991). Normal breast structure is composed of two epithelial layers, the inner luminal epithelium from which luminal epithelial breast cancer is derived and the outer basal epithelial layer from which the basal-like breast cancer originates. The confinement of breast cancer to breast ducts or lobes is referred to as DCIS (ductal carcinoma in situ) and LCIS (lobular carcinoma in situ) (Li et al., 2006). Breast cancer can be further classified into subtypes based on the incorporation of molecular markers of prognosis and recurrence such as ER, PR, Her/2neu and p53 (Silverstein et al., 1995).

There is evidence for immunosurveillance in breast cancer supported by the presence of CD4, CD8, CD20 and NK cells in DCIS lesions (Macchetti et al., 2006 and Czerniecki et al., 2007). This suggest that these effector cells might infiltrate the tumor to promote or eliminate the tumor. For example, breast tumors infiltrated with DCs that express the CD83 (maturation marker) exhibit prolonged disease-free survival in those patients (Czerniecki et al., 2007). However, the presence of CD4, CD8 positive T cells or macrophages showed no prognostic significance. The infiltration rate of T cells into tumors of patients with lymph node positive breast cancer was significantly increased relative to those without lymph node metastases (Macchetti et al., 2006). Similar to mouse studies (Knutson et al., 2006 and Santisteban et al., 2009) the presence of CD8 T cells in human breast cancer has not shown an association with increased survival. Some studies showed that increased tumor grade and Ki-67 staining (a marker of proliferation) were associated with increased infiltration of CD8, CD4, tumor-associated macrophages, and increased tumor angiogenesis. These results could be explained by: (i) the active immune response toward poorly differentiated tumors increases tumor proliferation, angiogenesis, and dissemination; (ii) high grade tumors secrete many cytokines in the tumor microenvironment, which attracts immune cells and increases microvessel density (Murri et al., 2008 and Matkowski et al., 2009). Collectively, the tumor immunogenicity and its microenvironment will likely dictate the type of infiltrating immune cells and their function whether to promote a tumor or impede it.

5.8 The NURF Complex

5.8.1 The Three Main Subunits of NURF Complex and Their Role in Cancer.

The NURF complex is a member of ISWI family and consists of the three main subunits: bromodomain PHD-finger containing transcription factor (BPTF); the ISWI ATPase SNF2L; the WD repeat protein pRBAP46/48 (Xiao et al., 2001and Barak et al., 2003). BPTF is the unique and largest subunit of NURF complex and it is crucial for the maintenance of complex integrity (Xiao et al., 2001). BPTF contains several conserved domains that form platforms for recruitment of modified histones, transcription factors and other NURF subunits, which include DDT domain, PHD finger, WAC and WAKZ in the N-terminal domain. The DDT domain interacts with the slide domain and this interaction is essential for maintaining the complex integrity (Xiao et al., 2001). The BPTF subunit has two PHD domains as mentioned above, which has Cys4HisCys3 (4 cysteines a histidine and 3 cysteines). The C-PHD domain strongly interacts with H3K4me3 or 2 while it interacts weakly with H3K4me1 (Wysocka et al., 2006). The bromodomain binds acetylated histones (H3K16ac) and cooperate with the C-terminal PHD which binds H3K4me3 to facilitate NURF localization to sites in chromatin with modified histones (Ruthenburg et al., 2011).

SNF2L is essential for both catalytic and remodeling functions of the NURF complex. The N-terminal domain of SNF2L includes ATP binding domain and helicase domain. The ATP binding domain is enriched with acidic residues that interact with the positive residues in the N-terminal tail of H4 to facilitate the NURF remodeling activity (Mueller et al., 2013). The C-terminus of SNF2L has three domains, HAND, SANT

(Swi3 Ada2-N-cor TfIIIB) and SLIDE (Sant like Domain) (Clapier and Carins et al., 2009). The HAND domain is required for the interaction with the nucleosomal DNA (Dang and Bartholomew 2007). The SANT domain is believed to enable the NURF complex to interact with histone H3 (Boyer et al., 2004). The SLIDE domain interacts with nucleosomal linker DNA and this interaction is required for the complex remodeling activity (Hota et al., 2013).

RbAp46 and RbAp48 are homologous proteins with WD (Tryptophan-Asparatic) repeats that form the platform to facilitate protein-protein interactions to tether the remodeler complex to its chromatin. Both proteins act as histone chaperones for histone deposition into nucleosomes. RbAp48 interacts with H3-H4 dimer to mediate its incorporation into assembled nucleosomes (Zhang et al., 2013). For example, the interaction between RbAp46/48 and the transcription factor FOG1 (Friend of Gata1) recruit the NURD complex to specific sites of chromatin (Hong et al., 2005). Both proteins are also involved in cancer. Overexpression of the RbAp46 in the human breast epithelial cells, MCF10AT3B, induced suppression of cell growth *in vitro* and reduced tumor formation *in vivo* (Li et al., 2003). Similarly, knockdown of the RbAp48 protein in the cervical cell line, H8, induced tumor formation in nude mice through the control of the HPV16 transforming activity (Kong et al., 2007).

5.8.2 NURF Remodeling Activity

As mentioned above, NURF complex subunits involved in protein-protein interactions which facilitate the complex remodeling activity by its recruitment to nucleosomes. Upon NURF recruitment, it binds the nucleosome at two separate sites,

at linker DNA beside the entry site, and the nucleosomal DNA at the exit site. After binding, the NURF complex utilizes ATP hydrolysis to move nucleosomes ~ 10bp in either direction (Schwanbeck and Wu 2004). The remodeling activity of NURF can be regulated by many mechanisms, which include: incorporation of a SNF2L variant that produce non-functional ATPase (Barak et al., 2004) or PTM of the NURF complex reduces its remodeling function. For example, ISWI acetylation by the histone acetyl transferase GCN5 has been thought to reduce the complex remodeling activity (Ferreira et al., 2007). In addition, the composition of the histone octamer and nucleosome structure can modulate the NURF activity. For example, the incorporation of the histone variant H2AZ enhances ATP hydrolysis ~9 fold greater than H2A and increases its remodeling activity (Goldman et al., 2010). Collectively, the NURF remodeling activity is affected by incorporation of an inactive ATPase, histone variants or the PTM of the complex (Alkhatib and Landry, 2011).

5.8.3 The Biological Roles of NURF Complex

The NURF complex interacts with many transcription factors and DBPs with consequences on gene expression and function (Xiao, et al. 2001). In Drosophila, NURF is required for the expression of homeotic genes and its disruption affects the determination of body segments (Badenhorst, Voas, et al. 2002). In addition, NURF is a co-activator of the Wingless pathway through its interaction with the pathway signal transducer β-Catenin/Armadillo, which is a transcription factor that recruit NURF to promoters of Wingless downstream genes to initiate their expression (Song, Spichiger-Haeusermann and Basler 2009). NURF is essential for self-renewal and maintenance of

germline stem cells through its positive regulation of the JAK/STAT pathway (Cherry and Matunis 2010). In human breast cancer cell lines, BPTF interacts directly with PR (progesterone receptor) to recruit NURF, which in turn recruits other co-activators to promote gene expression (Vicent, et al. 2011).

As a chromatin remodeler, NURF is involved in the regulation of the chromatin structure. NURF directly interacts with the histone chaperone Nap1 to regulate nucleosomes assembly at heterochromatin domains (Stephens , et al. 2006). NURF is also, involved in the separation between euchromatin and heterochromatin regions. In chicken erythroleukemia cell lines USF1 interact with NURF to mediate its recruitment to the HS4 element of the β-globin insulator. HS4 element is required to prevent the heterochromatin from disrupting β-globin locus expression (Li, et al. 2011). In addition, recent work in our lab supports the role of NURF in regulation of chromatin structure. CTCF is the main insulator in vertebrates with roles in chromatin looping to enhance gene expression like the ring-like structure cohesion. Insulators are DNA-protein complexes, which prevent enhancer-promoter interactions and/or form barriers to isolate the silencing effects of heterochromatin (Jingping et al., 2011). NURF interacts with both CTCF and cohesion suggesting a possible role in chromatin looping and organization (Qiu, et al. 2015).

In mammals, NURF is essential for early embryonic development since KO of the complex's essential subunit (BPTF) resulted in early embryonic lethality. *BPTF* KO embryos fail to gastrulate due to defective DVE differentiation, which could be due to its

co-activation role of the TGF/Smad pathway. Moreover, *BPTF* KO mESCs were defective in their differentiation potential, which is supported by the defective differentiation of embryoid bodies and teratoma *in vitro* (Landry et al., 2008). This observation was further verified by investigating the role of NURF in T cell development. Thymocyte maturation is accomplished by TCR (T-cell receptor) pathway to determine the lineage specification of a double positive cell that express both CD8 and CD4 to be a single positive cells that express CD8 or CD4. Thymocytes isolated from BPTF KO mice exhibited normal proliferation rate but fail to specify their lineage, which suggest the NURF role as cell type-specific regulator of gene expression (Landry, et al. 2011).

5.8.4 NURF and Cancer

BPTF and by extension NURF is located on chromosome 17 at q24.2, this region is amplified in many cancers including neuroblastoma (Bown, et al. 1999), breast cancer (Monni, et al. 2001), prostate cancer (Levin, et al. 2008), liver cancer (Raidl, et al. 2004) and lung cancer (Choi, et al. 2006), which suggest advantageous role for this region to tumor survival. BPTF overexpression is associated with more aggressive disease in HCC (hepatocellular carcinoma) and colorectal cancer (Xiao, Liu and Fang, et al. 2015). BPTF overexpression in melanoma is associated with poor prognosis, in addition, KD of BPTF reduced proliferation rate of melanoma cell lines both *in vitro* and *in vivo* (Dar, et al. 2015). *C-myc* is a proto-oncogene that is deregulated in many cancers (Vita et al., 2006). Recently, Richart et al. showed that BPTF is a co-partner of *c-myc* to regulate the transcription program of *c-myc* in MEFs and *in vivo* depletion of BPTF reduced tumor growth (Richart et al., 2015). Recent work in our lab revealed that

BPTF knock-down enhance tumor immunogenicity by directly regulating the immunoproteasome subunits *Psmb8* and *Psmb9*, *Tap1* and *Tap2*, which enhance antigen presentation and production (Mayes et al., 2016).

Chapter 6

Material and Methods

6.1 Cell Culture

67NR, 66cl4, 4T1 (Fred Miller, Wayne State University) and SY5Y, HeLa, HEK 293T (ATCC) were cultured in DMEM (Thermo-Fisher), 10% FBS (Hyclone), 1% NEAA (Thermo-Fisher), 1% glutamine (Thermo-Fisher), and 1% penicillin/streptomycin (Thermo-Fisher). T47D and MDA-MB-436 were cultured in RPMI (Thermo-Fisher), 10% FBS, 1% NEAA, 1% glutamine, 1% penicillin/streptomycin and 5 µg/ml insulin (Sigma). NK-92 cells (ATCC) were cultured in Alpha MEM (Thermo-Fisher), 12.5% horse serum (Sigma), 12.5% FBS, 2 mM L-glutamine, 1.5 g/L sodium bicarbonate (Sigma), 0.2 mM inositol (Sigma), 0.1 mM β-mercaptoethanol (Sigma), 0.02 mM folic acid (Sigma) and 200 U/ml Il-2 (R&D Systems). OT1 T cells were cultured in DMEM containing 10% FBS, 1% NEAA, 1 % glutamine, 1% penicillin/streptomycin, 1% HEPES (Thermo-Fisher), 50 µM β-mercaptoethanol and 500 U/ml mouse IL-2.

6.2 Western Blotting

Monolayer cells, cell pellet or collected tumors homogenate were homogenized by pipetting using 1 ml pf TRI-Reagent for 5 min. The homogenates were incubated with 200 µl chloroform for 15 min. Then, samples were centrifuged for 15 min at 20,000 RCF at 4°C. Three layers were formed; an aqueous phase contains the RNA, an interphase contains the DNA and an organic phase contains the proteins (bottom layer). After removing the aqueous and interphase, 1 ml isopropanol was added to samples and the

tubes were incubated at room temperature for 10 min. Then, the samples were centrifuged at 20,000 RCF for 15 min at 4°C. The supernatants were discarded and 1 ml of 0.3 M guanidine in 95% ethanol was added for overnight wash at 4°C on shaker. Then, the guanidine was removed by centrifugation at high speed and protein pellets were washed overnight with 1 ml of 100 % ethanol at 4°C on shaker. Next, proteins were dissolved in 250 µl of 8 M urea in 1% SDS at 65°C overnight. Protein concentration was measured using Bio-Rad Dc Protein Assay provided by Bio-Rad Laboratories (Hercules, CA) using BSA standards. 50 µg of protein was loaded into 4% SDS-PAGE, and run for 1 hour at 200 V and 300 mA. Next, proteins were transferred into PVDF (polyvinylidene fluoride) membrane for 17 hours at 20 V and 30 mA. Transfer buffer for Ino80 was 10 mM CAPS-NaOH [ph10.5] and 2.5 mM DTT. After transfer, the PVDF membranes were blocked with 5% non-fat dry milk for 1 h, and incubated with primary antibody for overnight at 4°C. Primary antibodies used in this study include; BPTF (custom rabbit polyclonal) at 2 µg/ml; anti-heparanase (Santa Cruz Cat# sc25826) at 1 µg/ml; anti-HS (Millipore Cat# MAB2040) at 2µg/ml. Next, membranes were washed three times with PBST (phosphate buffer saline with 0.1% tween 20) for 10 min each, and the membranes were incubated with horseradish peroxidase (HRP)-conjugated anti-rabbit or anti-mouse secondary antibody (Cell Signaling) at 0.1 µg/ml for 1hour. The plots were then washed for 10 min with PBST for three times and developed using Super Signal West Femto Substrate (Thermo Scientific).

6.3 BPTF KD (in OT1 & NK Cells Using Replication-Deficient Adenovirus)

Spleens from OT-l mice were harvested and dispersed into single cell suspensions in MACS buffer and erythrocytes were removed by suspension in RBC lysis buffer. The cells were then washed, suspended in DMEM containing 10% FBS, 1% NEAA, 1% glutamine, 1% penicillin/streptomycin, 1% HEPES, 50μM β-mercaptoethanol (Sigma) and 500 U/ml mouse IL-2 (R&D Systems), and co-incubated with mitomycin C-treated B16F10-OVA cells for 3 weeks with continuous medium change until we got a high population of OT1 T cells. $3X10^6$ NK-92 or $5X10^5$ OT1 T cells were infected with $2X10^7$ rADV or $2X10^6$ in a volume of 10 ml or 1 ml for 5 days and then collected for Western blot analysis. Remaining cells were used for cytotoxicity assays as described below.

6.4 Tumor Studies

$1x10^5$ 67NR cells, $1x10^4$ 66cl4 cells or $1X10^5$ 4T1 cells were injected into the fourth mammary fat pad of BALB/cJ or NSG mice. Tumors were analyzed at 21 days (67NR), 28 days (66cl4) or 35 days (4T1). For rADV studies, BALB/cJ mice were inoculated with $1x10^6$ 66cl4 or $3x10^5$ 4T1 cells and injected intratumorally with rADV-Luc or rADV-BPTF (1×10^9 PFU in 100ul) every 3 days for 3 weeks once tumors were ~5 mm in any dimension. Animals were euthanized 1 week after the last injections and tumors were collected for analysis. For all 4T1 studies, mice were injected I.P. with 1.2 mg/mouse gemcitabine 5 days after tumor inoculation and once every 7 days thereafter. The mice used in these studies were BALB/cJ (Jackson Laboratories Cat# 000651) and

NOD/SCID/Ifrg2r -/- (NSG) (Jackson Laboratories Cat# 005557) female mice 6-8 weeks of age were housed under aseptic barrier conditions. The Institutional Animal Care and Use Committee at Virginia Commonwealth University have approved these studies.

6.5 Mouse NK Cells Purification

The spleens of BALB/c mice and NK cells were purified by negative selection using a magnetic separation MACS column (Miltenyi Biotech, cat# 130-690-864.). The spleens were cut and pressed gently to release the splenocytes. The splenoctytes were collected with 5 ml of MACS column buffer (PBS [pH 7.2], 2 mM EDTA, 0.5% BSA) and passed through a 0.45 µm filter to create a single cell suspension. The cells were counted and centrifuged for 10 min at 300 x *g* before resuspending into 400 µl of buffer per 1 x 10^8 cells. 100 µL of a primary biotin-conjugated antibody cocktail (Miltenyi Biotec) was added per 1 x 10^8 cells and incubated on ice for 20 min. This cocktail binds all non-NK cells. 300 µL of buffer was subsequently added followed by 200 µL of secondary magnetic microbead-strepavidin antibody per 1 x 10^8 cells and incubated for 10 min on ice. The samples were then washed with 4 mL of buffer per 10^8 cells and centrifuged for 10 min at 300 x *g*. After carefully aspirating the supernatant, the cells were resuspended into 500 µL of buffer per 1 x 10^8 cells and separated on MACS LS columns (Miltenyi Biotec). The LS columns pre-rinsed with 3 mL of buffer before adding 500 µL of the prepared splenocytes suspension. Following this, 3 mL of buffer was added to the column to elute the unlabeled NK cells, while the column retained the biotin-labeled cell fractions. NK cells were eluted using three additions of buffer. The

eluted NK cells were centrifuged for 10 min at 300 x *g* and resuspended into 2 mL of complete RPMI-10 medium (10% FBS, 2 mM glutamine, 1x penicillin-streptomycin, 50 μM β-mercaptoethanol and 50 U/ml IL-2) and counted.

6.6 NK Cell Cytotoxicity Assay

NK 92 cells were cocultured with the targets, which were plated at the indicated E:T ratios for 4 hrs. For antibody blocking experiments, NK cells were pre-incubated for 1 hr with blocking antibodies to hNKp46 (Biolegend Cat# 13614), hNKp30 (Biolegend Cat# 325204) or hNKG2D (BD Pharmingen Cat# 552866) at 10 μg/ml. NK cells were then plated on mitomycin C treated cells for assay. Cell death was measured using the CytoTox 96® Non-Radioactive Cytotoxicity Assay (Promega). The plate was then placed on a plate reader and the wells were read at 490 nm absorbance for LDH release by spectrophotometer (Synergy H1 Multi-Mode Plate Reader, BioTek). Percent cytotoxicity was calculated using (Experimental – Effector Spontaneous – Target Spontaneous)/ (Target Maximum – Target Spontaneous) x 100.

6.7 Flow Cytometry

To measure NK activity, purified mouse splenic NK cells were incubated with mitomycin C treated cells for 24 hours. NK cells were removed and stained with BD Pharmagen antibodies; 0.25 μg anti-NKp46 (FITC), (Cat# 137605); 0.1 μg anti-CD69 (PE), (Cat# 561932) and 7AAD viability dye.

For tumor infiltrating lymphocyte analysis, tumors were minced and digested in 0.04% DNase 1, 0.1% collagenase IV (Sigma) at 37°C for 30 min. Tumor digests were

filtered with a 40 µM nylon filter and centrifuged at 500 x g for 5 min at room temperature. Cells were resuspended in 40% percoll (Sigma), layered on top of 70% percoll and centrifuged at 3000-x g for 30 min at room temperature. Lymphocytes at the interphase were removed, diluted in PBS, and centrifuged at 500 x g for 5 min at room temperature. Cells were stained with BD Pharmagen antibodies: 0.25 µg anti-NKp46 (FITC), (Cat# 137605); 0.1 µg anti-CD69 (PE), (Cat# 561932); 0.25 µg anti-CD3 (PE), (Cat# 553060); 0.25 µg anti-CD8 (FITC), (Cat# 100706) antibodies and 0.5 µg 7AAD viability dye.

For the *Ncr*1-Ig fusion protein was purified by protein G chromatography from the culture supernatant of stably transfected HEK293 cell line (gift from Ofer Mandelboim). $1X10^5$ Cells were incubated with 5 µg of the soluble receptor for 45min at 4°C, washed, stained with PE- anti-Human-IgG Fc (Biolegend Cat# 409304) for 20 min and analyzed by flow cytometry using a FACS Calibur flow cytometer (Becton Dickinson).

6.8 Enzyme Linked Immunosorbent Assay (ELISA)

Tumors were minced with a clean razor blade and placed in HBSS supplemented with complete protease inhibitor (Roche). After 3 of freeze-thaw cycles, samples were centrifuged at 15000 x rpm at 4°C for 15 min supernatant was collected and tested for total protein using a DC protein assay kit (Biorad). ELISA for IFNγ was performed according to the manufacturer's instructions (R&D systems). IFNγ concentrations was then normalized to total protein.

6.9 Ncr1- ζ Chain Reporter Assay

Murine BW thymoma cells (TCR α/β negative) were transfected with constructs encoding chimeric proteins in which the extracellular portion, which has the ligand binding domain of NKp46 is fused to the transmembrane and tail domains of the CD3 ζ chain. The cytoplasmic domain of the T-cell receptor ζ-chain is sufficient to trigger IL-2 secretion upon ligation of extracellular portion of NKp46 to its cognate ligand (Gili et al., 2009). To measure the levels of NCR1 and its ligands expressed by target tumor cell lines, BW Ncr1-ζ and target cell lines were co-incubated at 1:1 E: T ratio for 48 h at 37°C and 5% CO2. Total RNA was extracted from cultured cells with TRI Reagent and 5 µg RNA was reverse transcribed using Superscript II First-Strand Kit (Invitrogen). qRT-PCR was performed using SYBR green PCR master mix (Biorad) with a 7900 HT Fast Real-Time qPCR System (Applied Biosystems). The ΔΔCT method was performed using normalization to GAPDH. Primer pairs are provided in Table 6.1

Table 6.1: Primers Used for *IL-2* qRT-PCR

NCR1-Zeta IL2 Reporter Assay Primers	
NCR1	For GAGGATCAACACTGAAAAGGAGAC
	Rev ACTCTGCTTGGATGTTCCCA
IL- 2	For CCTGAGCAGGATGGAGAATTACA
	Rev TCCAGAACATGCCGCAGAG

6.10 qRT-PCR

qRT-PCR was performed as described in chapter two. Primers used for heparanase quantification are provided in Table 6.2.

Table 6.2: Primers for Heparanase Quantification

Heparanase qRT-PCR Primers	
mGapdh	For TGGCAAAGTGGAGATTGTTGCC
	Rev AAGATGGTGATGGGCTTCCCG
mHeparanase (67NR)	For GAGCGGAGCAAACTCCGAGTGTATC
	Rev GATCCAGAATTTGACCGTTCAGTT
mHeparanase (66cl4)	For GGAAATCTCAAGTCAACCATGATAT
	Rev ATCTCCACTGAGCTTCTTGAGTAG

6.11 Chromatin Immunoprecipitation (ChIP)

ChIP was performed as described in chapter two and primers used for heparanse promoter are provided in Table 6.3.

Table 6.3: Primers for Heparanae ChIP Analysis

Heparanase ChIP Primers	
Promoter Site	For GGTGGCCAGAATCCAAGATCC
	Rev AAAAACAGGGTCCCCACCAC

6.12 Statistics

Standard deviation was used to calculate error bars throughout the study. *P* values were calculated using two tailed T tests. Number of replicates are designated in the repetitive figure legends.

Chapter 7

Results

7.1 BPTF Depletion in Tumors Enhances NK Cell Antitumor Activity

To uncover the possible role for BPTF in breast cancer biology, we transduced the well-established 67NR and 66cl4 mouse breast cancer cell lines (Aslakson and Miller, 1992) with retroviruses expressing control (Ctrl-sh1, Ctrl-sh2) or BPTF (Bptf-sh1, Bptf-sh2) short hairpin RNAs (Figure 7.1 A). Both Ctrl and BPTF KD 66cl4 and 67NR cell lines were inoculated into the 4th mammary fat pad of syngeneic BALB/c mice and tumors were collected 3-4 weeks later and tumor weights were assessed. We observed a significant reduction in BPTF KD tumor weight compared to controls (Figure 7.1 B). Microarray analysis of control and BPTF KD tumors discovered an enrichment of genes with gene ontology (GO) terms that included immune response genes (data not shown) suggesting a possible role for the immune system in the BPTF KD reduced tumor weight. To validate our hypothesis, we have inoculated both Ctrl and BPTF KD 66cl4 and 67NR cell lines into an immune-deficient NOD/SCID, Ifrg2r -/- (NSG) background. Both Ctrl and BPTF KD 66cl4 and 67NR cell lines showed equivalent tumor weights to controls, suggesting an immune response toward BPTF KD tumors (Figure 7.1 C).

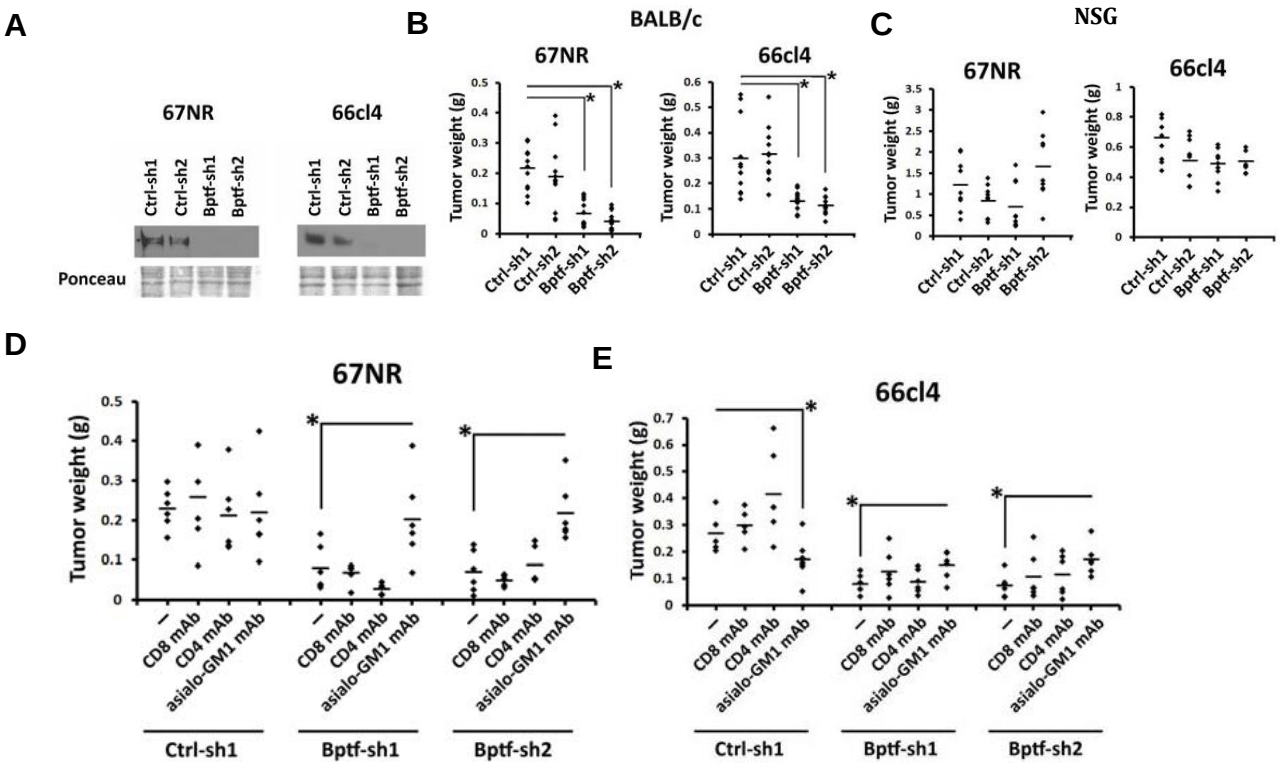

Figure 7.1: NK Cells Are the Key Effectors in BPTF KD 67NR and 66cl4 Tumor Weight Reduction.
A) BPTF Western blot analysis from control (Ctrl-sh1, Ctrl-sh2) and BPTF KD (Bptf-sh1, Bptf-sh2) 67NR and 66cl4 total cell extracts. Membranes were stained with Ponceau as a loading control.
B) 67NR and 66cl4 tumor weights harvested from BALB/c mice. Control and BPTF KD cells were injected subcutaneously into the fourth mammary fat pad of BALB/c mice and tumors were weighed on day 21 (67NR) or day 28 (66cl4) ($n \geq 11$, * = t-test p-value < 0.0005).
C) 67NR and 66cl4 tumor weights harvested from NSG mice ($n = 9$).
D&E) 67NR and 66cl4 tumor weights harvested from undepleted, or CD8+, CD4+ or asialo-GM1+ mAb depleted BALB/c mice ($n = 6$, * = t-test p-value < 0.05).
This figure is done by Suehyb Alkhatib and Kimberly Mayes.

The immune system executes its elimination function against tumors using immune effector cells. These immune effector cells infiltrate the tumor tissue to lyse tumor cells. Lymphocytes populations have been identified in breast cancer, which include ($CD8^+$) T cells, helper ($CD4^+$) T cells and NK cells (Whitford et al., 1992 and Chin et al., 1992). To characterize the main effector immune cells that are involved in BPTF KD reduced tumor weights, we depleted the major immune effector cells in mice that have been inoculated with both Ctrl and BPTF KD 66cl4 and 67NR cell lines using monoclonal antibodies against NK cells, CD8+ T cells, or CD4+ T cells. Depletion of CD8+ T-cell or CD4+ T-cell did not reduce the weight BPTF KD tumors (Figure 7.1 D, E). However, NK cell depletion resulted in approximately equal tumors weight in both Ctrl and BPTF KD 67NR and 66cl4 cell lines. These results suggest that NK cells are the major effector immune cells that are responsible for the reduced BPTF KD tumor weight.

To quantify and characterize the NK cell population in the tumor microenvironment (TME), we have conducted flow cytometry analysis on lymphocytes isolated from both Ctrl and BPTF KD 67NR and 66cl4 tumors. The gating strategy is illustrated in (Figure 7.2 A, C). To evaluate the abundance of lymphocytes in the TME, we stained lymphocytes with CD3 and NKp46 to select for the CD3- and NKp46+ population. We used the CD3 marker to exclude the NKT cell population that express NKp46 on their cell surface. As shown in (Figure 7.2 B) the rate of NK cells infiltration was very high in these tumors. To eliminate the possibility of non-specific staining, we repeated the same experiment using 4T1 tumors that are known to be poorly infiltrated

with NK cells (duPre et al., 2008). To assess the activation status of NK cells we used CD69, a known marker for lymphocytes activation. As shown in (Figure 7.2 D), that NK cell abundance in the TME was approximately equal in both Ctrl and BPTF KD 67NR and 66cl4 tumors. However, NK cells in BPTD KD TME were more active than those in Ctrl tumors (Figure 7.2 D). These results demonstrate that BPTF KD cells enhance NK cytotoxic activity, which could result in the observed reduced tumor weight.

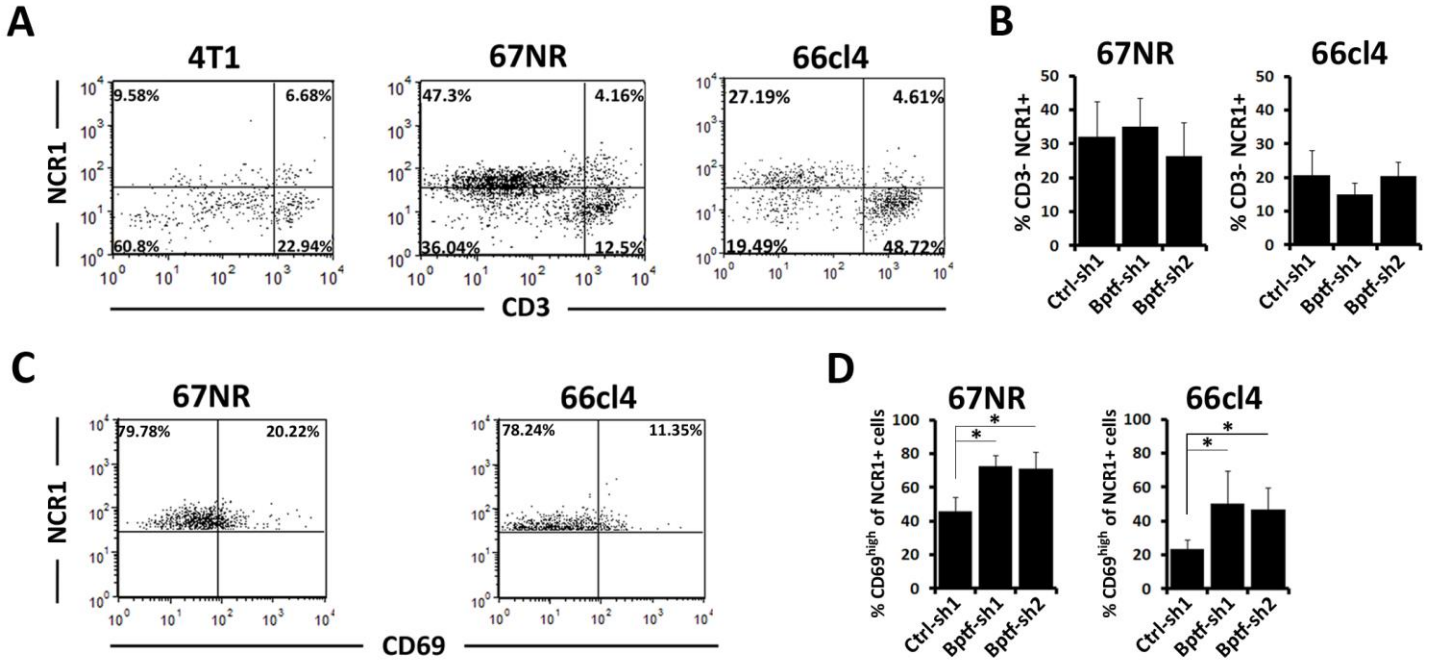

Figure 7.2: NK Cells Are More Active in the BPTF Depleted Tumor Microenvironments.
A) Representative flow cytometry dot plots of live tumor infiltrating NK cells stained with CD3ε and NCR1.
B) Percentages of live CD3-, NCR1+ NK cells from of all live lymphocytes isolated from tumors (n ≥ 6).
C) Representative flow cytometry dot plots of live tumor infiltrating NK cells stained with CD69 and NCR1.
D) Percentages of live NCR1+ cells that are $CD69^{high}$ (n = 6, * = t-test p-value < 0.006).
This figure is done by Mark Roberts and Zeinab Elsayed.

7.2 BPTF Depletion in Cancer Cells Enhances NK Cell Cytotoxic Activity *in Vitro* Through NCR Receptors

The ability of NK cells to kill BPTF KD cells *in vivo* suggests that BPTF KD cells are better targets than Ctrl cells for NK cells and enhance their cytotoxicity. To verify this observation *in vitro* we cocultured the purified splenic mouse NK cells with both Ctrl and BPTF KD 67NR and 66cl4 cells. Results showed that NK cells are more active when cocultured with BPTF KD targets as was indicated by the elevated expression of cell surface activation markers CD69 and NKp46 (Figure 7.3 A, B). The question now, how BPTF KD targets enhance NK cytotoxic activity. The most likely explanation is that BPTF KD cells overexpress or downregulate activating or inhibitory NK receptor ligands, respectively. However, NK cells have a hundred of activating and inhibitory receptors, which make it difficult to screen the ligands of all these receptors on the cell surface of BPTF KD targets.

In an attempt to narrow down our possible ligands, we have tested the ability of the human NK-92 cells to lyse both Ctrl and BPTF KD targets. NK-92 cells are IL-2-dependent human cell line that expresses high levels of activating receptors (NKp30, NKp46, 2B4, NKG2D and CD28), high levels of cytotoxic molecules such as perforins and granzymes, and few inhibitory receptors (Guitta et al., 2000). The number of major killing receptors that are involved in cancer elimination and conserved between NK-92 and naïve mouse NK cells are limited. Towards this end, we co-cultured our NK-92 cells with both Ctrl and BPTF KD targets and measured the cytotoxic effect of NK-92 cells. As illustrated in (Figure 7.3 C), NK-92 cells showed significantly more cytotoxic effects

toward BPTF KD targets compared to controls. These same results were observed using native mouse NK cells (data not shown). These results in combination suggest that NK-92 cytotoxic activities toward BPTF KD targets is due to a conserved cell surface receptor on both NK-92 and mouse naïve NK cells.

To identify the receptor on NK-92 which recognizes a BPTF-dependent ligand, we have blocked the major activating receptors on NK-92 cells using monoclonal antibodies against NKp46, NKp30 and NKG2D. The results showed that NKp30 blocking significantly diminished the NK-92 cytotoxic activity toward BPTF KD 66cl4 (Figure 7.4 A-C). NKp30 is highly expressed on NK-92 and it is also the major NCR used by NK92 cells for antitumor activity (Maki et al., 2001). Also, NKp46 reduced NK-92 cell activity but the results were not statistically significant. However, blocking of NKG2D has almost no effect on NK-92 cytolysis. These results demonstrate that NCRs are the major receptors involved in the killing of BPTF KD targets.

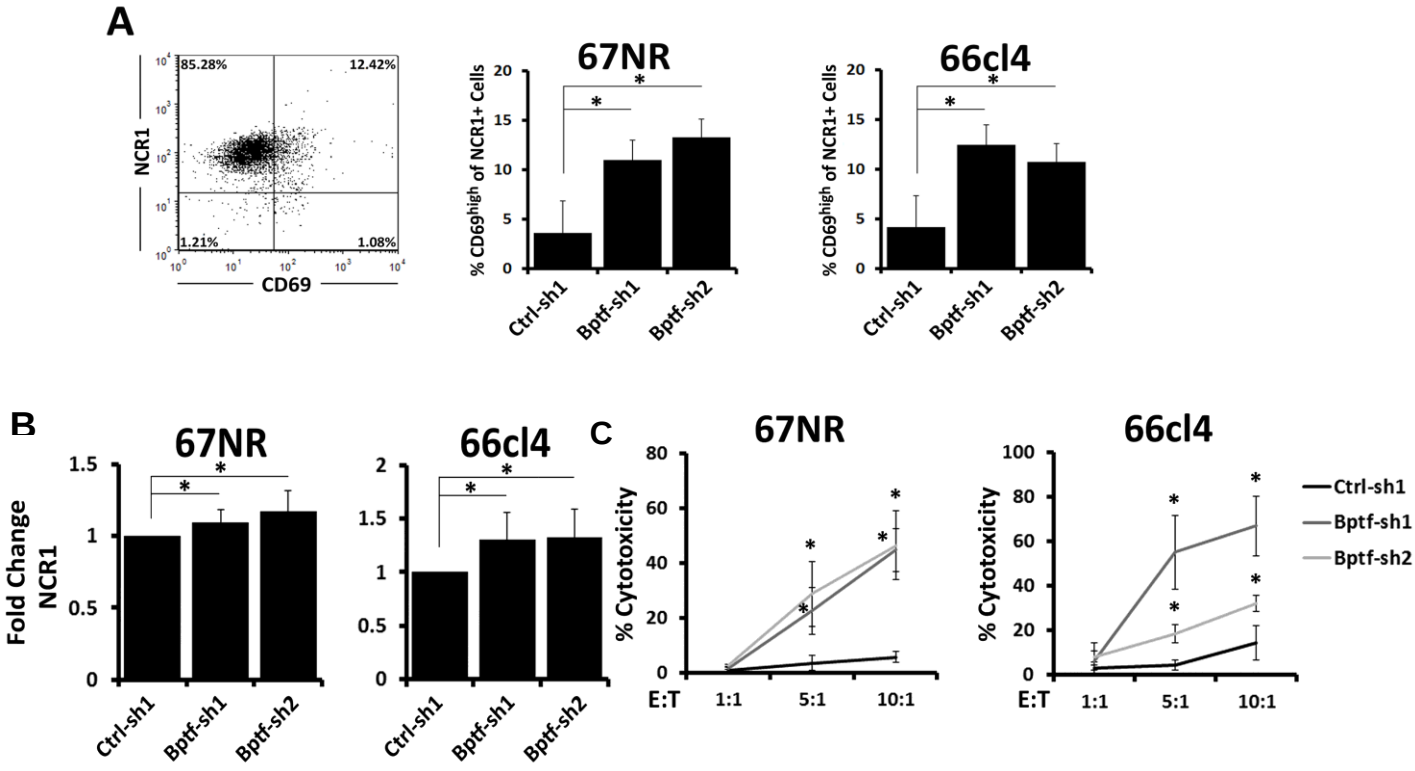

Figure 7.3: A Cell Surface Factor Enhances Mouse NK Cells and NK-92 Cells Activation Toward BPTF Depleted Tumor Cells.

A) Representative flow cytometry dot plot and percentages of live mouse NK cells stained with NCR1 and CD69 after coculture with 67NR or 66cl4 targets at a 5:1 E: T ratio (n = 3, * = t-test p-value < 0.04).

B) Fold change of NCR1 MFI on mouse NK cells after co-culture with 66cl4 or 67NR target cells at a 5:1 E: T ratio. (n ≥ 4, * = t-test p-value < 0.05).

C) NK-92 cells were cocultured with 67NR and 66cl4 at the indicated E: T ratios (n = 3, * = t-test p-value < 0.05).

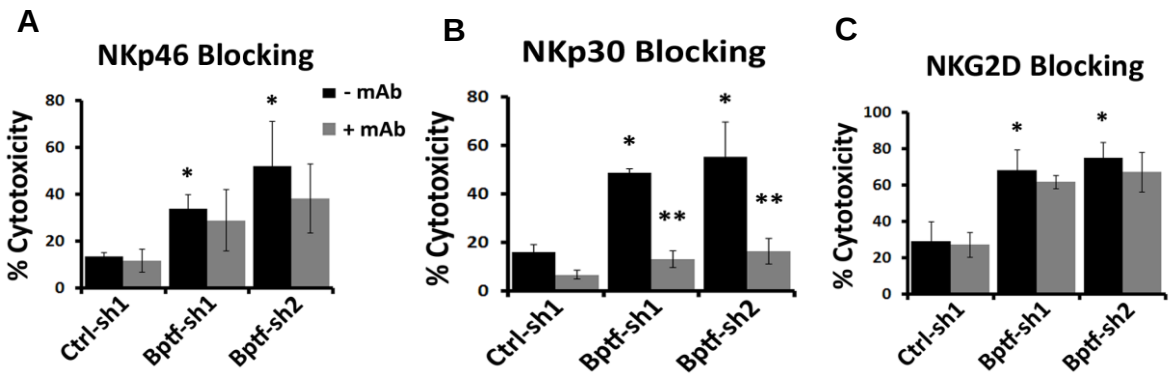

Figure 7.4: NKp30 is Required for BPTF KD Targets Killing by NK-92 Cells *in vitro.*
A) Cytolytic activity of NK-92 cells non-treated or pretreated with anti-NKp46 using the LDH assay,
B) Cytolytic activity of NK-92 cells non-treated or pretreated with anti-NKp30 using the LDH assay,
C) NK-92 cells non-treated or pretreated with anti-NKG2D mAb when cocultured with control or BPTF KD 66cl4 targets at a 10:1 E: T ratio (n = 3, * = t-test p-value < 0.05).

To verify our observation, we repeated our cytotoxicity assay in the presence of heparin. Soluble heparin is known to inhibit NCRs binding to their ligands on tumor cells and enhancement of NK cells activity. When BPTF KD targets cocultured with NK-92 cells in the presence of heparin, NK-92 cytotoxic activity was significantly reduced, which further supports that NKp30 is the NK-92 receptor that enhances their cytolysis activity toward BPTF knock-down targets (Figure 7.5 A, B).

NKp46, and its mouse orthologue NCR1, are important activation receptors that are involved in the killing of tumor cells *in vitro* and *in vivo* (Sivori et al.,1999, Sivori et al., 2000 and Gili et al., 2009). It has been shown that the proximal domain of NCR1 is the ligand binding domain that activates NK cells degranulation upon engagement (Alon et al., 2005). The fusion of this domain to the FC portion of the human IgG have been widely used to identify the receptor ligands (Gazit et al., 2006).

In order to assess the levels of NKp46/NCR1 ligands on the surface of both Ctrl and BPTF KD 67NR and 66cl4 cell lines, we stained cells with recombinant NCR1-Fc receptor. Flow cytometry analysis revealed equal binding of NCR1 in both Ctrl and BPTF KD cells (Figure 7.5 C). Based on cytotoxicity assay results that exhibited more NK cytotoxic activity toward BPTF KD targets suggests the presence of more activating ligand on BPTF KD targets. We explored the ability of both Ctrl and BPTF KD targets to induce *IL-2* expression in BW reporter cells.

The BW cells are a mouse thymoma cell line that lack the expression of α and β of TCR chains and can be induced to secrete IL-2. When the NCR1 ligand binding

domain is fused to the CD3-ζ chain and stably expressed in BW cells, the chimeric protein can induce the expression of *IL-2* upon ligand binding (Gili et al., 2009). As shown in Figure 7.5 D, co-incubation of both Ctrl and BPTF KD target with BW cells resulted in higher expression of IL-2 in BPTF KD targets, suggesting the presence of a functional NCR1 ligand on the cell surface of BPTF KD cells.

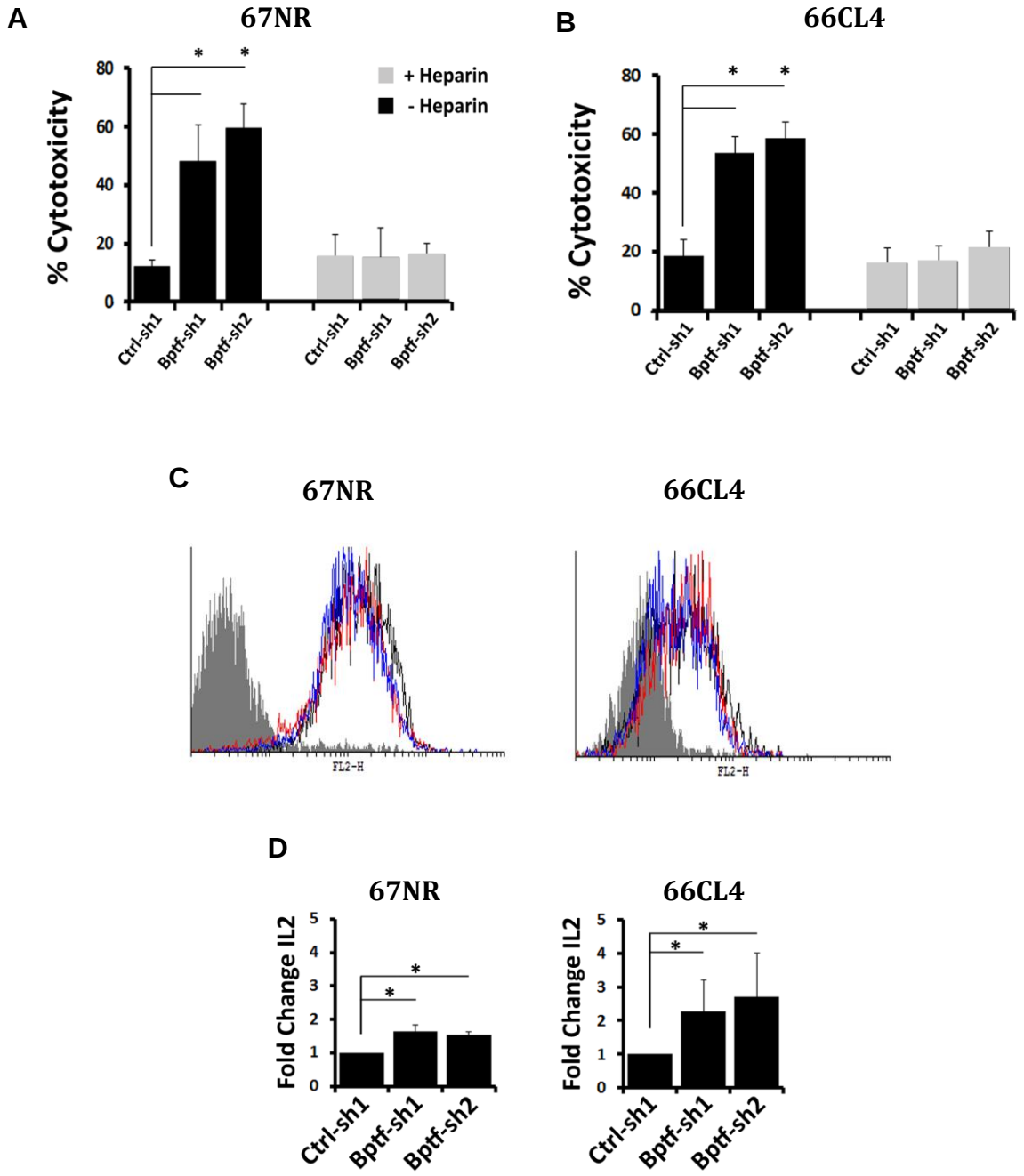

Figure 7.5: NK Cell Cytolysis Activity to BPTF KD Cells Requires NCR Receptors.
A and B) Percent target cell cytotoxicity as measured by LDH assay. NK-92 cells were cocultured with 67NR or 66cl4 targets at a 5:1 E: T ratio with or without heparin. (n = 3,* = t-test p-value < 0.05).
C) Representative flow cytometry histograms of NCR1-Ig binding to 67NR and 66cl4.
D) qRT-PCR analysis of *IL-2* expression in Ncr1-ζ, IL-2 reporter BW cells incubated with control or BPTF KD 66CL4 and 67NR cell lines for 48 hrs (n ≥ 3, * = t-test p-value < 0.05).

7.3 BPTF Regulates Cell Surface HS Abundance on HSPG and Heparanase Expression.

HS (heparin sulfates), also known as HSGAGs (heparin sulfate glycosaminoglycans), are members of the glycosaminoglycan family. HS are complex polysaccharides that are characterized by a repeat disaccharide unit of iduronic or glucuronic acid linked to a glucosamine. When the HS are covalently attached to proteins, they are called heparin sulfate proteoglycans (HSPGs). Although HS are expressed on the cell surface of both normal and tumor cells, their fine structure and sequence are modulated in both cell types to play diverse roles (Ram et al., 2002). It has been shown that the presence of HS on tumor cells induce NK cytotoxic activity through engagement with NCRs (Hershkovitz et al., 2008 and Hecht et al., 2009). Our microarray data (data not shown) revealed alteration in HS metabolism genes, which encouraged us to look at the levels of HS on the cell surface of both Ctrl and BPTF KD cells. As expected, the levels of HS were upregulated on the surface of BPTF KD 67NR and 66cl4 targets when compared to Ctrl cells (Figure 7.6 A) suggesting that high levels of HS on the surface of BPTF KD cells enhance NCR engagement and activate NK cell cytotoxicity.

Heparanase is an endo-glycosidase that cleaves the HS side chain of HSPGs on the cell surface. Heparanase is overexpressed in human tumors such as breast cancer (Gomes et al., 2013), hepatocellular carcinoma (El-Assal et al., 2001) and gastric cancers (Endo et al., 2001). Since it plays important roles in metastasis, angiogenesis

and inflammation. The levels of heparanase affect many physiological processes in the cell so its expression is tightly regulated (Nta et al., 2006).

So far, heparanase is the only known mammalian enzyme to regulate the levels of HSPGs on cell surface (Fuxt al., 2009 and Caruana et al., 2015). In an attempt to identify BPTF regulated genes that are involved in the regulation of HS on cell surface. We investigated the levels of heparanase using qRT- PCR and Western blot analysis. As shown in Figure 7.6 B, C, the levels of heparanase are substantially downregulated at both the levels of RNA and protein in BPTF KD 67NR and 66cl4 when compared to Ctrl. These data suggest that BPTF could directly regulate the levels of heparanase. To test this hypothesis, we have conducted ChIP experiment, which revealed heparanase promoter occupancy by BPTF supporting a direct role for BPTF in regulating the levels of heparanase in 67NR and 66cl4 cell lines (Figure 7.6 D) (Kuo and Allis, 1999).

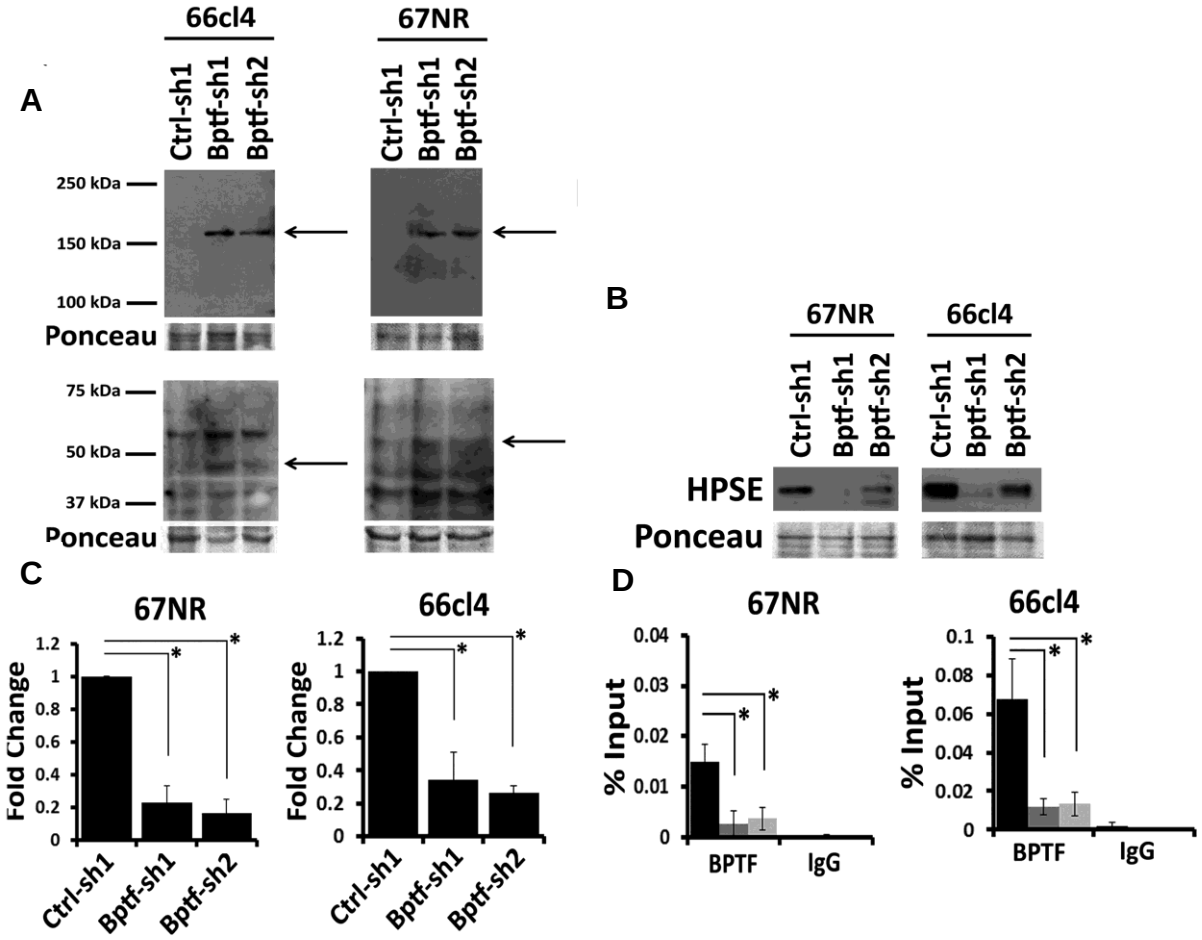

Figure 7.6: BPTF Regulates Heparanase Expression
A) HSPG Western blot analysis of cell surface extracts using anti-HS primary mAb. Arrows indicate reproducible changes in HSPG abundance with BPTF KD.
B) Heparanase Western blot analysis of cell surface extracts from control and BPTF KD cell lines.
C) qRT-PCR analysis of heparanase (HPSE) expression from 67NR and 66cl4 cells (n = 3, * = t-test p-value < 0.006).
D) BPTF ChIP at the mouse heparanase′ promoter (n = 3, * = t-test p-value < 0.04).
This figure is done by Kimberly Mayes.

7.4 BPTF Depletion Enhances the Immune Response to Established Tumors

In our transplantation experiments, we have used cell lines that constitutively express BPTF-shRNAs. Therefore, we decided to determine the antitumor effect of BPTF KD in established tumors. Toward this end, we constructed a replication-deficient adenovirus (rADV) expressing control or BPTF KD shRNAs. The ability of rADV to efficiently KD BPTF in both 66cl4 and 4T1 cells was first demonstrated *in vitro* (data not shown). Both 66cl4 and 4T1 cell lines were inoculated into BALB/c and once the tumors reached a palpable size (~5 mm), we started an intra-tumor injection with $1x10^9$ PFU rADV of either virus, three times a week for three weeks. BPTF levels in established tumors were reduced in response to rADV treatment as measured by Western blotting (Figure 7.7 A). BPTF KD in those tumors resulted in significant reduction in tumor weight (Figure 7.7 B) and in some cases to complete tumor regression in 66cl4 tumors. To evaluate the anti-tumor effect of BPTF KD, we measured the levels of infiltration and activation of NK cells in 66cl4 tumors and CD8+ T cells 4T1 tumors, respectively. We previously showed that BPTF KD enhances the CD8+ T cell response to 4T1 tumors because of improved tumor antigenicity (Mayes et al., 2016). BPTF KD in established tumors enhanced both NK and CD8+ T cells' activity (Figure 7.7 C).

Active immune effector cells are characterized by cytokine secretion such as IFNγ that modulate TME. To assess the ability of active of NK and CD8+ T cells for cytokine secretion, we measured the levels of IFNγ in the TME. As illustrated in Figure 7.7 D, BPTF KD tumors exhibit high levels of IFNγ demonstrating a conversion to a Th1 TME. rADV injection into established tumors could KD BPTF in tumor and non-tumor

cells. To monitor the effect of BPTF KD on NK cells and CD8 T cells, we transduced NK92 cells and splenic mouse OT1 T cells with rADV to knock-down BPTF, which was verified by Western blot analysis (Figure 7.8 A, C). After BPTF KD in NK-92 and OT1 T cells, we measured their cytolytic activity *in vitro*. Results showed that BPTF KD did not alter NK cells or T cell cytotoxic activity (Figure 7.8 B, D) indicating that rADV treatment of established tumors did not compromise effector cell function.

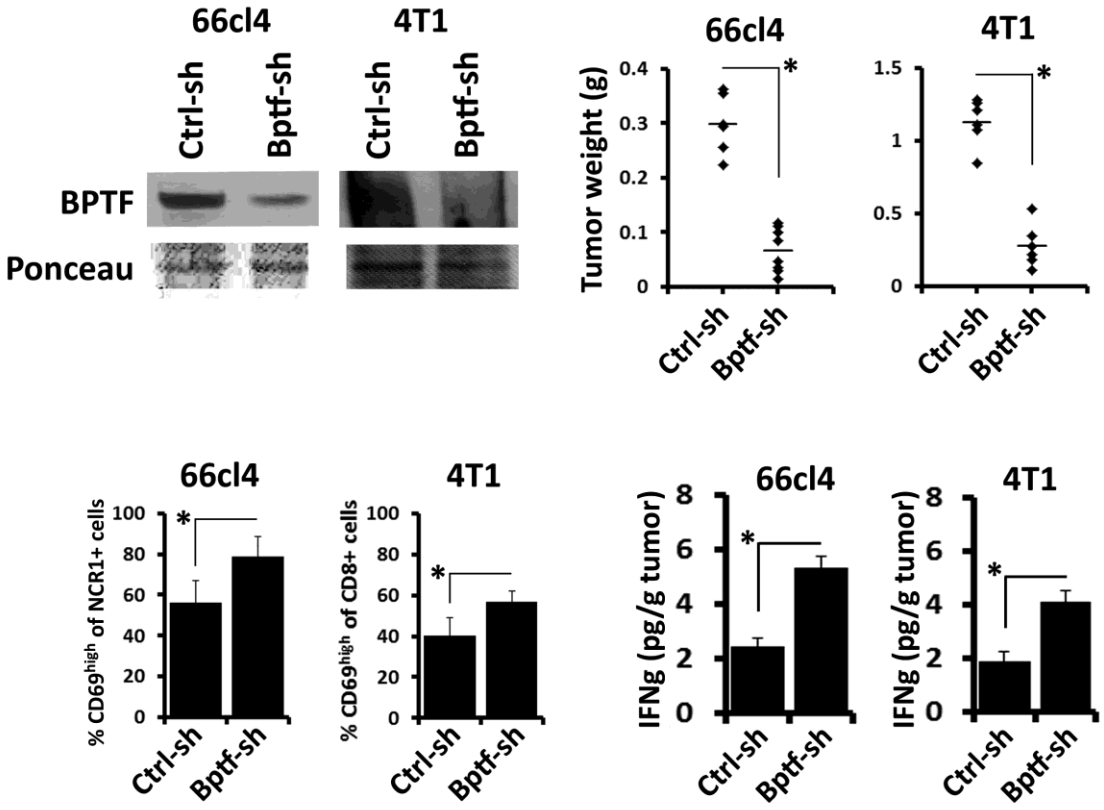

Figure 7.7: BPTF is Required for an Immune Suppressive Tumor Microenvironment.
A)BPTF Western blot analysis of 66cl4 and 4T1 tumors injected with replication-deficient adenovirus (rADV) expressing either control (Ctrl-sh) or BPTF KD (Bptf-sh) shRNAs.
B) Weights of 66cl4 and 4T1 tumors after treatment with rADV ($n \geq 6$, * = t-test p-value < 0.003).
C)Flow cytometry analysis of 66cl4 tumor infiltrating NK cells and 4T1 tumor infiltrating CD8+ T cells. Active lymphocytes are quantified as percent $CD69^{high}$ of total infiltrating NK cells (NKp46+) or CD8+ T cells (CD8+) ($n \geq 4$, * = t-test p-value < 0.01).
D) IFNγ concentrations from 66cl4 and 4T1 tumor extracts measured by ELISA ($n \geq 6$, * = t-test p-value < 0.04).
This figure is done by Mark Roberts and Zeinab Elsayed.

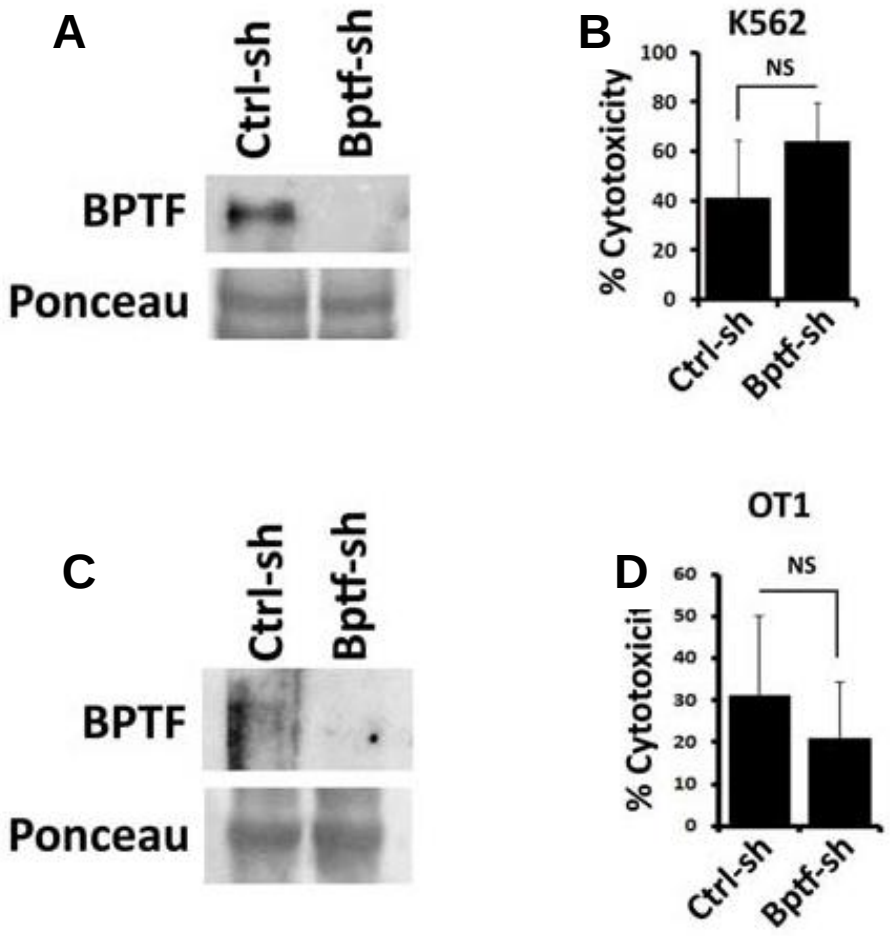

Figure 7.8: **BPTF is Not Required for NK or CD8+ T Cell Cytolytic Activity**.
A and C) BPTF Western blot analysis on total cell extracts from control and BPTF KD NK-92 or (*c*) mouse OT1 T cells after rADV infection.
B and D) Percent target cell cytotoxicity. (B) NK-92 or (D) mouse OT1 T cells were incubated with K562 cells for 4 hrs or B16F10-OVA targets or 24 hrs, respectively, at a 10:1 E: T ratio (n = 3).

7.5 NK Cytolysis Activity Toward BPTF KD Cells is Conserved in Human

In a first step toward understanding the mechanism for the enhanced cytolytic activity of NK cells to BPTF KD tumor cells, we determined if the effect is conserved between mice and humans. Toward this end, we transduced the human breast adenocarcinoma cell lines, T47D and MDA-MB-436, and the neuroblastoma cell line SH-SY5Y with lentiviruses expressing control or BPTF shRNAs (Figure 7.9 A, B). These human cell lines and the mouse 67NR and 66cl4 cell lines were cocultured with human NK-92 cells, an immortalized human NK cell line (Gong et al., 1994), and monitored for cytolytic activity. Similarly, we observed enhanced NK-92 cytolytic activity toward human BPTF KD targets compared to controls (Figure 7.9 C). Moreover, the levels of heparanase were also down regulated in these cells indicating that the mechanisms leading to NK enhanced cytolytic activity are conserved.

Collectively, our data suggest a model for BPTF in the suppression of NK antitumor activity as shown in Figure 7.10. BPTF is a positive regulator of heparanase in 67NR and 66cl4 cells and its depletion increases cell surface HSPG levels. HSPGs are activating ligands for the NK cells activating receptor NCR1 (in mouse) and NKp30 (in human), and their abundance on the cell surface made them better targets for NK cells cytolytic activity. In addition, active NK cells secrete IFNγ, which promotes the Th1 response, which in turn secrete more IFNγ that activate APCs and recruit more immune effector cells. We speculate that dead tumor cells in the TME result in more *de novo* antigens and enhance CD8 T cells effector function upon presentation. The combined effect of these responses promotes tumor elimination and host protection.

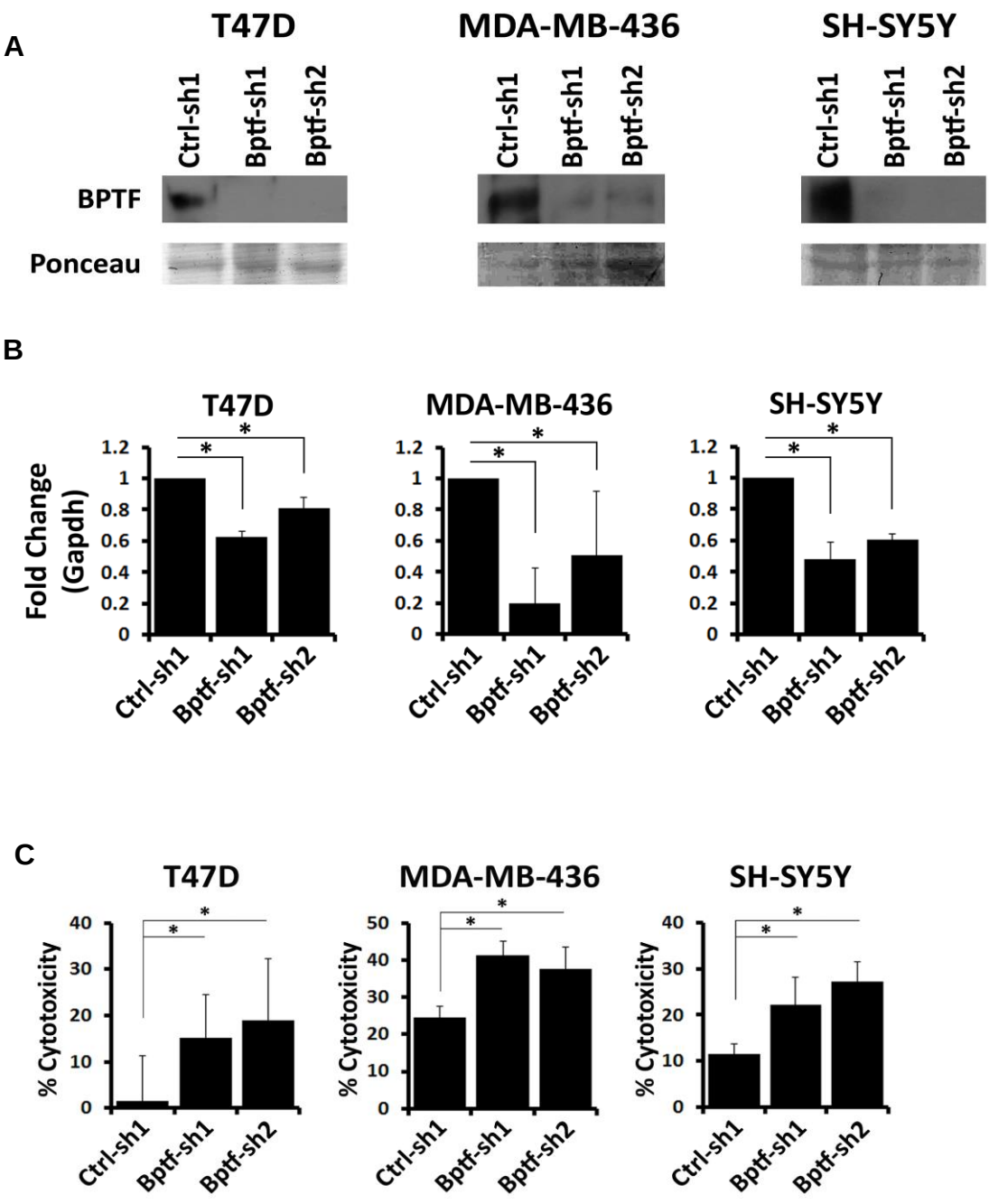

Figure 7.9: NK Cytolysis Activity is Conserved in Human Cell Lines.
A) BPTF Western blot analysis of heparanase in control and BPTF KD T47D, MDA-MB-436 and SH-SY5Y total cell extracts. **This is done by Dr.Joseph Landry.**
B) qRT-PCR analysis of heparanase expression in T47D, MDA-MB-436 and SH-SY5Y cells (n = 3, * = t-test p-value < 0.05). **This is done by Kimberly Mayes.**
C) NK-92 cells were co-cultured with T47D, MDA-MD-436 or SH-SY5Y at a 10:1 E: T ratio (n = 3, * = t-test p-value < 0.05).

A Model for the Effect of BPTF KD in Anti-Tumor Immunity

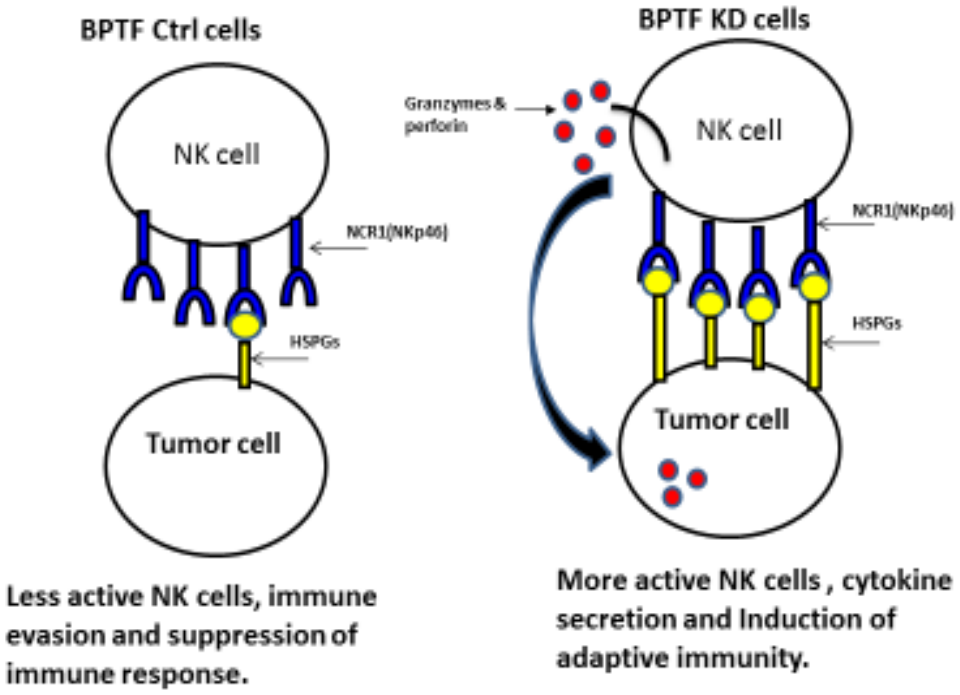

Figure 7.10: A Model for BPTF Suppression of Anti-Tumor Activity.
In BPTF Ctrl cells, NURF stimulates heparanase expression, which consequently reduces cell surface HSPGs (NCR1 co-ligand) abundance, inhibiting NK-cell antitumor activity. However, in BPTF KD cells, heparanase levels are reduced resulting in elevated HSPGs on the cell surface and enhancement of NK cell-mediated antitumor activity.

Chapter 8

Discussion and Future Directions

Tumor immune evasion is an important step for cancer progression, which is accomplished by acquiring genetic and epigenetic modifications. These changes can result in defective antigen presentation, upregulation of immune suppressive mediators and/or down regulation of NK ligands for activating receptors (Vinay et al., 2015). Genetic changes are irreversible and occur at lower frequency than reversible epigenetic changes making them appealing therapeutic targets (Kornel et al., 2007). ATP dependent chromatin remodeling complexes are gate-keepers that regulate the accessibility to DNA or histone modifiers predicting an essential role for these complexes in cancer biology. To understand how the ATP dependent remodeling complex NURF is involved in breast cancer progression, we used mouse transplantable tumor models. In these models BPTF KD induced NK antitumor response and polarized TME toward tumor rejection and eradication by inducing Th1 response.

BPTF is the largest and essential subunit of the NURF complex (Barak et al., 2003, Xiao et al., 2001). BPTF is unique subunit for the NURF complex so; its knockdown will not cause pleotropic effects that could complicate our results. BPTF has a tumorigenic role in skin, lung, colon and liver (Dai et al., 2015, Xiao et al., 2015, Buganim et al., 2010, Xiao et al., 2015)**.** However, its exact role in breast cancer biology is not well understood. To uncover its roles in breast cancer biology we used well-characterized mouse models of breast cancer. The cell lines used in this study (67NR,

66cl4 and 4T1) were isolated from same tumor (Aslakson and Miller, 1992). Both 4T1 and 66cl4 cell lines are metastatic while 67NR is not. 4T1 is highly immunogenic and it is characterized by high infiltration rate of suppressive immune cells such as immature DCs, Tregs, MDSCs and both M1&M2 macrophages (Aslakson and Miller, 1992 and Zaidi et al., 2011). However, the immunogenicity of both 67NR and 66cl4 is not defined. BPTF knock-down in both immunogenic and non-immunogenic cell lines resulted in reduced tumor weights suggesting that BPTF depletion can overcome immune suppressive mechanisms developed by tumor cells. Our depletion experiments revealed that NK are the major effector cells involved in the reduction of BPTF KD cells. NK cells represent the key component of the innate immune system that recognize and eliminate cancer cells. There is recent clinical and experimental evidence that NK cells are critically involved in the immune surveillance of tumors (Waldhauer and Steinle 2008).

NK cell cytotoxic activity results from the integration of multiple activating and inhibitory signals (Chester et al., 2015). We looked at the levels of NK inhibitory ligands but they were expressed equally on both Ctrl and BPTF KD targets (data not shown). We also tested the possibility that BPTF KD targets secrete a soluble factor to activate NK cells. These experiments revealed that NK activity is due to a cell surface receptor rather than a soluble ligand (data not shown). To complete cytotoxicity assays we took advantage of NK-92, a highly cytotoxic human cell line that is IL-2-dependent (Guitta et al., 2000). NK-92 express high levels of activating receptors such as NKp30, NKp46, and 2B4, NKG2D, E and CD28 and the expression levels of cytotoxic molecules such as perforins and-granzymes are also high (Guitta et al., 2000). Conversely, they

express few inhibitory receptors like NKG2A/B very low levels of KIR2DL4 and ILT-2 lack most the killer inhibitory receptors (KIRs). The increased cytotoxic activity of NK-92 cells toward BPTF KD targets supports the presence of a conserved active receptor-ligand between mice and human that is responsible for their enhanced activity. These results also excluded the possibility of an antibody dependent cell cytotoxicity (ADCC) since NK-92 do not express the FC-gamma receptor.

Our microarray data support the role of BPTF in regulating HSPGs (data not shown) leading us to a defined set of activating receptors on NK-92 cells (NCRs-NKp30, NKp44 and NKp46) and their conserved homologue in mice NCR1. Antibody blocking and heparin competitive inhibition experiments revealed that NKp30 (and NCR1 in mice) is most likely to be the target receptor. The NKp30 is involved in the crosstalk between NK cells and immature dendritic cells (iDCs) (Simhadri, and Reiners et al. 2008). The cross-talk may either result in a reciprocal activation and maturation of both cell types or in NK cell-dependent killing of immature dendritic cells, a mechanism that limits the supply of antigen-presenting DCs to the immune response (Walzer, Dalod et al. 2005). In this crosstalk, NKp30 on NK cells seems to be the driving and critical receptor for both processes (Ferlazzo, Tsang et al. 2002; Vitale, Della Chiesa et al. 2005; Walzer, Dalod et al. 2005; Simhadri, Reiners et al. 2008).

We used two approaches to support our finding; the first approach was the use of NCR-Fc soluble receptors that bind their cognate ligands if expressed on target cells. Although the binding of both BPTF Ctrl and KD targets was similar, the second

approach was enhancement of *IL-2* expression in BW reporter cell line. Although both Ctrl and BPTF KD targets bind equally to NCR1-Fc BPTF KD targets enhanced more *IL-2* expression when in contact with the Ncr1-zeta BW reporter line. This could be explained by different glycosylation pattern of the Ncr1 receptor in BW and HEK-293 cells which results in differential ligand binding (Ariella et al., 2015). Another possibility is that BPTF KD targets expresses adhesion molecules that synergize with NCR1 and enhance *IL-2* expression.

We have attributed the lower levels of HSPGs on BPTF Ctrl cells to higher expression levels of heparanase. Higher levels of heparanase expression was supported experimentally by Western blot and QPCR analysis. The BPTF dependent regulation of heparanase could be direct due to the fact that BPTF occupies the heparanase promoter region as illustrated by CHIP analysis. BPTF regulation of heparanase expression could have broader implications since heparanase is involved in many tumor promoting processes such as angiogenesis, metastasis, and inflammation (Hammond et al., 2014). It has been shown that BPTF KD in melanoma tumors reduced their metastatic potential (Dar et al., 2015). Our data suggest that BPTF could reduce metastasis through heparanase regulation. The connection between BPTF depletion and heparanase down-regulation and their effect on metastasis needs to be further tested.

In our model, depletion of BPTF in established tumors overcame the suppressive effect of TME and enhanced NK cytotoxic function. Antitumor activity of NK cells could be direct or indirect. The direct effect of NK cells is lysis of tumor cells and

secretion of IFNγ. IFNγ secretion in the TME can indirectly enhance Th1 cells to control tumor growth (Ribas et al., 2003). In addition, because of IFNγ secretion, tumor cells induce Fas expression and NK cells can kill them in a Fas ligand-dependent manner, the lysis of tumor cells release *de novo* antigens, which in turn enhance tumor antigenicity (Screpanti et al., 2001). Moreover, IFNγ stimulate the maturation of dendritic cells, which promote strong and protective CD8 T cell response (Mocikat et al., 2003; Adam et al., 2005). For 4T1 tumors, IFNγ is secreted by T cells, which can activate antitumor T cells and promote the production of nitric oxide synthetase (Shankaran et al., 2001). High levels of NO (nitric oxide) in the TME can directly induce apoptosis through caspase activation, DNA fragmentation and chromatin condensation (Dimmeler et al., 1997, Brune et al., 1998). Finally, BPTF depletion in 66cl4 or 4T1 tumors enhance immune effector cells activity generating a positive feedback loop that helps in tumor elimination (Heba et al., 2011).

BPTF depletion in 66cl4 tumors with rADV resulted in complete tumor regression in about 18% of the mice. This regression was not observed in 4T1 tumors possibly due to (i) 66cl4 tumors are infiltrated by significantly large number of NK cells, which upon activation by BPTF depletion can completely eradicate tumors (Figure 7.2 A). In addition, 4T1 cells is infiltrated by significant number of MDSCs, which are suppressive immune cells. Although we treated the mice with gemcitabine (Le et al., 2009) to eliminate MDSCs, the inability to achieve tumor regression could be a result of their residual activity. In the future, we can try high concentration of the rADV to treat 4T1 tumors to get a similar response to 66cl4.

BPTF depletion could synergize with other epigenetic modification inhibitors such as the currently used DNMTi (DNA methyltransferase inhibitors). DNMTi are demethylation agents that are known to induce the immune response by removing the methylation suppressive effect on tumor antigens such as cancer testis antigens (CTAs) and stimulating a CD8+ T cell response (James et al., 2006). DNMTis are also known to induce heparanase expression possibly by promoting cancer biology (Ateeq et al., 2008; Shteper et al., 2003). Combination of DNMTi and NURF inhibitors could possibly inhibit heparanase upregulation, enhance CD8 T, cells and synergize with the beneficial antitumor immune response by enhancing NK cells antitumor activities.

Chapter 9

References

Alatwi HE, Downs JA. Removal of H2A.Z by INO80 promotes homologous recombination. EMBO Rep. 2015; 16, 986-94.

Alén, Claudia, Nicholas A Kent4, Hannah S Jones, Justin O'Sullivan, Agustín Aranda, and Nicholas J Proudfoot. "A role for chromatin remodeling in transcriptional termination by RNA polymerase II." Molecular Cell 10, no. 6 (2002): 1441–1452.

Alkhatib, Suehyb, and Joseph W Landry. "The Nucleosome Remodeling Factor." FEBS Letter.2011; 3197-3207.

Andrew J Bannister and Tony Kouzarides.Regulation of chromatin by histone modifications. Cell Res. 2011; 21(3): 381–395.

Anfossi, N. et al. Human NK cell education by inhibitory receptors for MHC class I. Immunity. 2006; 25, 331–42.

Aparicio O, Geisberg JV, Struhl K. Chromatin immunoprecipitation for determining the association of proteins with specific genomic sequences in vivo. Curr Protoc Cell Biol. 2004; Chapter 17: Unit 17.7.

Arman E, Haffner-Krausz R, Chen Y, Heath JK, Lonai P. Targeted disruption of fibroblast growth factor (FGF) receptor 2 suggests a role for FGF signaling in pregastrulation mammalian development. Proc Natl Acad Sci. 1998; 95, 5082–5087.

Arnon, T., Markel, G. and Mandelboim, O. Tumor and viral recognition by natural killer cells receptors. Semin. Cancer Biol. 2006; 16, 348–358.

Arnon, T.I., Achdout, H., Levi, O., Markel, G., Saleh, N., Katz, G. et al. Inhibition of the NKp30 activating receptor by pp65 of human cytomegalovirus. Nat Immunol. 20056; 515–23.

Arnon, T.I., Achdout, H., Lieberman, N., Gazit, R., Gonen-Gross, T., Katz, G. et al. The mechanisms controlling the recognition of tumor- and virus-infected cells by NKp46. Blood.2004; 103, 664–72.

Ashby J Morrison & Xuetong Shen. Chromatin remodelling beyond transcription: the INO80 and SWR1 complexes. Nature. 2009; 10, 373-384.

Aslakson, C.J., and F.R. Miller. Selective events in the metastatic process defined by analysis of the sequential dissemination of subpopulations of a mouse mammary tumor. *Cancer Res*. 1992; 52, 1399-1405.

Augugliaro, R., Parolini, S., Castriconi, R., Marcenaro, E., Cantoni, C., Nanni, M. et al. Selective cross talk among natural cytotoxicity receptors in human natural killer cells. Eur J Immunol. 2003; 33, 1235–41.

Augugliaro, R., Parolini, S., Castriconi, R., Marcenaro, E., Cantoni, C., Nanni, M., Moretta, L., Moretta, A., and Bottino, C. Selective cross talk among natural cytotoxicity receptors in human natural killer cells. Eur J Immunol. 2003; 33, 1235.

B. Brune, A. von Knethen, K.B. Sandau. Nitric oxide and its role in apoptosis
Badenhorst, Paul, Matthew Voas, Ilaria Rebay, and Carl Wu. "Biological functions of the ISWI chromatin remodeling complex NURF." Genes Dev. 2002; 3186–3198.

Barak, Orr, Maribeth A Lazzaro, Neil S Cooch, David J Picketts, and Ramin Shiekhattar. "A Tissue-specific, Naturally Occurring Human SNF2L Variant Inactivates Chromatin Remodeling." The Journal of Biological Chemistry. 2004; 279, 45130-45138.
Barski, Artem, et al. "High-Resolution Profiling of Histone Methylations in the Human Genome." Cell. 2007; 129, 823–837.

Bartholomew, Blaine. "Regulating the Chromatin Landscape: Structural and Mechanistic Perspectives." Annu. Rev. Biochem. 2014; 83, 671–696.

Bauer, S., Groh, V., Wu, J., Steinle, A., Phillips, J.H., Lanier, L.L. and Spies, T. Activation of NK cells and T cells by NKG2D, a receptor for stress-inducible MICA. Science.1999; 285, 727.

Becker, Peter B, and Jerry L Workman. "Nucleosome Remodeling and Epigenetics." Cold Spring Harb Prespect Biol 5 (2013): a017905.

Biassoni, R., Pessino, A., Bottino, C., Pende, D., Moretta, L., Moretta, A. The murine homologue of the human NKp46, a triggering receptor involved in the induction of natural cytotoxicity. Eur J Immunol. 1999; 29, 1014–20.

Biron, C.A. and Brossay, L. NK cells and NKT cells in innate defense against viral infections. Curr Opin Immunol.2001; 13, 458.

Bloushtain, N., Qimron, U., Bar-Ilan, A., Hershkovitz, O., Gazit, R., Fima, E. et al. Membrane-associated heparan sulfate proteoglycans are involved in the recognition of cellular targets by NKp30 and NKp46. J Immunol. 2004; 173, 2392–401.

Bouabe H, Okkenhaug K. Gene targeting in mice: a review. Methods Mol Biol. 2013; 1064, 315–36.

Bown, Nick, et al. "Gain of Chromosome Arm 17q and Adverse Outcome in Patients with Neuroblastoma." N Engl J Med 1999; 340, 1954-1961.

Boyer, Laurie A, Robert R Latek, and Craig L Peterson. "The SANT domain: a unique histone tail binding module?" Nature review | Molcular cell biology. 2004; 5, 1-6.

Bryceson, Y. & March, M. Activation, coactivation, and costimulation of resting human natural killer cells. Immunol. Rev. 2006; 214, 73–91.

Bryceson, Y.T., March, M.E., Ljunggren, H.G. and Long, E.O. Synergy among receptors on resting NK cells for the activation of natural cytotoxicity and cytokine secretion. Blood. 2005; 107, 159-66.

Burnet FM. The concept of immunological surveillance. Prog. Exp. Tumor Res. 1970; 13, 1–27.

Burdon, T., Smith, A. and Savatier, P. Signalling, cell cycle and pluripotency in embryonic stem cells. Trends Cell. Biol. 2002; 12, 432-438.

David Allis and Thomas Jenuwein. The molecular hallmarks of epigenetic control.Nature Rev. 2016; 17, 487-500.

Carmeliet P, Jain RK. Angiogenesis in cancer and other diseases. Nature. 2000; 57, 407-249.

Castriconi, R., Cantoni, C., Della Chiesa, M., Vitale, M., Marcenaro, E., Conte, R., Biassoni, R., Bottino, C., Moretta, L. and Moretta, A. (2003). Transforming growth factor

beta 1 inhibits expression of NKp30 and NKG2D receptors: consequences for the NK-mediated killing of dendritic cells. Proc Natl Acad Sci. 2003; 100, 4120.

Cerwenka, A., Bakker, A.B., McClanahan, T., Wagner, J., Wu, J., Phillips, J.H. and Lanier, L.L. Retinoic acid early inducible genes define a ligand family for the activating NKG2D receptor in mice. Immunity. 2000; 12, 721.

Chan, H.-W. et al. DNA Methylation Maintains Allele-specific KIR Gene Expression in Human Natural Killer Cells. J. Exp. Med. 2003; 197, 245–255.

Chia NY, Chan YS, Feng B, Lu X, Orlov YL, Moreau D, Kumar P, Yang L, Jiang J, Lau MS, et al. A genome-wide RNAi screen reveals determinants of human embryonic stem cell identity. Nature. 2010; 468, 316–320.

Cherry, Christopher, and Erika L Matunis. "Epigenetic Regulation of Stem Cell Maintenance in the Drosophila Testis via the Nucleosome Remodeling Factor NURF." Cell Stem Cell.2010; 6, 557–567.

Choi, Jin Soo, et al. "Comparative Genomic Hybridization Array Analysis and Real-Time PCR Reveals Genomic Copy Number Alteration for Lung Adenocarcinomas." Lung.2006; 184, 355-362.

Clapier, Cedric R, and Bradley R Cairns. "The Biology of Chromatin Remodeling Complexes." Annual Review of Biochemistry.2009; 78, 273-304.

Cosman, D., Mullberg, J., Sutherland, C.L., Chin, W., Armitage, R., Fanslow, W., Kubin, M. and Chalupny, N.J. ULBPs, novel MHC class I-related molecules, bind to CMV glycoprotein UL16 and stimulate NK cytotoxicity through the NKG2D receptor. Immunity.2001; 14, 123.

Costello, R.T., Sivori, S., Marcenaro, E., Lafage-Pochitaloff, M., Mozziconacci, M.J., Coughlin CM, Salhany KE, Gee MS, LaTemple DC, Kotenko S, et al. Tumor cell responses to IFNγ affect tumorigenicity and response to IL-12 therapy and antiangiogenesis. Immunity.1998; 9:25.

Czerniecki BJ, Koski GK, Koldovsky U, Xu S, Cohen PA, Mick R, Nisenbaum H, Pasha T, Xu M, Fox KR, Weinstein S, Orel SG, Vonderheide R, Coukos G, DeMichele A, Araujo L, Spitz FR, Rosen M, Levine BL, June C, Zhang PJ. Targeting HER-2/neu in

early breast cancer development using dendritic cells with staged interleukin-12 burst secretion. Cancer Res. 2007; 67, 1842-52.

Dang, Weiwei, and Blaine Bartholomew. "Domain architecture of the catalytic subunit in the ISW2-nucleosome complex." Molecular and cellular biology. 2007; 8306-8317.

Dar, Altaf A, et al. "The Role of BPTF in Melanoma Progression and in Response to BRAF-Targeted Therapy." JNCI J Natl Cancer Inst.2015 107, 5.

Diefenbach, A., Jensen, E.R., Jamieson, A.M. and Raulet, D.H. Rae1 and H60 ligands of the NKG2D receptor stimulate tumor immunity. Nature. 2001; 413, 165.

Dimitrios C. Mastellos, Robert A. DeAngelis, and John D. Lambris. Inducing and characterizing liver regeneration in mice: Reliable models, essential “readouts” and critical perspectives. Curr Protoc Mouse Biol. 2013; 3, 141–170.

Dunn, C., Chalupny, N.J., Sutherland, C.L., Dosch, S., Sivakumar, P.V., Johnson, D.C., and Cosman, D. Human cytomegalovirus glycoprotein UL16 causes intracellular sequestration of NKG2D ligands, protecting against natural killer cell cytotoxicity. J Exp Med. 2003; 197, 1427.

Ebbert, R. et al.The product of the SNF2/SWI2 paralogue INO80 of *Saccharomyces cerevisiae* required for efficient expression of various yeast structural genes is part of a high-molecular-weight protein complex.Mol. Microbiol. 1999; 32, 741–751.

Ebara S, Kawasaki S, Nakamura I, Tsutsumimoto T, Nakayama K, Nikaido T, Takaoka K. Transcriptional regulation of the mBMP-4 gene through an E-box in the 5'-flanking promoter region involving USF. Biochem Biophys Res Commun. 1997; 240, 136-41.

Elliott, J. M., and Yokoyama, W. M. Unifying concepts of MHC-dependent natural killer cell education. Trends Immunol. 2011; 32, 364-372.

El-Assal ON, Yamanoi A, Ono T, Kohno H, Nagasue N. The clinicopathological significance of heparanase and basic fibroblast growth factor expressions in hepatocellular carcinoma. Clin Cancer Res. 2001; 7, 1299–305.

Elston, C. W. & Ellis, I. O. Pathological prognostic factors in breast cancer. I. The value of histological grade in breast cancer: experience from a large study with long-term follow-up. Histopathology. 1991; 19, 403–410.

Endo K, Maejara U, Baba H, Tokunaga E, Koga T, Ikeda Y, et al. Heparanase gene expression and metastatic potential in human gastric cancer. Anticancer Res. 2001; 21, 3365–9.

Evans, M. J. and Kaufman, M. H. Establishment in culture of pluripotential cells from mouse embryos. Nature. 1981; 292, 154-156.

Falco, M., Cantoni, C., Bottino, C., Moretta, A. and Biassoni, R. Identification of the rat homologue of the human NKp46 triggering receptor. Immunol Lett.1999; 68, 411.

Fernandez, N.C., Lozier, A., Flament, C., Ricciardi-Castagnoli, P., Bellet, D., Suter, M. et al. Dendritic cells directly trigger NK cell functions: crosstalk relevant in innate anti-tumor immune responses in vivo. Nat Med.1999; 5, 405–11.

Fernandez NC, Treiner E, Vance RE, Jamieson AM, Lemieux S, Raulet DH. A subset of natural killer cells achieves self-tolerance without expressing inhibitory receptors specific for self-MHC molecules. Blood. 2005; 105, 4416–23.10.

Ferreira, Roger, Anton Eberharter, Tiziana Bonaldi, Mariacristina Chioda, Axel Imhof, and Peter B Becker. "Site-specific acetylation of ISWI by GCN5." BMC Molecular Biology. 2007; 8, no. 73.

Ferlazzo, G., M. L. Tsang, et al. "Human dendritic cells activate resting natural killer (NK) cells and are recognized via the NKp30 receptor by activated NK cells." J Exp Med. 2002; 195, 343-351.

FitzGerald J. E., Grenon M., Lowndes N. F. 53BP1: function and mechanisms of focal recruitment. Biochem. Soc. Trans. 2009; 37, 897–904.

Gardiner, C. M. Killer cell immunoglobulin-like receptors on NK cells: the how, where and why. Int. J. Immunogenet. 2008; 35, 1–8.

Gasser, S., Orsulic, S., Brown, E.J. and Raulet, D.H. (2005). The DNA damage pathway regulates innate immune system ligands of the NKG2D receptor. Nature 436, 1186.

Gazit, R., Garty, B.Z., Monselise, Y., Hoffer, V., Finkelstein, Y., Markel, G., Katz, G., Hanna, J., Achdout, H., Gruda, R., Gonen-Gross, T. and Mandelboim, O. (2004).

Expression of KIR2DL1 on the entire NK cell population: a possible novel immunodeficiency syndrome. Blood 103, 1965.

Christopher V.E. Wright. Mechanisms of Left-Right Asymmetry: What's Right and What's Left? Cell.2001; 1,179–186.

Goldman, Joseph A, Joseph D Garlick, and Robert E Kingston. "Chromatin remodeling by imitation switch (ISWI) class ATP-dependent remodelers is stimulated by histone variant H2A.Z." The Journal of Biological Chemistry 285, no. 7 (2010): 4645-4651.

Gomes AM, Stelling MP, Pavão MSG. Heparan sulfate and heparanase as modulators of breast cancer progression. Biomed Res Int (2013) 2013:852093.

Gospodinov A, Vaissiere T, Krastev DB, Legube G, Anachkova B, Herceg Z. Mammalian Ino80 mediates double-strand break repair through its role in DNA end strand resection. Mol Cell Biol. 2011; 31, 4735-45.

Groh V, Wu J, Yee C, Spies T. 2002. Tumour-derived soluble MIC ligands impair expression of NKG2D and T-cell activation. Nature 419:734–38

Groh, V., Rhinehart, R., Randolph-Habecker, J., Topp M.S., Riddell, S. R. and Spies, T. Costimulation of CD8alphabeta T cells by NKG2D via engagement by MIC induced on virus-infected cells. Nat Immunol. 2001; 2, 255.

Groh, V., Wu, J., Yee, C. and Spies, T. Tumor-derived soluble MIC ligands impair expression of NKG2D and T-cell activation. Nature. 2002; 419, 734.

Douglas Hanahan, Robert A. Weinberg. Hallmarks of Cancer: The Next Generation. Cell. 2011; 144, 646–674.

Hanna, J., Gonen-Gross, T., Fitchett, J., Rowe, T., Daniels, M., Arnon, T. I., Gazit, R., Joseph, A., Schjetne, K.W., Steinle, A. et al. Novel APC-like properties of human NK cells directly regulate T cell activation. J. Clin. Invest. 2004; 114, 1612–1623.

Heba A Alshaker and Khalid Z Matalka. IFN-γ, IL-17 and TGF-β involvement in shaping the tumor microenvironment: The significance of modulating such cytokines in treating malignant solid tumors. Cancer Cell Int. 2011; 11, 33.

Hodge-Dufour J, Noble PW, Horton MR, Bao C, Wysoka M, et al. Induction of IL-12 and chemokines by hyaluronan requires adhesion-dependent priming of resident but not elicited macrophages. J. Immunol.1997; 159, 2492–500.

Hong, Wei, et al. "FOG-1 recruits the NuRD repressor complex to mediate transcriptional repression by GATA-1." EMBO J.2005; 24, 2367–2378.

Hota, Swetansu K, Saurabh K Bhardwaj, Sebastian Deindl, Yuan-chi Lin, Xiaowei Zhuang, and Blaine Bartholomew. "Nucleosome mobilization by ISW2 requires the concerted action of the ATPase and SLIDE domains." Nat Struct Mol Biol. 2013; 20, 222–229.

Hoeijmakers J. H. 2001. Genome maintenance mechanisms for preventing cancer. Nature. 2001; 411, 366–374.

Hu G, Kim J, Xu Q, Leng Y, Orkin SH, Elledge SJ. A genome-wide RNAi screen identifies a new transcriptional module required for self-renewal. Genes Dev. 2009; 23, 837–848.

Hur SK, Park EJ, Han JE, et al. Roles of human INO80 chromatin remodeling enzyme in DNA replication and chromosome segregation suppress genome instability. Cell Mol Life Sci. 2010; 67, 2283–2296.

Jamieson, A.M., Diefenbach, A., McMahon, C.W., Xiong, N., Carlyle, J.R. and Raulet D.H. The role of the NKG2D immunoreceptor in immune cell activation and natural killing. Immunity. 2002; 17, 19.

Jingping Yang and Victor G. Corces. Chromatin Insulators: A Role in Nuclear Organization and Gene Expression. Adv Cancer Res. 2011; 110, 43–76.

Jollie, W.P. Development, morphology, and function of the yolk sac placenta of laboratory rodents. Teratology.1990*;* 41, 361-381.

Kagey MH[1], Newman JJ, Bilodeau S, Zhan Y, Orlando DA, van Berkum NL, Ebmeier CC, Goossens J, Rahl PB, Levine SS, Taatjes DJ, Dekker J, Young RA. Mediator and cohesin connect gene expression and chromatin architecture. Nature. 2010; 23, 430-435.

Kaplan DH, Shankaran V, Dighe AS, Stockert E, Aguet M, et al. Demonstration of an interferon γ-dependent tumor surveillance system in immunocompetent mice. Proc. Natl. Acad. Sci. 1998; 95, 7556–61.

Karina B. Falbo and Xuetong Shen. Function of the INO80 chromatin-remodeling complex in DNA replication. Front Biosci (Landmark Ed). 2012; 17, 970–975.

Karre, K., Ljunggren, H.G., Piontek, G. and Kiessling, R. Selective rejection of H-2-deficient lymphoma variants suggests alternative immune defense strategy. Nature.1986; 319, 675.

Kazutoshi Takahashi1 and Shinya Yamanaka. Induction of Pluripotent Stem Cells from Mouse Embryonic and Adult Fibroblast Cultures by Defined Factors. Cell. 2006; 126, 663–676.

Khong HT, Restifo NP. Natural selection of tumor variants in the generation of “tumor escape” phenotypes. Nat. Immunol. 2002; 3, 999–1005.

Kiessling R, Klein E, Wigzell H."Natural" killer cells in the mouse. I. Cytotoxic cells with specificity for mouse Moloney leukemia cells. Specificity and distribution according to genotype. Eur J Immunol.1975; 5, 112-7.

Kim, S., Iizuka, K., Aguila, H.L., Weissman, I.L. and Yokoyama, W.M. In vivo natural killer cell activities revealed by natural killer cell-deficient mice. Proc. Natl. Acad. Sci.2000; 97, 2731–2736.

Klagsbrun M., Soker S. (1993). VEGF/VPF: the angiogenesis factor found. Curr. Biol. 3, 699–702 10.1016/0960-9822(93)90073-W.

Kolasinska-Zwierz, Paulina, Thomas Down, Isabel Latorre, Tao Liu, X. Shirley Liu, and Julie Ahringer. "Differential chromatin marking of introns and expressed exons by H3K36me3." Nat Genet. 2009; 41, 376–381.

Lai, Anne Y, and Paul a Wade. "Cancer biology and NuRD: a multifaected chromatin remodeling complex." Nature reviews Cancer. 2011; 11, 588-596.

Landry, Joseph, et al. "Essential Role of Chromatin Remodeling Protein Bptf in Early Mouse Embryos and Embryonic Stem Cells." PLOS Genetics. 2008; 4, 10.
.

Lanier, L. NK cell receptors. Annu. Rev. Immunol.1998; 16, 359–393.

Lanier, L.L. NK cell recognition. Annu Rev Immunol. 2005; 23, 225-74.

Levin, Albert M, Mitchell J Machiela, Kimberly A Zuhlke, Anna M Ray, Kathleen A Cooney, and Julie a Douglas. "Chromosome 17q12 variants contribute to risk of early-onset prostate cancer." Cancer Res. 2008; 68, 6492–6495.

Leitch HG[1], McEwen KR, Turp A, Encheva V, Carroll T, Grabole N, Mansfield W, Nashun B, Knezovich JG, Smith A, Surani MA, Hajkova P. Naive pluripotency is associated with global DNA hypomethylation. Nat Struct Mol Biol. 2013 Mar; 20(3):311-6.

Li CI, Malone KE, Saltzman BS, Daling JR. Risk of invasive breast carcinoma among women diagnosed with ductal carcinoma in situ and lobular carcinoma in situ, 1988-2001. Cancer. 2006; 106, 2104-12.

Li, Guohong, and Danny Reingberg. "Chromatin higher-order strucutres and gene regulation." Current Opinion in Genetics & Development. 2011; 21, 175-186.

Li, P., Morris, D.L., Willcox, B.E., Steinle, A., Spies, T. and Strong, R.K. Complex structure of the activating immunoreceptor NKG2D and its MHC class I-like ligand MICA. Nat Immunol. 2001; 2, 443.

Liao, N. S., Bix, M., Zijlstra, M., Jaenisch, R. & Raulet, D. MHC class I deficiency: susceptibility to natural killer (NK) cells and impaired NK activity. Science. 1991; 253, 199–202.

Livak KJ, Schmittgen TD. Analysis of relative gene expression data using real-time quantitative PCR and the 2 (-Delta Delta C (T)) Method. Methods. 2001; 4, 402-8.

Li Wang, Ying Du, James M. Ward, Takashi Shimbo, Brad Lackford, Xiaofeng Zheng, Yi-liang Miao, Bingying Zhou, Leng Han, David C. Fargo, Raja Jothi, Carmen J. Williams, Paul A. Wade, and Guang Hu. INO80 Dependent Promoter Access Facilitates Activation of Pluripotency Genes in Embryonic Stem Cell Self-Renewal, Reprogramming, and Blastocyst Development. Cell Stem Cell. 2014; 14, 575–591.

Loizou J. I., et al. Epigenetic information in chromatin: the code of entry for DNA repair. Cell Cycle. 2006; 5, 696–701.

Luger, Karolin, Armin W Mader, Robin K Richmond, F David Sargent, and Timothy J Richmond. "Crystal structure of the nucleosome core particle at 2.8 A resolution." Nature. 1997; 389, 251-260.

Luster AD, Leder P. IP-10, a −C−X−C−chemokine, elicits a potent thymus-dependent antitumor response in vivo. J. Exp. Med. 1993; 178, 1057–65.

Lu Chen,Yong Cai,Jingji Jin, Laurence Florens,Selene K. Swanson, Michael P. Washburn, Joan Weliky Conaway, andRonald C. Conaway. Subunit Organization of the Human INO80 Chromatin Remodeling Complex. An Evolutionarily conserved core complex catalyzes ATP Dependent Nucleosome Remodeling. J Biol Chem. 2011; 286, 11283–11289.

Manolis Papamichos-Chronakis, Shinya Watanabe,[1] Oliver J. Rando,[2] and Craig L. Peterson. Global regulation of H2A.Z localization by the INO80 chromatin remodeling enzyme is essential for genome integrity. Cell. 2011; 144, 200–213.

Margueron R, Trojer P, Reinberg D. The key to development: interpreting the histone code? Curr Opin Genet Dev. 2005; 15,163–176.

Marincola FM, Jaffee EM, Hicklin DJ, Ferrone S. 2000. Escape of human solid tumors from T-cell recognition: molecular mechanisms and functional significance. Adv. Immunol.2000; 74, 181–273.

Markel, G., Lieberman, N., Katz, G., Arnon, T.I., Lotem, M., Drize, O., Blumberg, R.S., Bar-Haim, E., Mader, R., Eisenbach, L. and Mandelboim, O. CD66a interactions between human melanoma and NK cells: a novel class I MHC-independent inhibitory mechanism of cytotoxicity. J Immunol. 2002; 168, 2803.

Markel, G., Wolf, D., Hanna, J., Gazit, R., Goldman-Wohl, D., Lavy, Y., Yagel, S. and O. Mandelboim. Pivotal role of CEACAM1 protein in the inhibition of activated decidual lymphocyte functions. J Clin Invest. 2002; 110, 943.

Martin-Fontecha, A., Thomsen, L.L., Brett, S., Gerard, C., Lipp, M., Lanzavecchia, A. et al. Induced recruitment of NK cells to lymph nodes provides IFNgamma for T(H)1 priming. Nat Immunol. 2004; 5, 1260–5.

Martin, G. R. Isolation of a pluripotent cell line from early mouse embryos cultured in medium conditioned by teratocarcinoma stem cells. Proc. Natl. Acad. Sci. 1981; 78, 7634-7638.

Matkowski R, Gisterek I, Halon A, Lacko A, Szewczyk K, Staszek U, Pudelko M, Szynglarewicz B, Szelachowska J, Zolnierek A, Kornafel J. The prognostic role of tumor-infiltrating CD4 and CD8 T lymphocytes in breast cancer. Anticancer Res. 2009; 29, 2445-51.

Mayes, K., S.G. Alkhatib, K. Peterson, A. Alhazmi, C. Song, V. Chan, T. Blevins, M. Roberts, C.I. Dumur, X.Y. Wang, and J.W. Landry. BPTF Depletion Enhances T Cell Mediated Antitumor Immunity. Cancer Res.2016; 76, 6183-6192.

Michaelsson, J., Teixeira de Matos, C., Achour, A., Lanier, L.L., Karre, K. and Soderstrom, K. A signal peptide derived from hsp60 binds HLA-E and interferes with CD94/NKG2A recognition. J Exp Med. 2000; 196, 1403.

Mocikat, R., Braumuller, H., Gumy, A., Egeter, O., Ziegler, H., Reusch, U. et al. Natural killer cells activated by MHC class I(low) targets prime dendritic cells to induce protective CD8 T cell responses. Immunity.2003; 19, 561–9.

Momcilovic O, Navara C, Schatten G. Cell cycle adaptations and maintenance of genomic integrity in embryonic stem cells and induced pluripotent stem cells. Results Probl Cell Differ. 2011; 53, 415–458.

Monni, Outi, et al. "Comprehensive copy number and gene expression profiling of the 17q23 amplicon in human breast cancer." PNAS. 2001; 98, 10.

Moretta, A., Biassoni, R., Bottino, C., Mingari, M.C. and Moretta, L. Natural cytotoxicity receptors that trigger human NK-cell-mediated cytolysis. Immunol. 2000; 21, 228.

Moretta, A., Sivori, S., Vitale, M., Pende, D., Morelli, L., Augugliaro, R., Bottino, C. and Moretta, L. Existence of both inhibitory (p58) and activatory (p50) receptors for HLA-C molecules in human natural killer cells. J Exp Med. 1995; 182, 875.

Moretta, L., Bottino, C., Pende, D., Mingari, M.C., Biassoni, R. and Moretta, A. Human natural killer cells: their origin, receptors and function. Eur J Immunol. 2002; 32, 1205.

Mueller-Planitz, Felix, Henrike Klinker, Johanna Ludwigsen, and Peter B Becker (2013). "The ATPase domain of ISWI is an autonomous nucleosome remodeling machine." Nature Structural &Molecular Biology. 2013; 20, 82-91.

Murri AM, Hilmy M, Bell J, Wilson C, McNicol AM, Lannigan A, Doughty JC, McMillan DC. The relationship between the systemic inflammatory response, tumour proliferative activity, T-lymphocytic and macrophage infiltration, microvessel density and survival in patients with primary operable breast cancer. Br J Cancer. 2008; 99, 1013-9.

Nowotschin S., Hadjantonakis A. K. (2010). Cellular dynamics in the early mouse embryo: from axis formation to gastrulation. Curr. Opin. Genet. Dev. 20, 420–427.

Parham, P. MHC class I molecules and KIRs in human history, health and survival. Nat. Rev. Immunol. 2005; 5, 201–14.

Pessino, A., Sivori, S., Bottino, C., Malaspina, A., Morelli, L., Moretta, L. et al. Molecular cloning of NKp46: a novel member of the immunoglobulin superfamily involved in triggering of natural cytotoxicity. J Exp Med. 1998; 188, 953–60.

Petter Höglund & Petter Brodin. Current perspectives of natural killer cell education by MHC class I molecules. Nature Reviews Immunology. 2010; 10, 724-734.

Piccioli, D., Sbrana, S., Melandri, E., Valiante, N.M. et al. Contact-dependent stimulation and inhibition of dendritic cells by natural killer cells. J Exp Med. 2002; 195, 335–41.

Qin Z, Blankenstein T. CD4+ T cell-mediated tumor rejection involves inhibition of angiogenesis that is dependent on IFNγ receptor expression by nonhematopoietic cells. Immunity. 2000; 12, 677–86.

Qiu, Zhijun, et al. "Functional Interactions between NURF and CTCF Regulate Gene Expression." Mol. Cell. Biol. 2015; 35, 224-237.

Raidl, Maria, et al. "Multiple chromosomal abnormalities in human liver (pre)neoplasia." Journal Hepatol.2004; 40, 660-668.

Raulet, D. H. & Vance, R. E. Self-tolerance of natural killer cells. Nat. Rev. Immunol. 2006; 6, 520–31.

Raulet, D.H., Vance, R.E. and McMahon, C.W. Regulation of the natural killer cell receptor repertoire. Annu Rev Immunol. 2001; 19, 291.

Reviron, D., Gastaut, J.A., Pende, D., Olive, D. and Moretta, A. Defective expression and function of natural killer cell-triggering receptors in patients with acute myeloid leukemia. Blood. 2002; 99, 3661.

Richardson, L., Torres-Padilla, M. E. & Zernicka-Goetz, M. Regionalised signalling within the extraembryonic ectoderm regulates anterior visceral endoderm positioning in the mouse embryo. Mech. Dev. 2006; 123, 288–296.

Rowland, B.D., Bernards, R., and Peeper, D.S. The KLF4 tumour suppressor is a transcriptional repressor of p53 that acts as a context-dependent oncogene. Nat. Cell Biol.2005; 7, 1074–1082.

Ruthenburg, Alexander J, et al. "Recognition of a Mononucleosomal Histone Modification Pattern by BPTF via Multivalent Interactions." Cell. 2011; 145, 692–706.

S. Dimmeler, A.M. Zeiher. Nitric oxide and apoptosis: another paradigm for the double-edged role of nitric oxide. Nitric Oxide: Biol. Chem. 1997; 1, pp. 275–28.

Sakaguchi S, Sakaguchi N, Shimizu J, Yamazaki S, Sakihama T, et al. 2001. Immunologic tolerance maintained by CD25+ CD4+ regulatory T cells: their common role in controlling autoimmunity, tumor immunity, and transplantation tolerance. Immunol. Rev. 2011; 182, 18–32.

Santisteban M, Reiman JM, Asiedu MK, Behrens MD, Nassar A, Kalli KR, Haluska P, Ingle JN, Hartmann LC, Manjili MH, Radisky DC, Ferrone S, Knutson KL. Immune-induced epithelial to mesenchymal transition in vivo generates breast cancer stem cells. Cancer Res. 2009; 69, 2887-95.

Savatier, P., Lapillonne, H., van Grunsven, L. A., Rudkin, B. B. and Samarut, J. Withdrawal of differentiation inhibitory activity/leukemia inhibitory factor up-regulates D-type cyclins and cyclin-dependent kinase inhibitors in mouse embryonic stem cells. Oncogene. 1996; 12, 309-322.

Schwanbeck, Ralf, Hua Xiao, and Carl Wu. "Spatial Contacts and Nucleosome Step Movements Induced by the NURF Chromatin Remodeliong Complex." The Journal of Biological Chemistry. 2004; 279, 39933-39941.

Shalaby F, Rossant J, Yamaguchi TP, Gertsenstein M, Wu XF, Breitman ML, Schuh AC. Failure of blood-island formation and vasculogenesis in Flk-1-deficient mice. Nature. 1995; 376, 62-6.

Shen X., Ranallo R., Choi E., Wu C. Involvement of actin-related proteins in ATP-dependent chromatin remodeling. Mol. Cell. 2003; 12, 147–155.
Seoane, J., Le, H.V., and Massague, J. Myc suppression of the p21(Cip1) Cdk inhibitor influences the outcome of the p53 response to DNA damage. Nature. 2002; 419, 729–734.

Simhadri, V. R., K. S. Reiners, et al. (2008). "Dendritic cells release HLA-B-associated transcript-3 positive exosomes to regulate natural killer function." PLoS One. 2008; 3, e3377.

Sims, Robert J, Chi-Fu Chen, Helena Santos-Rosa, Tony Kouzarides, Smita S Patel, and Danny Reinberg. "Human but not yeast CHD1 binds directly and selectively to histone H3 methylated at lysine 4 via its tandem chromodomains." Journal of biological chemistry. 2005; 280, 41789–92.

Sivori, S., Vitale, M., Morelli, L., Sanseverino, L., Augugliaro, R., Bottino, C., Moretta, L., and Moretta, A. p46, a novel natural killer cell-specific surface molecule that mediates cell activation. J Exp Med. 1997; 186, 1129.

Smyth, M.J., Kelly, J.M., Baxter, A.G., Korner, H., Sedgwick, J.D. et al. (1998). An essential role for tumor necrosis factor in natural killer cell-mediated tumor rejection in the peritoneum. J Exp Med. 1998; 188, 1611–9.

Smyth, M.J., Swann, J., Cretney, E., Zerafa, N., Yokoyama, W.M., Hayakawa, Y. et al. NKG2D function protects the host from tumor initiation. J Exp Med. 2005; 202, 583-8.

Smyth, M.J., Thia, K.Y., Cretney, E., Kelly, J.M., Snook, M.B., Forbes, C.A. et al.
Song, Haiyun, Chloe Spichiger-Haeusermann, and Konrad Basler. "The ISWI-containing NURF complex regulates the output of the canonical Wingless pathway." EMBO reports. 2009; 10, 1140-1146.

Spies, Noah, Cydney Nielsen, Richard A Padgett, and Christopher B Burge. "Biased Chromatin Signatures around Polyadenylation Sites and Exons." Moleculare Cell. 2009; 36, 245–254.

Stephens, Gena E, Hua Xiao, Dirk-H Lankenau, Carl Wu, and Sarah C. R. Elgin. "Heterochromatin Protein 2 Interacts with Nap-1 and NURF: A Link between Heterochromatin-Induced Gene Silencing and the Chromatin Remodeling Machinery in Drosophila." Biochemistry. 2006; 45, 14990-14999.

Stephen Frankenberg, Lee Smith, Andy Greenfield, and Magdalena Zernicka-Goetz. Novel gene expression patterns along the proximo-distal axis of the mouse embryo before gastrulation. BMC Dev Biol. 2007; 7: 8.

Sternlicht MD, Werb Z. How matrix metalloproteinases regulate cell behavior. Annu. Rev. Cell. Dev. Biol. 2001; 17, 463–516.

Street, S.E., Cretney, E., Smyth, M.J. et al. Perforin and interferon-gamma activities independently control tumor initiation, growth, and metastasis. Blood. 2001; 97, 192–7.

Sutherland, C.L., Chalupny, N.J., Schooley, K., VandenBos, T., Kubin, M. and Cosman D. UL16-binding proteins, novel MHC class I-related proteins, bind to NKG2D and activate multiple signaling pathways in primary NK cells. J Immunol. 2002; 168, 671.

Taylor, Gillian C, Ragnhild Eskeland, Betül Hekimoglu-Balkan, Madapura M Pradeepa, and Wendy a Bickmore. "H4K16 acetylation marks active genes and enhancers of embryonic stem cells, but does not alter chromatin compaction." Genome Research. 2013; 23, 2053–2065.

Tortorella, D., Gewurz, B.E., Furman, M.H., Schust, D.J. and Ploegh, H.L. Viral subversion of the immune system. Annu Rev Immunol. 2000; 18, 861.

Trinchieri, G. Biology of natural killer cells. Adv. Immunol. 1989; 47, 187–376.

Trojer, Patrick, and Danny Reinberg. "Facultative Heterochromatin: Is There a Distinctive Molecular Signature?" Molecular Cell. 2007; 28, 1-13.

Vales-Gomez, M., Reyburn, H.T., Erskine, R.A., Lopez-Botet, M. and Strominger J.L. Van den Broek, M.F., Kagi, D., Zinkernagel, R.M., Hengartner, H. et al. Perforin dependence of natural killer cell-mediated tumor control in vivo. Eur J Immunol. 1995; 25, 3514–6.

Vargo-Gogola T, Rosen JM. Modelling breast cancer: one size does not fit all. Nat Rev Cancer. 2007; 7, 659-72.

Vicent, Guillermo Pablo, et al. "Four enzymes cooperate to displace histone H1 during the first minute of hormonal gene activation." Genes & Deve. 2011; 25, 845-862.

Vitale, M., Bottino, C., Sivori, S., Sanseverino, L., Castriconi, R., Marcenaro, E., Augugliaro, R., Moretta, L. and Moretta, A. NKp44, a novel triggering surface molecule specifically expressed by activated natural killer cells, is involved in nonmajor histocompatibility complex-restricted tumor cell lysis. J Exp Med. 1998; 187, 2065.

Vita, M. & Henriksson, M. The Myc oncoprotein as a therapeutic target for human cancer. *Semin. Cancer Biol.* 2006; 16, 318–330.

Vivier, E., Raulet, D.H., Moretta, A., Caligiuri, M.A., Zitvogel, L., Lanier, L.L., Yokoyama, W.M., and Ugolini, S. (2011). Innate or adaptive immunity? The example of natural killer cells. Science. 2011; 331, 44-49.

Waldhauer.I., D.Goehlsdorf, et al. "Tumor-associated MICA is shed by ADAM proteases." Cancer Res. 2008; 68, 6368-6376.

Walzer, T., M. Dalod, et al. "Natural-killer cells and dendritic cells: "l'union fait la force"." Blood. 2005; 106, 2252-2258.

William S. Chen, Kada Manova, Daniel C. Weinstein Stephen A. Duncan, Andrew S. Plump, Vincent R. Prezioso/ Rosemary F. Bachvarova, and James E. Darnell Jr. Disruption of the HNF-4 eene, expressedin visceral endoderm, leads to cell deathin embryonic ectoderm and impaired gastrulation of mouse embryos. Genes & Development. 1994; 8, 2466-2477.

Wong, C. W., Hou, P. S., Tseng, S. F., Chien, C. L., Wu, K. J., Chen, H. F., Ho, H. N., Kyo, S. and Teng, S. C. Kruppel-like transcription factor 4 contributes to maintenance of telomerase activity in stem cells. Stem Cells. 2010; 28, 1510-1517.

Wu, J., Chalupny, N.J., Manley, T.J., Riddell, S.R., Cosman, D., and Spies, T. Intracellular retention of the MHC class I-related chain B ligand of NKG2D by the human cytomegalovirus UL16 glycoprotein. J Immunol. 2003; 170, 4196.

Wu S, Shi Y, Mulligan P, et al. A YY1-INO80 complex regulates genomic stability through homologous recombination-based repair. Nat Struct Mol Biol. 2007; 14, 1165–1172.

Wysocka, Joanna, et al. "A PHD finger of NURF couples histone H3 lysine 4 trimethylation with chromatin remodeling." Nature. 2006; 442, 86-90.

Wysocka, Joanna. "Identifying novel proteins recognizing histone modifications usinf peptide pull-down assay." Methods. 2006; 40, 339-343.

Xiao, Hua, et al. "Dual Functions of Largest NURF Subunit NURF301 in Nucleosome Sliding and Transcription Factor Interactions." Molecular Cell. 2001; 8, 531-543.

Xiao, Shuai, et al. "BPTF Associated with EMT Indicates Negative Prognosis in Patients with Hepatocellular Carcinoma." Dig Dis Sci.2015; 60, 910-918.

Xu Y, Ayrapetov MK, Xu C, Gursoy-Yuzugullu O, Hu Y, Price BD. Histone H2A.Z controls a critical chromatin-remodeling step required for DNA double-strand break repair. Mol Cell. 2012; 48, 723–733.

Yu J, Mitsui T, Wei M, Mao H, Butchar JP, Shah MV, Zhang J, Mishra A, Alvarez-Breckenridge C, Liu X, Liu S, Yokohama A, Trotta R, Marcucci G Jr, Benson DM, Loughran TP Jr, Tridandapani S, Caligiuri MA. NKp46 identifies an NKT cell subset susceptible to leukemic transformation in mouse and human. J Clin Invest. 2011; 121, 1456-70.

Yunhe Bao and Xuetong Shen. INO80 subfamily of Chromatin Remodeling Complexes. Mutat Res. 2007; 618, 18–29.

Zhang H, Roberts DN, Cairns BR. Genome-wide dynamics of Htz1, a histone H2A variant that poises repressed/basal promoters for activation through histone loss. Cell. 2005; 123, 219–231.

Zhang, Wei, et al. "Structural plasticity of histones H3-H4 facilitates their allosteric exchange between RbAp48 and ASF1." Nat Struct Mol Biol. 2013; 20, 29-35.

Zhou, Wenlai, et al. "Histone H2A Monoubiquitination Represses Transcription by Inhibiting RNA polymerase II Transcriptional Elongation." Mol Cell. 2008; 18, 69-80.

Zimmer, J. & Donato, L. Activity and phenotype of natural killer cells in peptide transporter (TAP) deficient patients (type I bare lymphocyte syndrome). J. Exp. Med.1998; 187, 117–122.

Vita

Zeinab Elsayed was born on January 29, 1979 in Giza, Egypt. She received her Bachelor of Science degree in Zoology from Al-Azhar University, Egypt in 2002. She received her master degree in cytogenetics from National Research Center, Egypt in 2011. She entered the Molecular Biology & Genetics program in the fall of 2012.